The effect of the direction of motion of a vibrating absorber on the response of an in-core neutron detector

by

Mohammad Kamaleddin Kalbasi-Isfahani

A Thesis Submitted to the
Graduate Faculty in Partial Fulfillment of the
Requirements for the Degree of
MASTER OF SCIENCE

Major: Nuclear Engineering

Iowa State University
Ames, Iowa

1985

TABLE OF CONTENTS

LIST OF TABLES

LIST OF FIGURES

LIST OF ACRONYMS

UTR-10 - University Training and Research Reactor - 10 kW

APSD - Auto Power Spectral Density

PRBS - Pseudo-Random Binary Signal

LVDT - Linear Variable Differential Transformer

CIC - Compensated Ion-Chamber

HP - Hewlett Packard

SQR - SQuare Root

DET - DETector

IC - Integrated Circuit

F - Flooded

@ - at the same time

NORM - NORMalization

w.r.t. - with respect to

CLK - CLocK

A.P. - Angular Position

L/G - Local to Global ratio

I. INTRODUCTION

Monitoring the motion of the different components such as control rods, fuel rods, and structural elements of a nuclear reactor core is vital to the safety of the plant. If, for example, one or more fuel rods or other components break due to vibration, they can block the flow channels of the coolant through the core, and cause the fuel to overheat. The vibrating component produces a time dependent perturbation of the neutron flux which can be observed with the reactor neutron instrumentation. In order to get familiar with the characteristics of the responses of a neutron detector located in different parts of a nuclear reactor to a vibrating core component, many theoretical and experimental investigations related to this subject have been carried out over the past few years [1-18]. It has been found, however, that the response of a neutron detector to a moving component is a complex function of the detector location relative to the component, and also the direction of motion of the component relative to the detector. To provide insight into the interpretation of neutron detector signals produced by a vibrating component, it is necessary to perform "separate effects" tests using simple systems that make it possible to study these various effects independently.

Most of the experimental research which has been done to date on the vibrations inside a nuclear reactor has been limited to motion of the vibrator relative to the detector in one or at most two directions, one perpendicular to the other [7, 9, 10, 15-17]. Since actual

vibrations usually are stochastic, elements could vibrate in many different directions of motion simultaneously. The purpose of this research is to study the response of a neutron detector as a function of the direction of vibrator motion relative to the detector using an experimental vibration system located in the Iowa State University UTR-10 reactor. Procedures used, involved turning the vibrator to different directions of motion and obtaining detector responses for each angular position of the vibrator. To do this, the vibration apparatus used in [10] was redesigned so that it could be remotely turned to different angular positions in the fuel tank.

In order to have fine control over the direction of motion and to avoid shutting down the reactor and manually changing the direction of motion for each test, a stepping motor was used and a control system designed which provided control by a computer. A reliable and economical control system was designed by the author and was built in the Engineering Research Institute shop at Iowa State University.

II. LITERATURE CITED

Research on the topic of the response of a neutron detector to an oscillating component has been carried out by many authors for years [1-18]. One of the most important theoretical developments is that of Van Dam [11] and Behringer et al. [12] who were able to demonstrate that the neutron fluctuations produced by a moving neutron absorber consist of two independendent effects: the 'local' effect which is space dependent and the 'global' effect, which is space independent. The local effect changes rapidly with position in the reactor.

Pazsit [13], working with one-dimensional, space-dependent one group theory, showed that the neutron noise generated by a vibrating neutron absorber is much different from the neutron noise which results from a stationary absorber of varying strength. Pazsit and Analytis [14] also developed a two-dimensional model for a system, which illustrated the dependence of the response of a detector on the direction of motion of the absorber.

Experimental measurements at Iowa State University were initiated by Al-Ammar [15] who constructed an apparatus which could be inserted into the UTR-10 in place of the central vertical stringer between the core tanks in the graphite. His apparatus consisted of a one-dimensional vibrating cadmium absorber and two neutron detectors. Al-Ammar found that the local effect was about 3.7 times greater than the global effect for an absorber vibrating in the North-South plane at a frequency of approximately 1.0 Hz. The detectors were located 4.5 Cm from the vibrator.

Al-Ammar's work was improved upon by Borland [16]. Borland constructed a vibrating absorber device which incorporated a better absorber position measuring system and a sturdier vibrator, thus eliminating some of the problems inherent in Al-Ammar's design. Borland's device also had the capability of measuring the flux response with different detector-vibrator configurations. His work verified Al-Ammar's results, and demonstrated the dependence of the response on the direction of motion of the absorber relative to the neutron detector.

The two-dimensional Green's function technique was used by Hennessy [17] to model the reactor response to a moving absorber. Borland's apparatus was used to check the experimental model. The results obtained showed the long range global and the short range local components and their interaction.

Sankoorikal [10] constructed an experimental apparatus consisting of a vibrating neutron absorber which could be located in a modified fuel assembly. His design was such that it was possible to have the absorber move in one of two perpendicular planes and measurements could be carried out with the thimble in which the absorber moved unflooded or flooded with water. He studied the local to global ratio, which he found to be an indicator of the distance of the vibrating absorber from the detector. He concluded that the detector response depends on its location as well as its relative orientation with respect to the direction of motion of the absorber.

III. REACTOR RESPONSE TO A VIBRATING ABSORBER

In this chapter, the response to a moving absorber is developed using the detector adjoint function. The analysis includes one- and two- dimensional analytic models.

A. One-Dimensional Model

Written in operator notation, the two-energy group, one-dimensional diffusion equation is [13, 15, 18]

$$L(x,t)\Phi(x,t) = 0 \tag{3.1}$$

where L is a 2X2 neutron diffusion operator matrix and Φ is the flux vector. If it is assumed that only the thermal absorption cross section is perturbed by the vibration, the cross section and flux vector may then be stated as [18]

$$\Sigma_{a2}(t) = \Sigma_{a20} + \delta\Sigma_{a2}(t) \tag{3.2}$$

and

$$\Phi(x,t) = \Phi(x,0) + \Delta\Phi(x,t)$$

where Σ_{a20} and $\Phi(x,0)$ represent the steady state components of the cross section and flux vector and $\delta\Sigma_{a2}(t)$ and $\Delta\Phi(x,t)$ describe their time dependent components. The index 2 represents the thermal group. The perturbed variables are substituted into Equation (3.1); these equations are then linearized and converted to the frequency domain by applying the Fourier transform. This yields

$$L(x,\omega)\Delta\Phi(x,\omega) = S(x,\omega) \tag{3.3}$$

where $\Delta\Phi$ is the complex frequency dependent flux perturbation vector, and S describes the frequency dependent cross section perturbation and is given by the product of $\Delta\Sigma_{a2}(x,\omega)$ and the steady state thermal flux Φ_{20}. Equation (3.3) has complex coefficients and can be solved for the real and imaginary components of $\Delta\Phi(x,\omega)$ [15, 18].

The adjoint function technique [12] is used to solve Equation (3.3). This gives

$$L^{+}(x,\omega)\Psi^{+}(x,\omega) = \Sigma_{d}(x,\omega) \tag{3.4}$$

where L^{+} is the complex 2X2 adjoint operator, Ψ^{+} is the complex adjoint flux vector, and Σ_{d} is the cross section vector (considered real) for a thermal detector of magnitude Q located at $x=x_{0}$. Thus,

$$\Sigma_{d}(x,\omega) = \begin{bmatrix} 0 \\ Q\delta(x-x_{o}) \end{bmatrix}. \tag{3.5}$$

Next, the inner product of Equations (3.3) and (3.4) with Ψ^{+} and $\Delta\Phi$, respectively, are calculated. From the definition of the adjoint function [19], it can be shown the left-hand sides of the two inner product equations are equal. Thus, the right-hand sides may be equated and, using an integral representation of the inner products [20], written as

$$\int_{x} \Delta\Phi(x,\omega)^{T}\Sigma_{d}(x,\omega)dx = \int_{x} S(x,\omega)^{T}\Psi^{+}(x,\omega)dx. \tag{3.6}$$

Equation (3.5) is substitued into Equation (3.6), which is solved for the perturbed thermal flux, yielding

$$\Delta\Phi_2(x_0,\omega) = (1/Q)\int_x \Delta\Sigma_{a2}(\omega)\Phi_2(x)\Psi_2^+(x,x_0,\omega)dx. \tag{3.7}$$

Equation (3.7) describes the response of a thermal detector located at $x=x_0$ to a thermal absorption perturbation at point x in the reactor.

In a one-dimensional analysis, the vibrating absorber may be described as a thermal neutron absorbing plate located at x_p, vibrating with an amplitude of $\pm\varepsilon$, and having an absorption strength of γ. Thus,

$$\delta\Sigma_{a2}(t) = \gamma\{\delta[x-x_p-\varepsilon(t)]-\delta(x-x_p)\}. \tag{3.8}$$

Equation (3.8) is substituted into Equation (3.7) and then the space integral is carried out which yields

$$\Delta\Phi_2(x_0,\omega) = (\gamma/Q)[\Phi_2(x_p)\partial\Psi_2(x,x_0,\omega)/\partial x|_{x=x_p\pm 0}$$

$$+\Psi_2^+(x_p,x_0,\omega)\partial\Phi_2(x)/\partial x|_{x=x_p}]\varepsilon(\omega). \tag{3.9}$$

Equation (3.9) describes the two basic components that comprise the detector response. The first component depends upon the static thermal flux and the gradient of the thermal adjoint function; it describes the response due to the movement of the local flux depression around the absorber and, consequently, it is called the "local" effect. The second term is dependent upon the thermal adjoint function and the thermal flux gradient; it describes the reactivity effect generated by

the absorber moving through a flux gradient. Since this effect is slowly varying in space, it is called the "global" effect. These two effects can add, or subtract, depending upon the signs of the gradient terms in Equation (3.9).

B. Two-Dimensional Model

For an absorber of strength γ located at $x=x_p$, $y=y_p$, and vibrating so that the vibration amplitude may be described by [14]

$$\varepsilon(x) = \varepsilon_x(t) + \varepsilon_y(t),$$

the response of a detector located at $x=x_0$, $y=y_0$, and with magnitude Q is [15]

$$\Delta\Phi_2(x_0,y_0,\omega) =$$

$$(\gamma/(QM^2\Sigma_{a2}))\{[\Phi_2(x_p,y_p,\omega)\partial G_2(x_p,y_p,x_0,y_0,\omega)/\partial x_p$$

$$+G_2(x_p,y_p,x_0,y_0,\omega)\partial\Phi_2(x_p,y_p,\omega)/\partial x_p]\varepsilon_x(\omega)$$

$$+[\Phi_2(x_p,y_p,\omega)\partial G_2(x_p,y_p,x_0,y_0,\omega)/\partial y_p$$

$$+G_2(x_p,y_p,x_0,y_0,\omega)\partial\Phi_2(x_p,y_p,\omega)/\partial y_p]\varepsilon_y(\omega)\} \qquad (3.10)$$

where M^2 is the thermal migration area and G_2 refers to the two-dimensional Green's function solution to the original differential equation.

As in the case of the one-dimensional model, the detector adjoint funtion $\Psi^+(x,\omega)$ and the adjoint operator $L^+(x,\omega)$ are both complex, while the detector cross-section $\Sigma_d(x)$, from a practical point of view, is real and frequency independent. Therefore, the adjoint Equation (3.4) can be written in the following form:

$$(L_R^+(x,\omega)+jL_I^+(x,\omega))(\Psi_R(x,\omega)+j\Psi_I(x,\omega)) = \Sigma_d(x) \tag{3.11}$$

where

$$L^+(x,\omega) = L_R^+(x,\omega) + jL_I^+(x,\omega)$$

$$\Psi(x,\omega) = \Psi_R(x,\omega)+j\Psi_I(x,\omega)$$

The real and imaginary parts of Equation (3.11) can be written separately as

$$L_R^+\Psi_R - L_I^+\Psi_I = \Sigma_d \tag{3.12a}$$

$$L_R^+\Psi_I + L_I^+\Psi_R = 0. \tag{3.12b}$$

The subscripts (x,ω) have been dropped for simplicity. Assuming that Ψ_R^+ is the main variable in (3.12a) and Ψ_I^+ is the main variable in (3.12b), then $L_I^+\Psi_I$ can be thought of as an "up scatter" term from (3.12a) to (3.12b) and $L_I^+\Psi_R$ is a "down scatter" term in these coupled equations. For a two-group calculation, the matrix Equations (3.12a) and (3.12b) will form four-"group" equations in the variables Ψ_{1R}, Ψ_{2R}, Ψ_{1I}, Ψ_{2I} and each of these equations will contain a coupling term

representing an "up scatter" or "down scatter" or both. To solve such equations using existing static codes, a code should be selected that can handle up and down scatter terms for four "energy" groups.

If the calculation is restricted to the plateau region of the global response, where $\lambda << \omega << \beta/\ell$, then $L_I \simeq 0$. This will reduce the equations to

$$L_R^+ \Psi_R = \Sigma_d$$

$$L_R^+ \Psi_I = 0.$$

In this form, the correspondence between Ψ_R^+ and Ψ_I^+ has been lost due to the missing coupling term.

As theoretical Equation (3.10) predicts and experimental results confirm, the detector response is a function of the directions of motion of the vibrator through the ε_x and ε_y functions. During the experiment performed in this study, the x(t) and y(t) components of the vibration amplitude change due to the rotation of the vibrator assembly, and the responses of the neutron detectors change accordingly. Experimental results are presented in section V of this thesis which support these observations.

IV. EXPERIMENTAL EQUIPMENT AND PROCEDURES

In this chapter, the equipment and computer software used in the study are discussed. Included are (A) the vibrator system, (B) the stepping motor, (C) stepping motor control system, (D) the software programs, and (E) experimental procedures.

A. The Vibrator System

The experimental apparatus used in this research is basically the same as the one used by Sankoorikal [10]. The modifications to the apparatus, and the experiment plan, including the safety analsis report, are explained in [21].

The vibrating absorber consists of a cadmium strip (2.54 cm by 0.63 cm by 0.16 cm typical) secured in a slot at the end of an aluminum rod (66.04 cm by 0.63 cm dia., see Figure 1). The other end of the aluminum rod is attached to an aluminum block (5, Figure 1) mounted on a horizontal pin. Power applied alternately to two 24v DC push-type coils, placed above the aluminum block, causes the armatures in the coils to push the aluminum block alternately down and up. This results in a vibrating motion of the aluminum rod and the cadmium absorber. An aluminum rod (10.16 cm by 0.32 cm dia., see Figure 1) attached to the aluminum block connects it to the core of a linear variable differential transformer (LVDT), which measures the vibrator position (the signal from LVDT decreases as its core goes into LVDT). The coils, LVDT and the pivoting aluminum block are mounted on an aluminum structure (Figure 1). This structure sits inside an aluminum

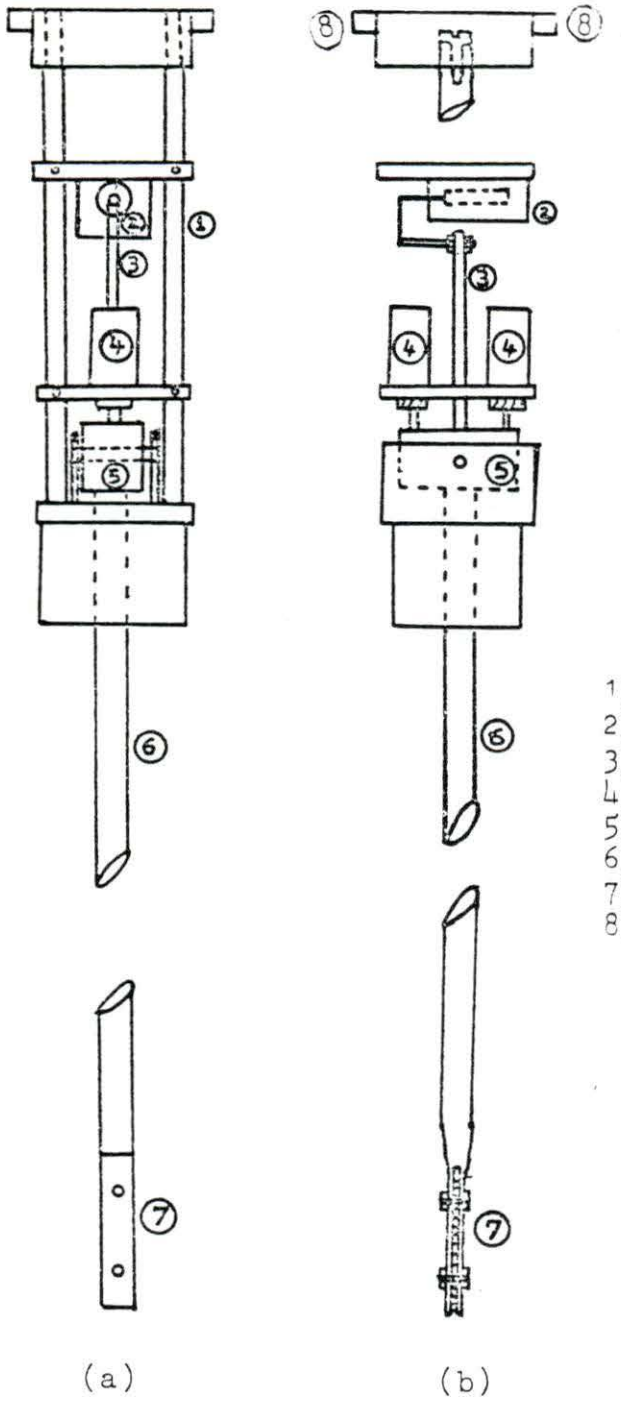

1) Aluminum structure
2) LVDT
3) LVDT connecting rod
4) Coils
5) Aluminum block
6) Aluminum rod
7) Cadmium (absorber)
8) Positioning hangers

FIGURE 1. Front and side views of the vibrator assembly

enclosure (Figures 2 and 3) made of two different diameter tubes, the top one 20.32 cm long by 3.81 cm OD and the bottom one 71.12 cm long by 2.14 cm OD. A fuel element was reassembled leaving the third fuel plate out resulting in a gap of width 2.23 cm between the second and fourth fuel plates. The 2.14 cm OD tube containing the vibrator was located in this space (Figures 4 and 5). Note that this tube extends below the mid elevation of the fuel element. A plastic screw at the bottom of the small tube can be tightened to make the tube water tight for "dry" operation or opened slightly to fill the tube with water. The coil arrangement (Figure 6) was well above (about 10.16 cm) the water level in the core tank during normal operation. The mounting plate rests on two separator plates in the core (Figure 4). The normal position of the neutron absorber is at the mid elevation of the fuel element. The aluminum vibrator structure (Figure 1) (without positioning hangers on the top side) can be rotated by increments of 1.8 degrees in the range of 0 to 180 degrees resulting in 100 possible planes of vibrations. The maximum displacement of the absorber from the neutral position is approximately 0.95 cm.

An aluminum tube (101.60 cm by 2.14 cm OD) with a water tight plastic screw at the bottom end, filled with Plexiglass "donuts" holds a (5.08 cm by 1.59 cm dia.) BF-3 detector (N. Wood model G-5-3, 60 cm of Hg gas pressure). This tube is also located between the second and fourth fuel plates (Figures 4 and 5) of the fuel element (this detector is located about 3.80 cm from the absorber). The BF-3 detector was

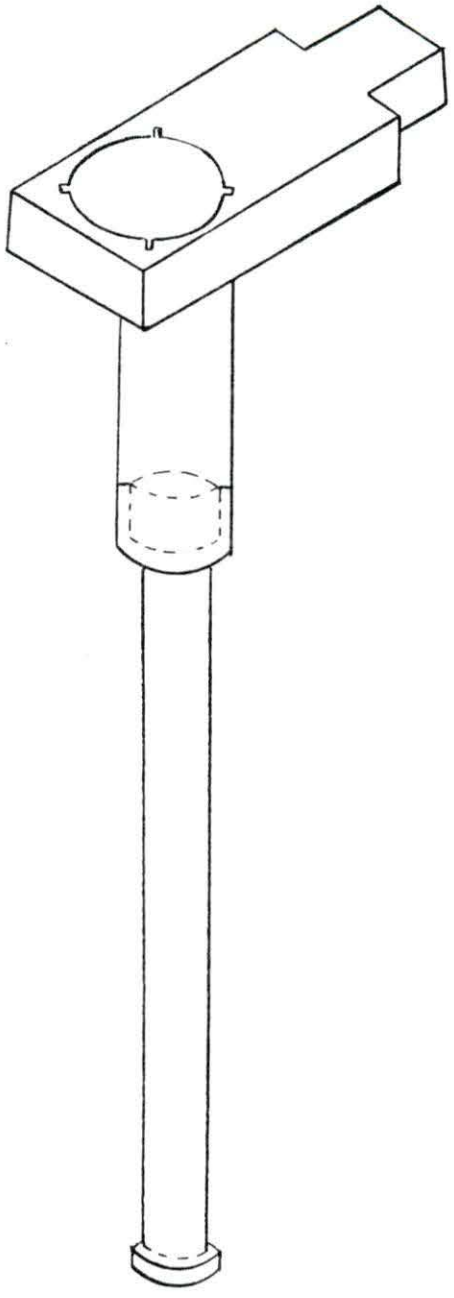

FIGURE 2. Vibrator thimble

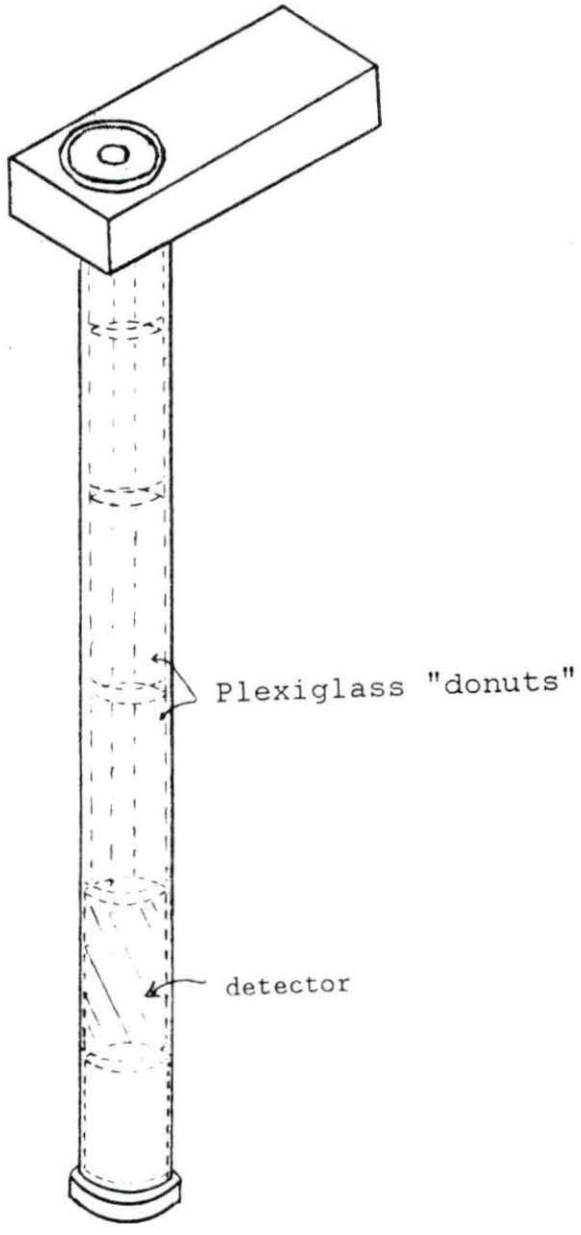

FIGURE 3. Detector cover

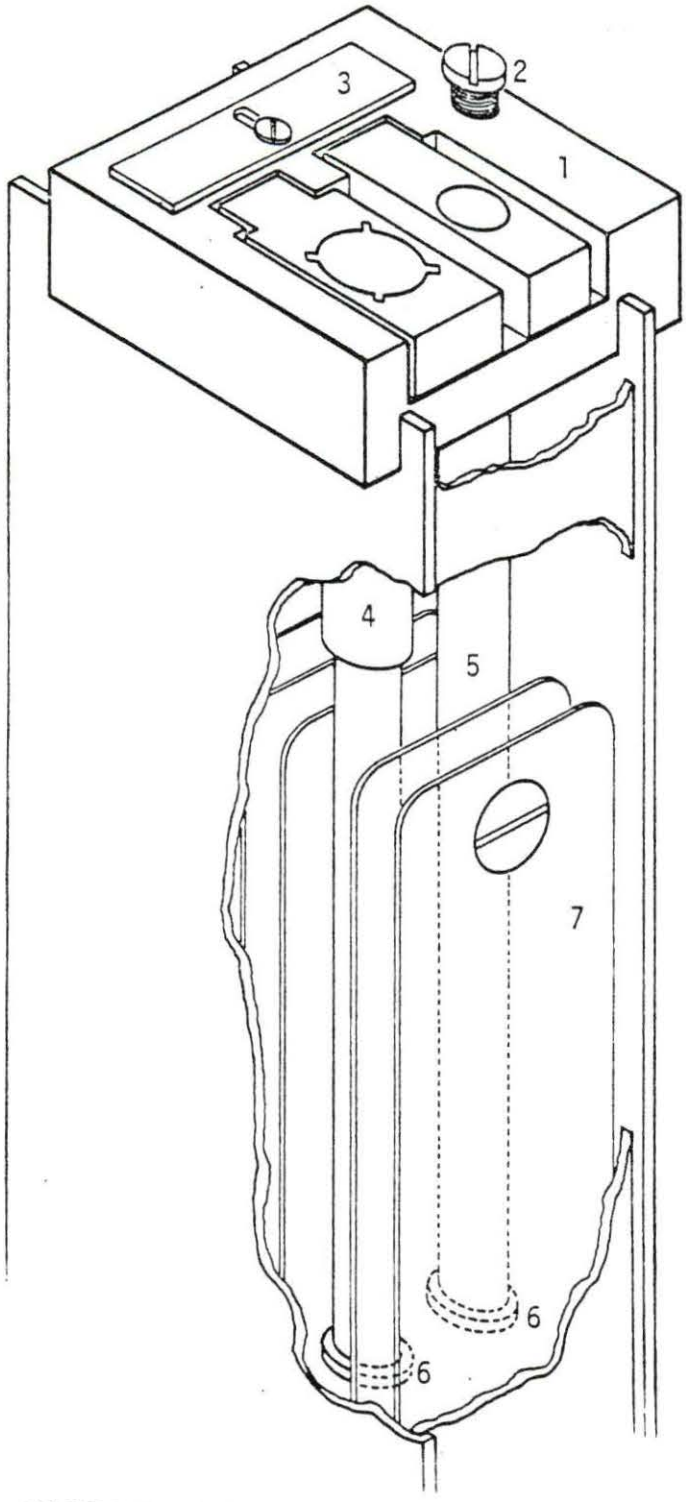

1. Mounting plate
2. Teflon screw
3. Tightening plate
4. Vibrator thimble
5. Detector thimble
6. Plastic screw
7. Fuel element

FIGURE 4. The vibrator assembly-core tank configuration

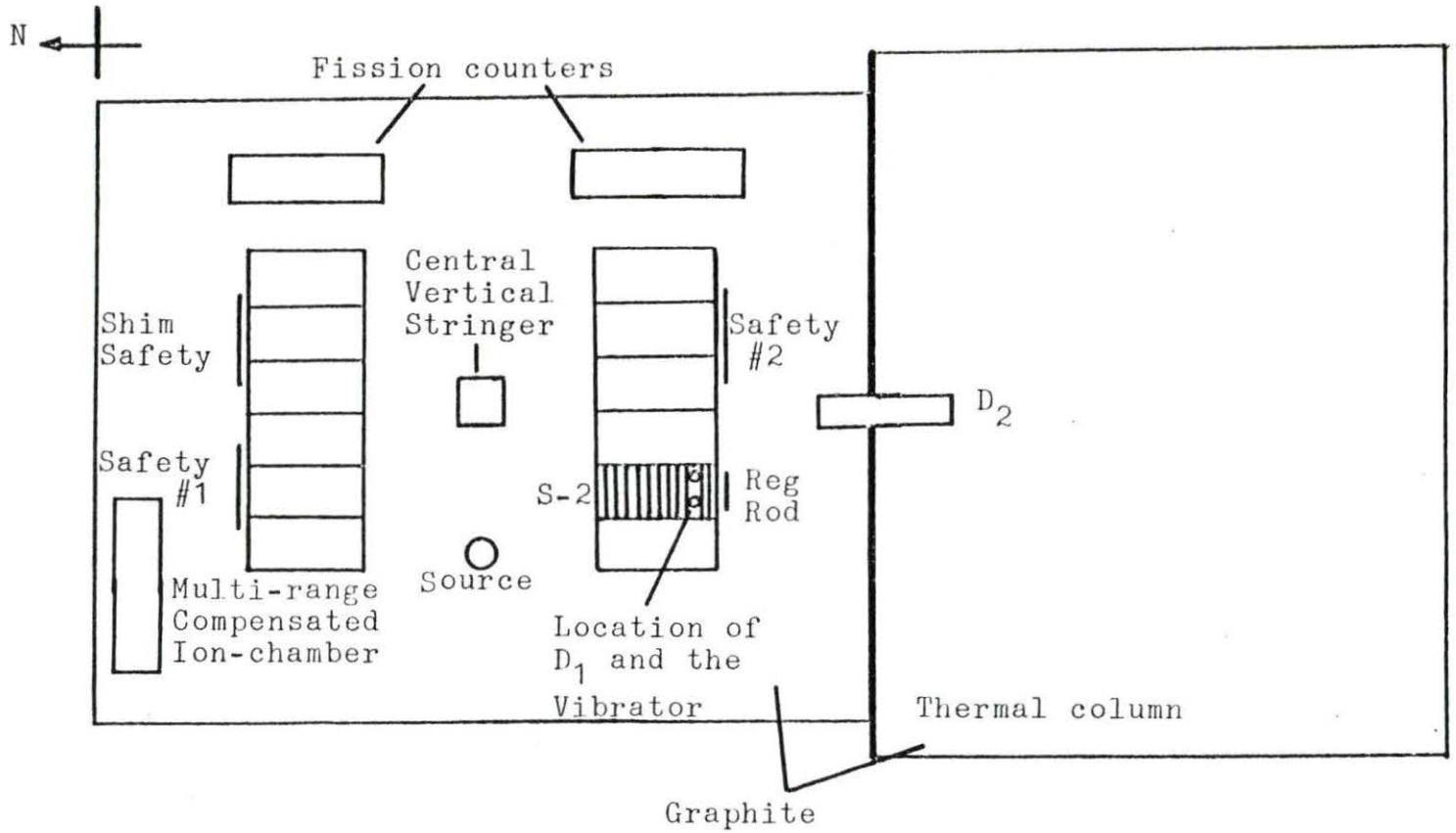

FIGURE 5. Plan view of the UTR-10 reactor

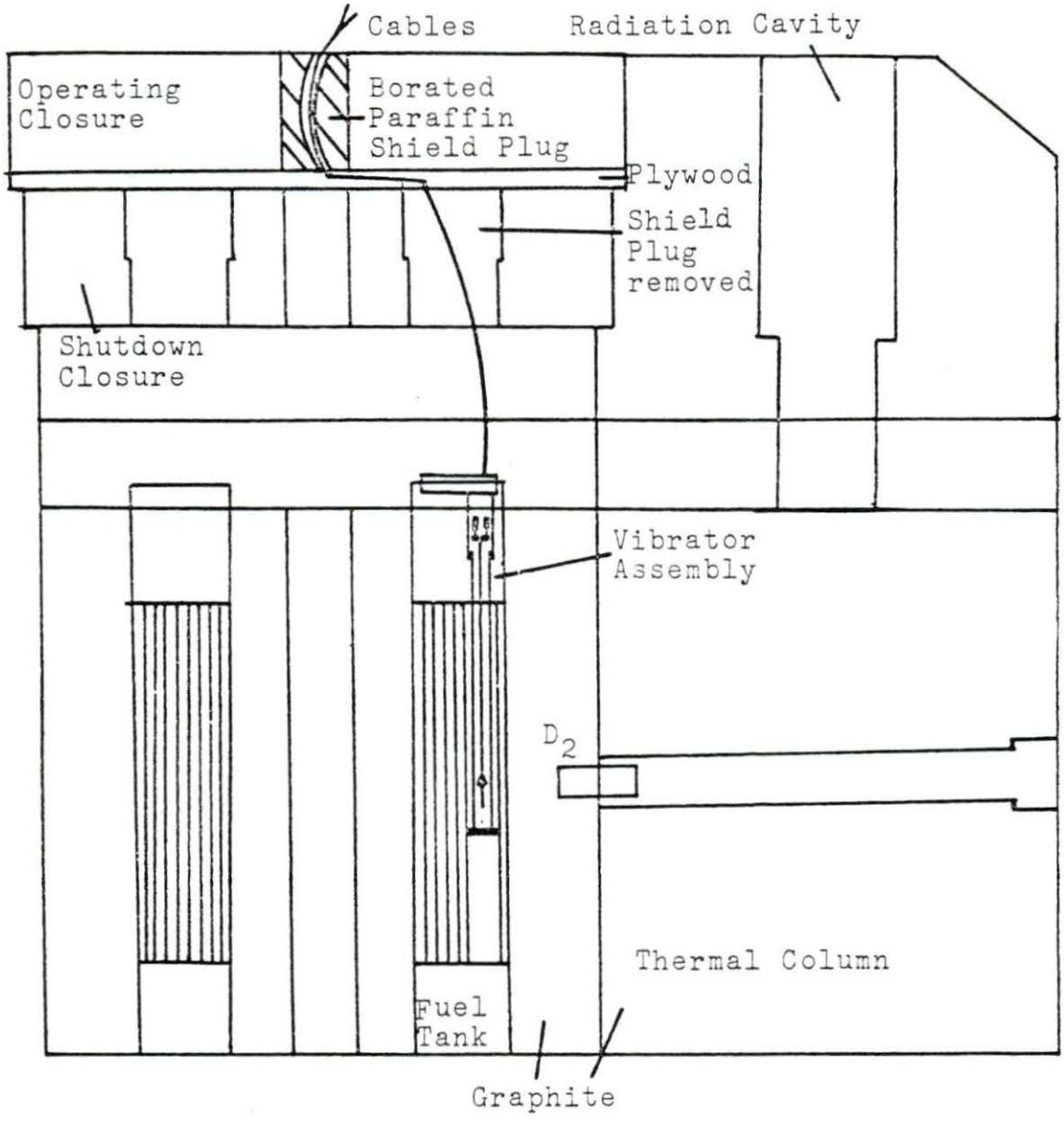

FIGURE 6. Elevation of the UTR-10 reactor

operated as an ion-chamber. The detector and vibrator enclosures are held securely in position by two aluminum screws and also by tightening the new elliptical shaped aluminum block (Figure 7) which can slide on the mounting aluminum plate. The mounting plate is held in position by the aluminum "fingers" extending down from it and can be secured by tightening a Teflon screw (see Figures 4 and 5).

The following paragraphs refer to Figures 7 and 8 and Table 1.

The DC-stepping motor (13) is held on the aluminum motor adapter (1) by three nylon screws (16), (18). One of these screws (18) plus one additional screw (17) are used to attach the aluminum motor adapter (1) to the vibrator enclosure. A larger screw (19), passing through an aluminum washer (20), is also used to adjust the horizontal motion of the aluminum motor adapter (1) on the aluminum mounting plate (2). The vibrator disc (5) of the rotatable vibrator structure is connected to the aluminum motor adapter (1) by an aluminum tube (7), an aluminum round cylinder (11), a nylon set screw (14) and a spur gear (4). By means of three equal radius spur gears (10), the torque of the motor is transferred to the vibrator assembly (Figure 1).

A thin aluminum disc (9), with two slits on the diameter is located on the shaft of the motor. This is used to monitor the position of the vibrator by the opto-electronic (12) instrument mounted (8) with two nylon screws (15) to the aluminum motor adapter (1).

FIGURE 7. Motor adapter assembly section, full scale

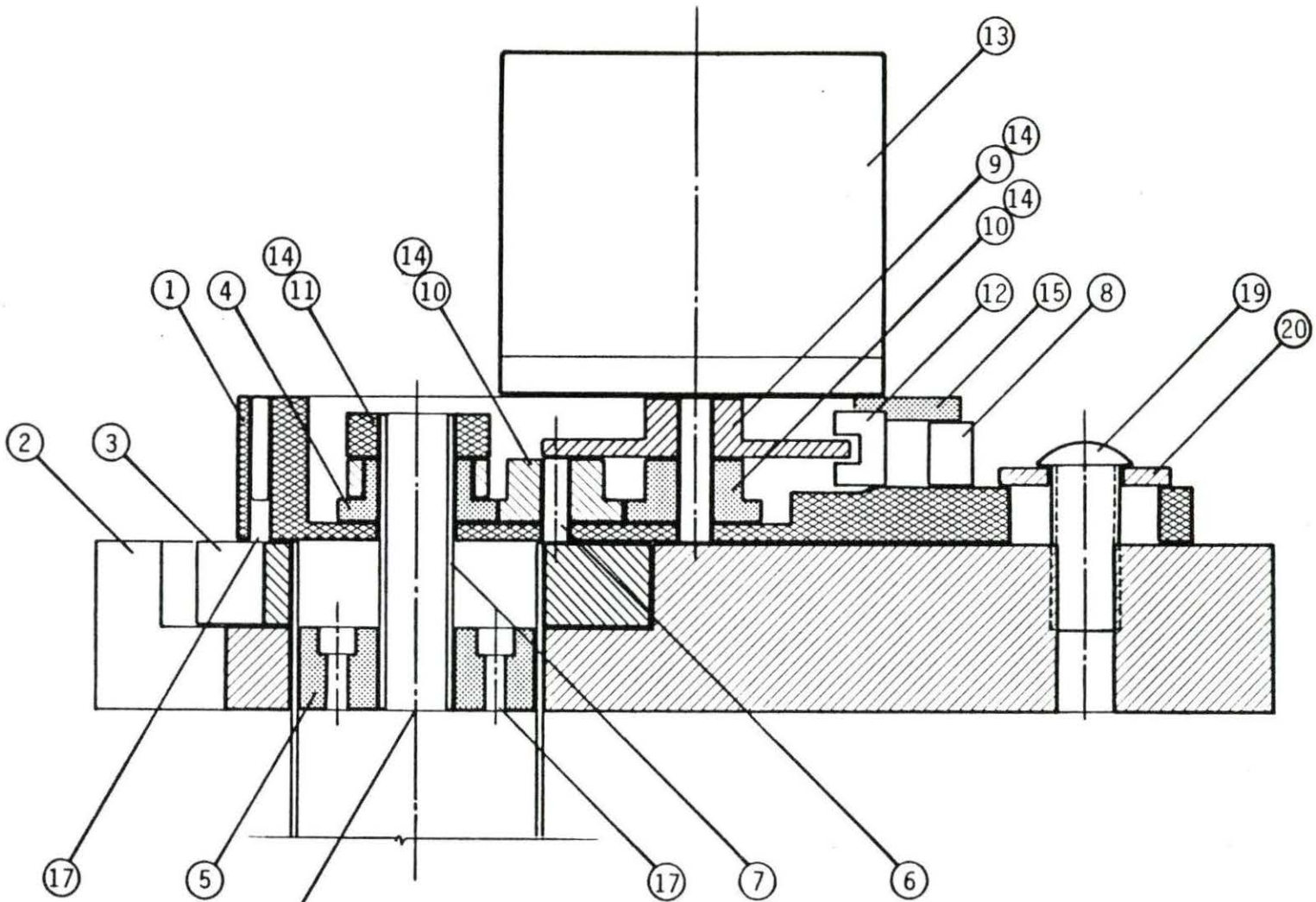
13
14
9
14
10
14
14
11
14
10
1
4
12
15
8
19
20
2
3
17
5
17
7
6
DRILL & REAM
.953(.375) .955(.376)
ADD SET SCREW ON O.D.

FIGURE 8. Top view of the motor adapter assembly, full scale

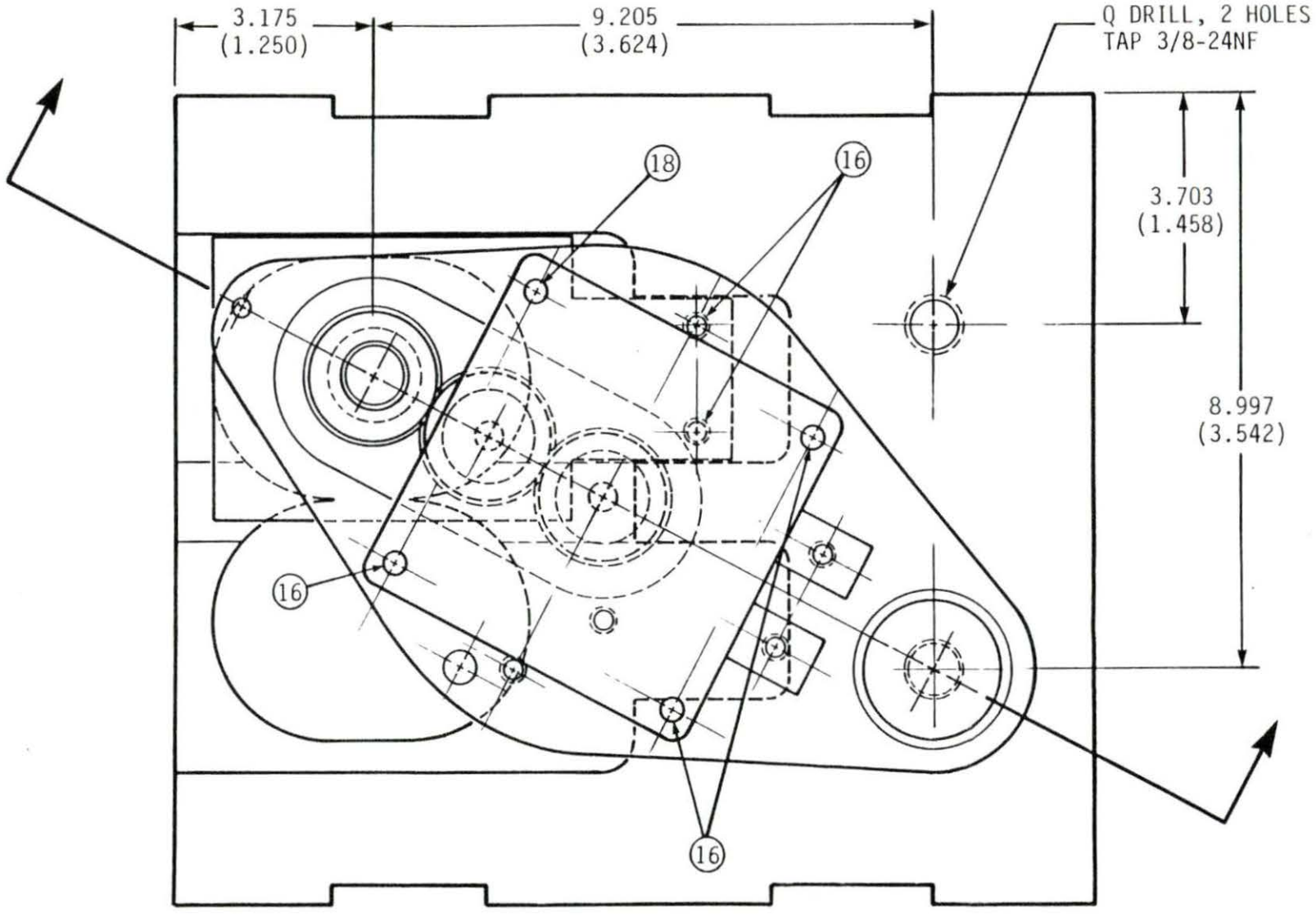
3.175
(1.250)
9.205
(3.624)
Q DRILL, 2 HOLES
TAP 3/8-24NF
3.703
(1.458)
8.997
(3.542)
18
16
16
16

TABLE 1. Bill of materials for the added parts

No.	Qty.	Names	Dimensions[1]
1	1	Motor Adapter	Alum. Flat 1X3.5X5.75 Long
2	1	Main Block	Existing
3	1	Shield Block	Existing
4	1	Spur Gear	See Detail Delrin
5	1	Vibrator Disc	Existing (must be modified)
6	1	Delrin Round	3/16 Dia.X1/3 Long
7	1	Alum. Tubing	3/8 O.D.X0.070 WallX1.5 Long
8	1	Delrin	0.5X0.5X1 Long
9	1	Delrin Round	1.75 Dia.X5/16 Long
10	2	Spur Gear Delrin	0.875 P.D.X3/16 Bore (42 teeth)
11	1	Aluminum Round	7/8 Dia.X0.5 Long
12	1	Electric Eye	Existing
13	1	Stepping Motor	Existing
14	4	Nylon Set Scr.	6-32X1/4 Long
15	2	Nylon Screw	10-32X1/2 Long Round Head
16	5	Nylon Screw	10-32X3/4 Long
17	1	Nylon Screw	10-32X1.25 Long
18	1	Nylon Screw	10-32X1.5 Long
19	1	Nylon Screw	3/8-24NFX1 Long
20	1	Alum. Washer	1 O.D.X3/8 P.D.X1/8 Thick

[1]All dimensions in inches.

The purpose of the DC-stepping motor is to rotate the vibrating structure to any angle between 0 and 180 degrees. Special control circuits (section-C) and software (section-D) were developed to control the stepping motor with an HP-85 computer.

The purpose of the opto-electronic device is to provide a fine reference point of the vibrator assembly angular position inside the reactor for the operator of the experiment. This electronic device sends signals to the stepping motor driver to light a reference light when one of the slits passes through the opto-electronic device. Note that the detector and vibrator positions can be interchanged by removing

the apparatus from the reactor and exchanging them. This is done by rotating the elliptical shaped aluminum block by about 60 degrees.

The cables to the detector, the coils, the DC-stepping motor, the electronic eye and the LVDT are taken out by removing the shutdown closure plug above the fuel element. Plywood strips (2.50 cm thick) were used to raise the operating closure so that the cables could be brought out to the operating closure plug (Figure 6). The cables pass through a special shield plug, with curved conduit, which is located in the operating closure. The cables to the coils and the LVDT are passed through the aluminum tube (7).

B. Stepping Motor

A SLO-SYN Stepping Motor (Superior Electric, M061-FC027) is a permanent magnet motor that converts electronic signals into mechanical motion. Each time the direction of the current in the motor windings is changed, the motor output shaft rotates a specific angular distance. The motor shaft can be driven in either direction.

These stepping motors have permanent magnet rotors and eight-pole stators. They have no brushes, ratchets or detents and use shielded ball bearings to insure maximum reliability and long life. The motors are totally enclosed, but are not sealed against direct splash of water, oil or other liquids. When the operating environment includes direct splash of water, oil, cutting fluids, etc., the motor should be protected from such exposure.

These motors have Class B (130 degree celsius) winding insulation and may be operated at ambient temperatures from -40 to +40 degree celsius. The continuous duty temperature rise is 65 degree celsius. They operate on phase-switch dc power. The motor shaft advances 200 steps per revolution (1.8 degrees per step) when a four-step input sequence (full-step mode) is used. Power transistors connected to flip-flops or other logic devices are normally used for switching as shown in the wiring diagram, Figure 9. The four-step input sequence is also given in Table 2. Since current is maintained on the motor windings when the motor is not being stepped, a high holding torque results.

During use, it was found that the stepping motor would occasionally turn in the wrong direction. The reason for this is due to the following problem which was not known during the actual experiment.

As the manufacturer of the DC-stepping motor points out, transient voltages are generated as current is switched through the windings during stepping. These voltages can cause faulty operation (in rotation) and damage to the motor or drive components unless a means of limiting or removing them is provided. The most common method for suppressing transient voltages uses shunting diodes as shown in the wiring diagram in Figure 10. The components which were used to correct the system were four (1N4007, 1000 Volts In Reverse, 1 Amp.) diodes (Figures 9, 10 and 11 components D). These modifications were done after the experiment.

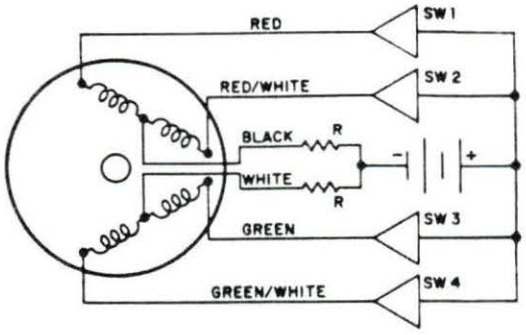

FIGURE 9. DC stepping circuit

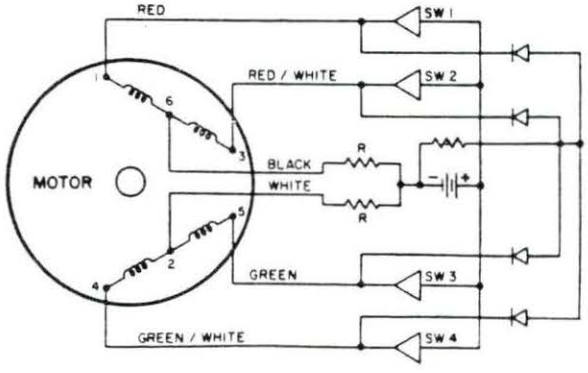

FIGURE 10. Typical transient voltage suppression circuit

C. Stepping Motor Control System

There are four windings in a stepping motor and a permanent magnet in the center, therefore, each winding should be energized and produce positive and negative polarities which can repel and/or attract the permanent magnet inside the structure of the motor and cause the permanent magnet to rotate 90 degrees around its center line. This is the internal shaft of the motor which drives gearing inside the motor structure making the output shaft of the motor rotate only 1.8 degrees, while the permanent magnet turns 90 degrees.

To design the control system for such a motor (see Figures 11, 12, and 13), there was a need for a solid state logic circuit to make it possible to control the motor with the HP-85 computer and the HP-3497 data acquisition system, or manually using the internal clock source, 555 timer integrated circuit. The speed of the motor also can be changed by adjusting the potentiometer nob on the stepping motor driver device when the system is in manual mode. Since there are four windings that make the motor turn, there should be at least four power transistor switches which can turn the power supply to these windings ON and OFF (see Table 2). The state diagram and logic design which would make the motor turn correctly were designed and are shown on Figures 11, 12, and 13.

TABLE 2. Four-step input sequence[1] (full-step mode)

STEP	SW1	SW2	SW3	SW4
1	ON	OFF	ON	OFF
2	ON	OFF	OFF	ON
3	OFF	ON	OFF	ON
4	OFF	ON	ON	OFF
1	ON	OFF	ON	OFF

[1]Provides CW rotation as viewed from nameplate end of motor. To reverse direction of motor rotation perform switching steps in the following order: 1, 4, 3, 2, 1.

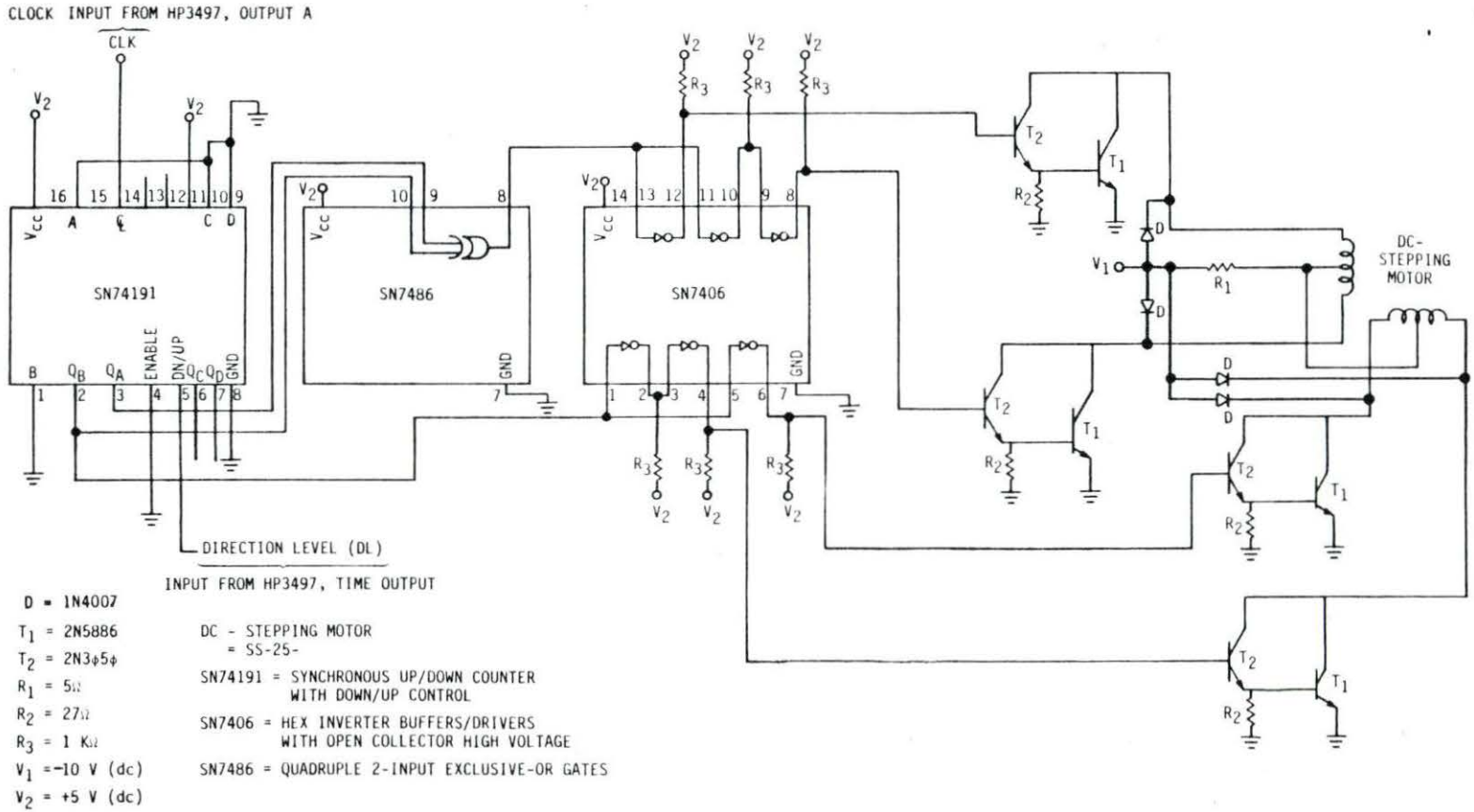

FIGURE 11. The sequencer circuit

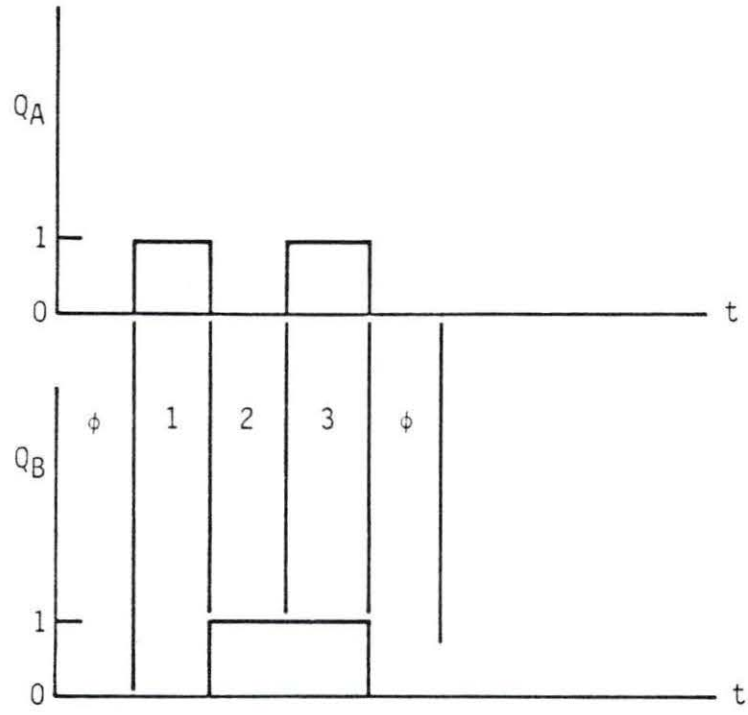

$A = \{0,3\}$
$B = \{0,1\}$

$$A = \bar{Q}_A \cdot \bar{Q}_B + Q_A \cdot Q_B = \overline{Q_A \oplus Q_B}$$
$$B = \bar{Q}_A \cdot \bar{Q}_B + Q_A \cdot \bar{Q}_B = \bar{Q}_B \underbrace{(\bar{Q}_A + Q_A)}_{1}$$
$$B = \bar{Q}_B$$

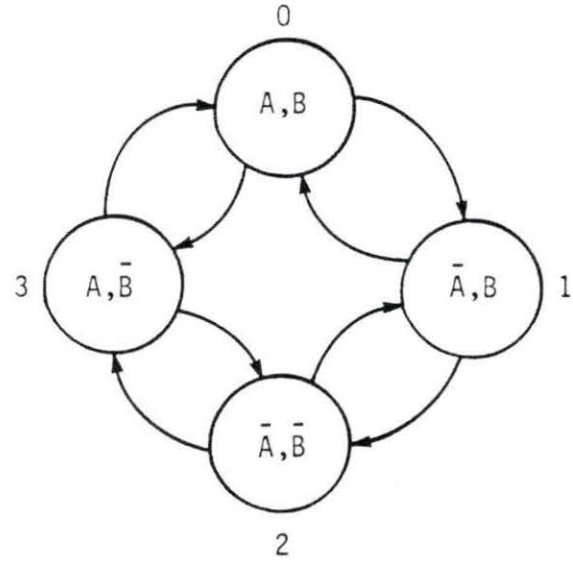

FIGURE 12. The state diagram of the sequencer

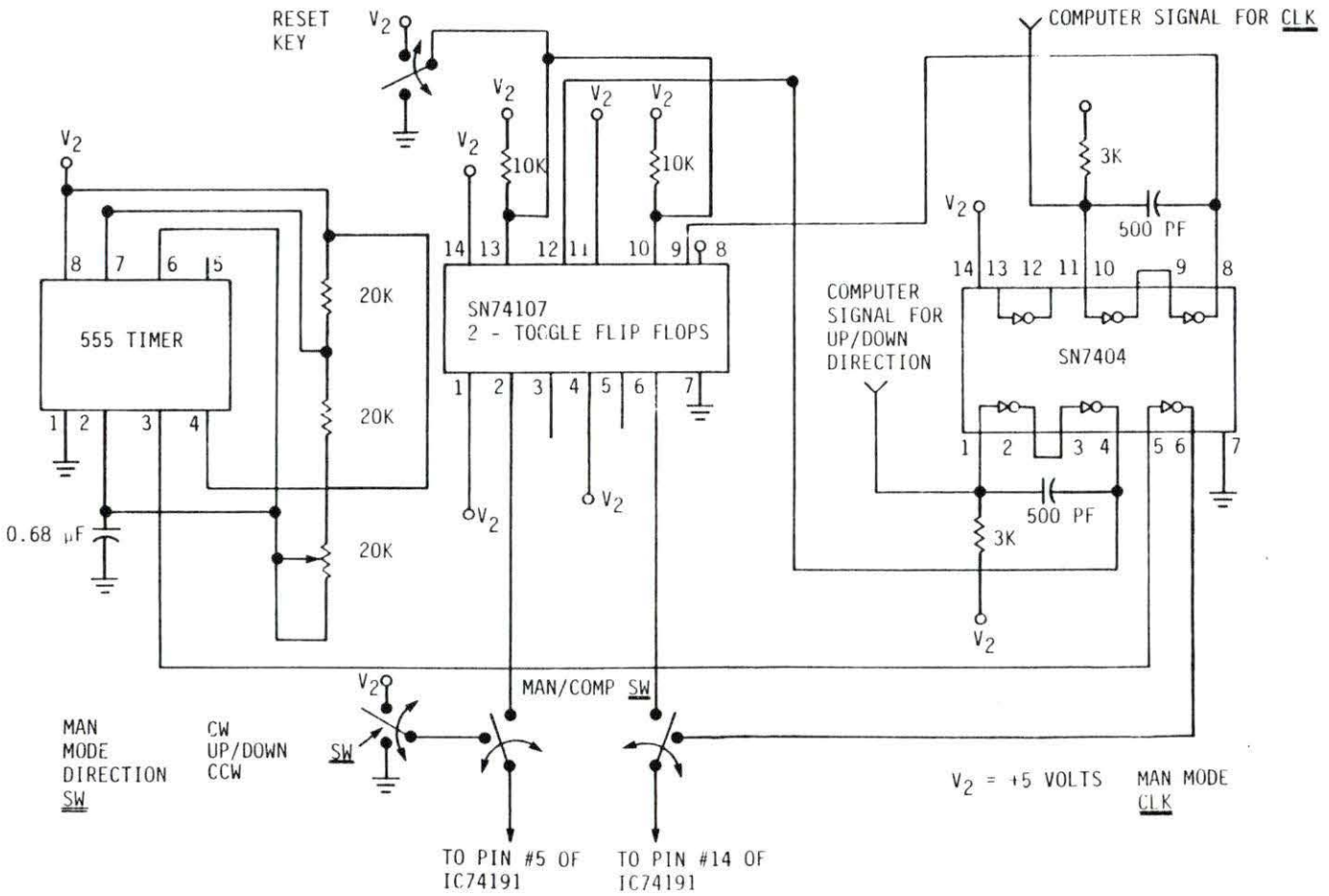

FIGURE 13. The conditioning and switching circuit

Figure 12 shows that each winding in the motor, which makes up the four states, is labelled from 0 to 3 and at each moment two of these windings (labelled A and B) should be energized, Table 2. In order to go through these states continuously, a solid state counter like a SN74191 (see Figure 11) was used to count from 0 to 3, binary wise (AB: 00, 01, 10, 11), continuously.

The SN74191 counter was chosen since it has the feature of up/down control. Using that, one can control the direction of rotation of the stepping motor. The signals from the HP-3497 data acquisition system are used for the clock and the directional control of the stepping motor while the DC-stepping motor device is in the computer mode. The HP-3497 has two software controllable outputs; one is the TIME OUTPUT which was used for direction level control and the other is OUTPUT A of the data acqusition frequency counter which was used for the clock sequence. Due to circuit constraints and the shape of the output signals from the HP-3497, the signals had to be passed through the filtering and delay circuits using invertors, capacitors and resistors as shown in Figure 13. In the same figure, one can see the locations of the manual switches which were used to change the modes of the DC-stepping motor driver device for computer mode, manual mode, and direction modes when the device is in the manual mode. The reset button or key is used to clear the SN74107 flip flops for initialization of the system when the system is in computer mode. This key is also used to block the signals from going through the motor and therefore, stopping the motor in an

emergency situation such as a mulfunction in the system where the motor tends to keep turning.

D. Software Programs

The software program "AUTOMATION", which was designed to run the motor automatically in the computer mode, is shown in Appendix A. This software program was designed based on the characteristics of the HP-85 computer, the HP-82902M storage system, the HP-3497 data acquisition system, the HP-3582A spectrum analyzer and the DC-stepping motor driver device. Using this program one can gather the following vibration measurement data using the HP-3582A spectrum analyzer: (1) the square root of the APSD of the input A, (2) the square root of the APSD of the input B, (3) the transfer function of input B with respect to input A, (4) the phase and (4) the coherence function. To aid in record keeping, these data were labelled using the designations A, B, M, P, C. Data were stored on disc using the HP-82902M disc drive. An indexing notation was developed using a number between 1 and 11 with each data set label, to indicate the angular position of the vibrator apparatus. The angles from 0 to 180 degrees were divided into steps of 18 degrees. The vibrator apparatus was turned from 0 to 180 degrees, and then the program automatically makes the stepping motor rotate back to 0 degrees, or to the reference for the second run, when the two inputs to the spectrum analyzer (HP-3582A) are changed. In this case, the combination of the inputs (input A-input B) is as follows (1) LVDT-DET1, (2) LVDT-

DET2, and (3) DET1-DET2. Since the typical time for a single step of the stepping motor is about 2.5 msec., enough waiting time was allocated between necessary software instructions. The program "DATA READER" (Appendix B) was used to read and store the values of different data at a frequency of 1.52 Hz (the fundamental vibrator frequency), for different angular positions. This program also made the data more understandable and useful for the purposes of normalization and graphing of profiles of the vibrations in different angular positions. The program "NORMALIZER" (Appendix C) was used to normalize DET1, and DET2 data with respect to the LVDT and DET1 with respect to DET2. The program "PLOTTER" (Appendix D) was used to graph most of the data gathered.

For more information on the experimental appratus, the experiment plan [21] written for this research by the author may be referred to.

E. Experimental Procedures

An experimental plan, including the safety analysis report [21], was prepared for the experiment. This was appoved by the Reactor Use Committee, and the pre-experimental tests were performed as outlined in it.

The locations of the modified assembly, the experimental apparatus, the in-core detector DET1 (BF3 detector, located about 3.8 cm from the absorber) are shown in Figures 5 and 6. The detector high voltage of approximately 240 volts is supplied by batteries. The second

detector, DET2 (Figures 5 and 6), (compensated ion chamber (CIC), Westinghouse type 6377) was located in the position of the 19-inch stringer in the thermal column at a distance of about 35 cm from the vibrator. The high voltage and the compensating voltage used were 600 volts positive and 30 volts negative, respectively. As mentioned previously, the vibrator-detector positions could be interchanged (east or west). Measurements were taken with the detector DET1 on the east.

By flooding the vibrator thimble, it was possible to change the magnitude of the flux gradient in the region in which the vibrator was moving. Two cases, thimble flooded and thimble unflooded, were studied. Another way of changing the flux gradient is by altering the regulating rod positions. All measurements were obtained with the regulating rod at 99.5% and the shim-safety rod at 75.8% withdrawn.

A 1.52 Hz square wave was used for the vibrator excitation. As mentioned before, for each experimental situation, three channels of data, viz. LVDT, DET1 and DET2, were available. For different combinations of these three signals, five sets of data (the square root of the APSD for the two channels, the transfer function magnitude and phase, and the coherence between the two channels) were measured. Since the 1.52 Hz signal was strong and statistically invarient, 8 rms averages with the spectrum analyzer were used during data collection. The "Flat top" mode of the Pass Band Shape of the spectrum analyzer was used because of the trade-off criteria between the frequency and

amplitude resolution of the system. For all the runs, the reactor power was 200 W and the coolant inlet temperature was 80 degree Fahrenheit. The reactor was operated manually and the data were collected during the time the reactor power was not drifting. In the software program "AUTOMATION", enough waiting time (1-2 min.) was allocated (between instructions) for the operator of the reactor to make any required control rod position changes to stablize the power while data was not being collected. The sensitivity of the analyzer was adjusted to the maximum without overloading. The analyzer and filter were zeroed before data collection to reduce the DC component that appears at the analyzer input.

As shown in Figure 14 and Table 3, the current output from the detector DET1 is fed into a DC-coupled preamplifier (Ames Laboratory) which converts the detector current to an output voltage. The phase between the input and the output signal is almost zero. The detector DET2 current was measured using a high-speed picoammeter (Keithley model 417) which was capable of giving an output voltage between zero and minus three volts for a meter deflection of zero to full scale on any range. This introduces a phase shift of 180 degree between the input and the output of the picoammeter.

At any time, two out of three channels of available data were passed through two identical band-pass filters and then to the spectrum analyzer. Each band-pass filter was formed using a low-pass filter (Burr-Brown model UAF11) with cut-off at about 15 Hz and a high-pass

filter (Krohn-Hite model 3321) with a cut off at 0.1 Hz. Since each filter has a time constant, and the output of the filter is meaningless for a time equivalent to several time constants, enough waiting time (1-2 min.) was allocated between the instructions in the software program "AUTOMATION", so that the data stored were meaningful.

For more information on the data acqusition and analysis system, the reader may refer to Sankoorikal's thesis [10].

Note that an exact way of obtaining the "physical" 0 degree position of the plane of vibrator motion relative to the detector was not available and that a small variation in angular placement position resulted in a significant rotation (36 degrees) of the direction of motion from physical 0 degree, Figure 15. Since for each set of inputs to the spectrum analyzer, the experiment had to be started from the 0 degrees, there were six rotational cases from 0 to 180 degrees (Figure 15). Referring to this figure, one can see the rotation direction of the stepping motor as inferred from the data obtained from available inputs to the spectrum analyzer. It was found that for data sets 1-4, the vibrator rotated CCW, and for data sets 5 and 6 it rotated CW.

Figure 16 shows the assumed and experimentally obtained signal characteristics of the input and output signals based on the data obtained (Figures 17-48,chapter V).

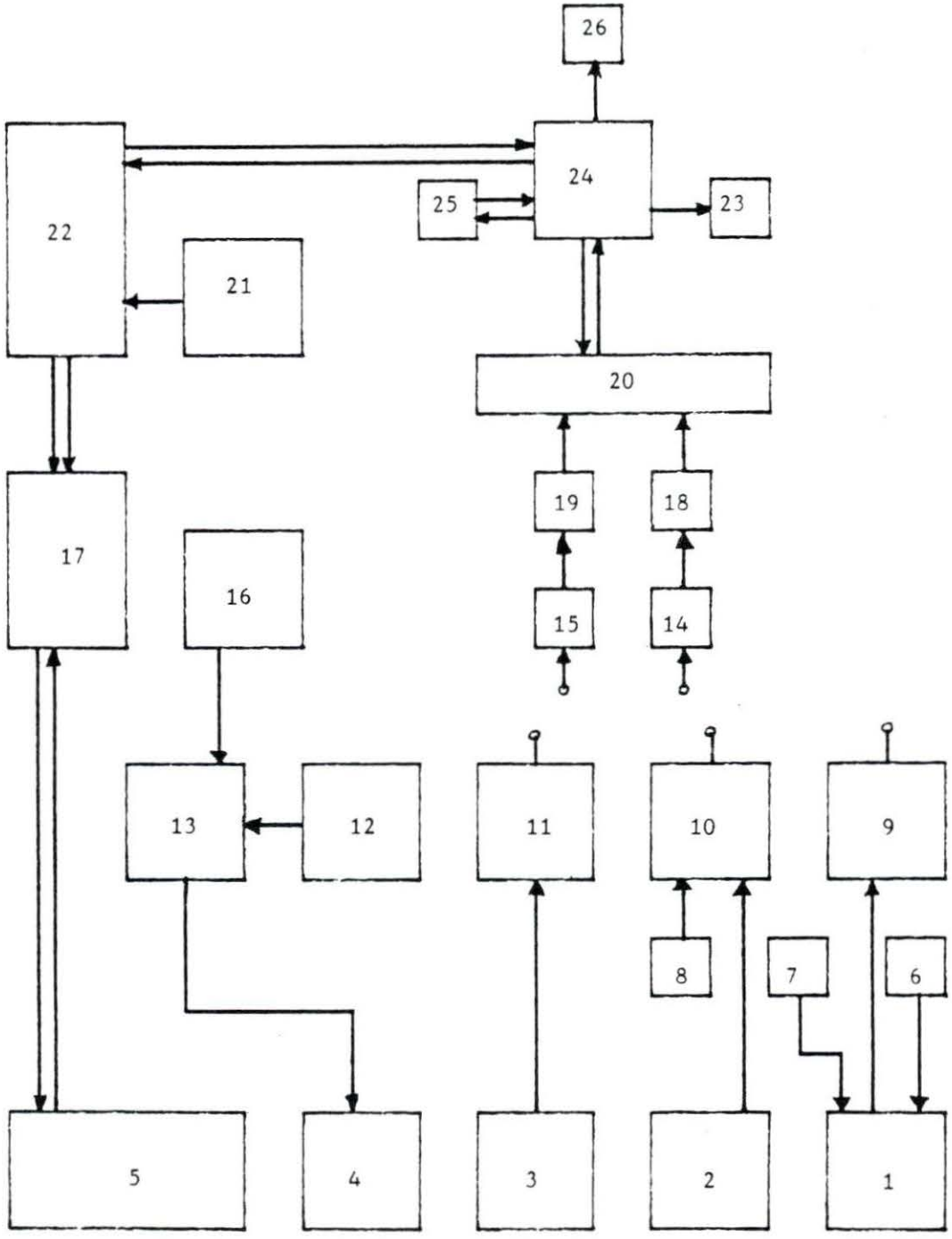

FIGURE 14. The automated data acquisition and analysis system

TABLE 3. Component numbers and their descriptions for Figure 14

No.	Descriptions
1	Detector2 (CIC), DET2
2	Detector1 (BF3), DET1
3	LVDT
4	Two 24 volt DC push-type Coils
5	DC-Stepping Motor and Electronic Eye
6	Compensating voltage (-30 volts)
7	High voltage (600 volts)
8	High voltage (240 volts)
9	Picoammeter
10	Preamplifier
11	LPM210 Signal Conditioner
12	Square Wave Generator (1.52 Hz, clock)
13	Coil Switching Unit
14	High pass filter (0.1 Hz)
15	High pass filter (0.1 Hz)
16	24-volt DC Power Supply
17	DC-Stepping Motor Driver System
18	Low pass filter (15 Hz)
19	Low pass filter (15 Hz)
20	Frequency Spectrum Analyzer
21	Square Wave Generator (400 Hz, clock)
22	HP-3497 Data Acquisition System
23	HP-Plotter
24	HP-85 Computer
25	HP-Disc Storage
26	HP-Printer

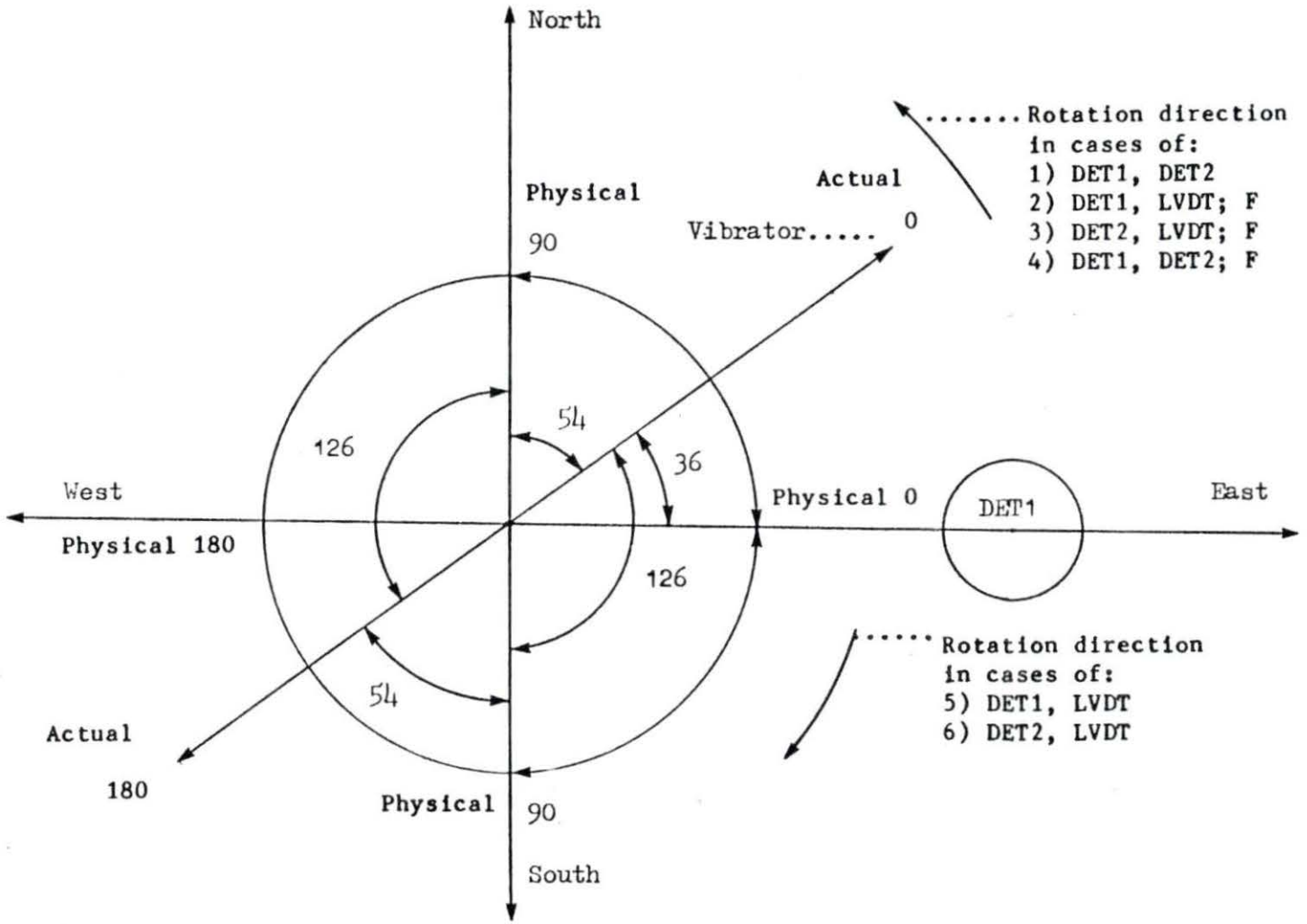

FIGURE 15. Directions of rotation of stepping motor in this test

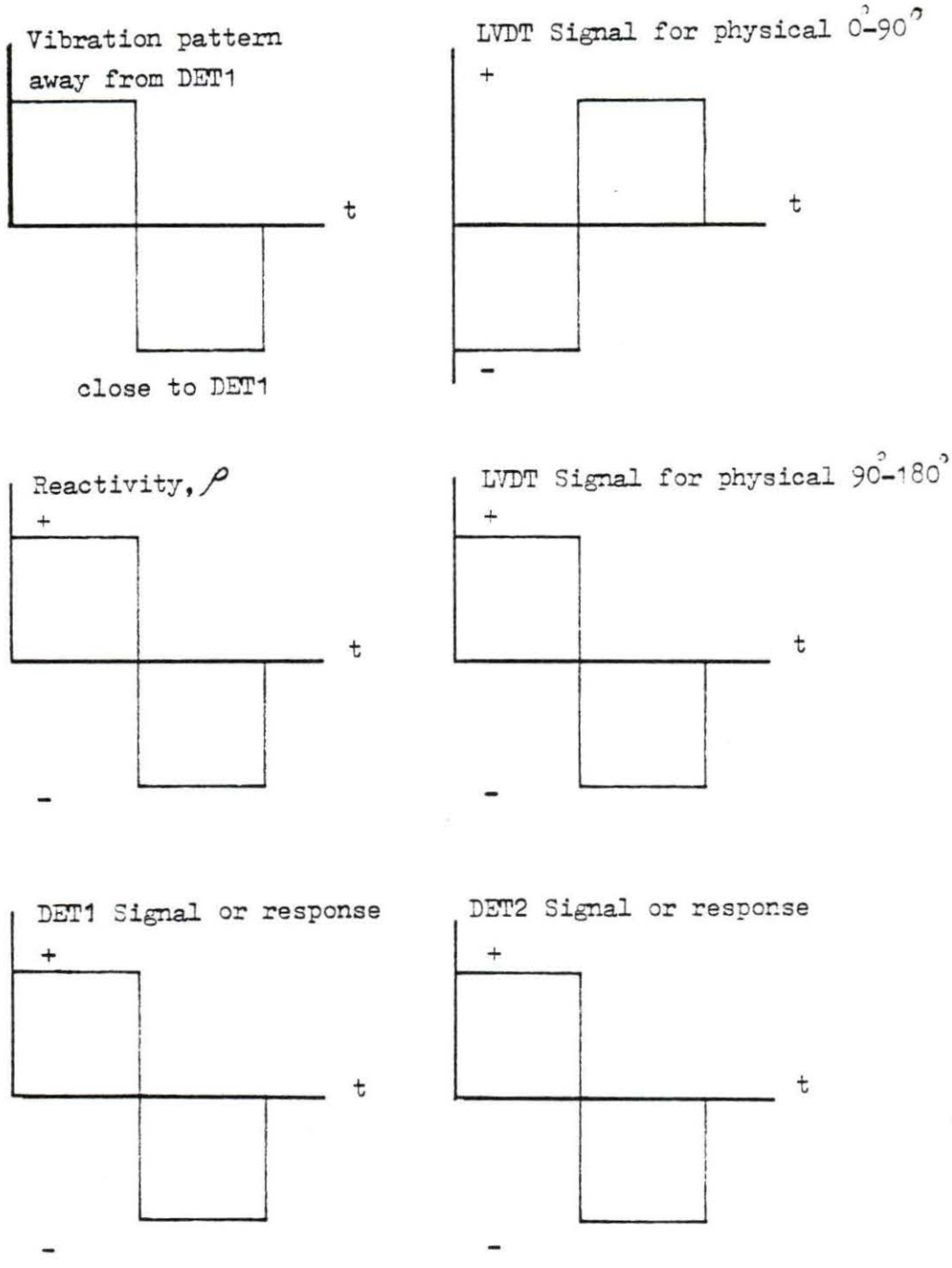

FIGURE 16. Reactor response and indicated detector responses

V. DISCUSSION OF RESULTS

Results obtained for the various combinations of signals studied are shown in Figures 17 to 46. Figures 17 through 31 correspond to the unflooded case, and Figures 32 through 46 correspond to the flooded case of the vibrating rod thimble. Every five consecutive figure numbers form a data set (1. normalization, 2. SQR. of APSD of the input A, 3. SQR. of APSD of the input B, 4. phase, 5. coherence) which were gathered from one of the input sets to the spectrum analyzer as follows: (LVDT to INPUT A @ DET1 to INPUT B), (LVDT to INPUT A @ DET2 to INPUT B), (DET1 to INPUT A @ DET2 to INPUT B). Results are presented in the general form of a particular output (normalization, magnitudeA, magnitudeB, phase, coherence) versus the angular direction of motion of the vibrator. All measurements are for a vibrator frequency of 1.52 Hz. A complete analysis of the behavior shown for all cases studied has not been possible. The results for all data taken are presented, however, to show the sensitivity of the detector response to the direction of vibrator motion and to provide an indication of the scope of the problem for future research.

Some explanation of notation is required before one looks at the figures of this chapter. To fully understand the meaning of the vertical axis label of these figures, one should also refer to the table of acronyms to check the meanings of some abbreviations used.

The notation Angle1@Angle2 (e.g. 126@90) means that Angle1 is equivalent to Angle2 (always physical 90 degrees) in the physical

environment of the direction of motion of the vibrator relative to DET1. The other notation is Signal1@Signal2 (e.g., DET1@LVDT), which means the graph shown was obtained from Signal1, and it also means that, at the same time ("@"), the other input to the spectrum analyzer was Signal2.

As mentioned before, it was found that the stepping motor would occasionally turn in the wrong direction. This is illustrated in Figures 17 through 26, which show that the vibrator actually turned in the other direction relative to the other figures (Figure 15).

As mentioned before, the spectrum analyzer was used for collecting and processing the data in this experiment. This system was used to calculate the square root of the APSD of the two inputs, the transfer function magnitude and phase, and the coherence between the two inputs. As also mentioned by Sankoorikal [10], it was observed that, due to design limitations, the LVDT frequency spectrum (and therefore vibrator motion) varied slightly for different runs (Figures 18, 23, 33, 38). In order to correct for this, and to compare the data from different runs, it was necessary to normalize the data. This was done by normalizing the detector signals to the LVDT signal, and also the DET2 signal was normalized to the DET1 signal to show the variations of DET2 with respect to DET1 (Figures 17, 22, 27, 32, 37, 42). The formula used was

NORMALIZED DATA = (UNNORMALIZED DATA)/(NORMALIZER DATA).

By observation, it was found that as the vibrator cadmium is moving away from DET1, by assumption the reactivity increases and by experiment the LVDT signal increases or decreases depending on the way

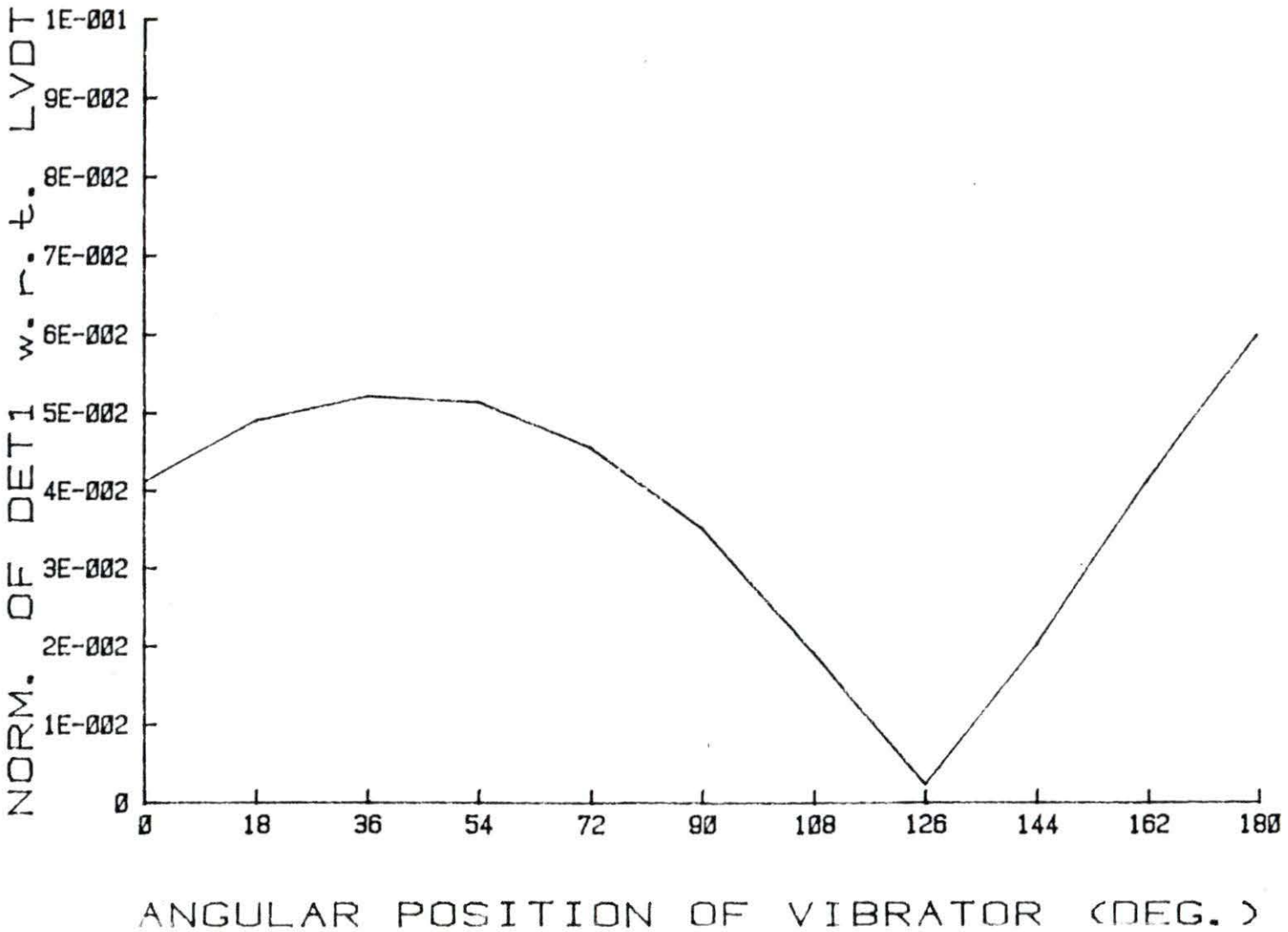

FIGURE 17. Normalization of DET1 to LVDT at 1.52 Hz vs angular position of the vibrator

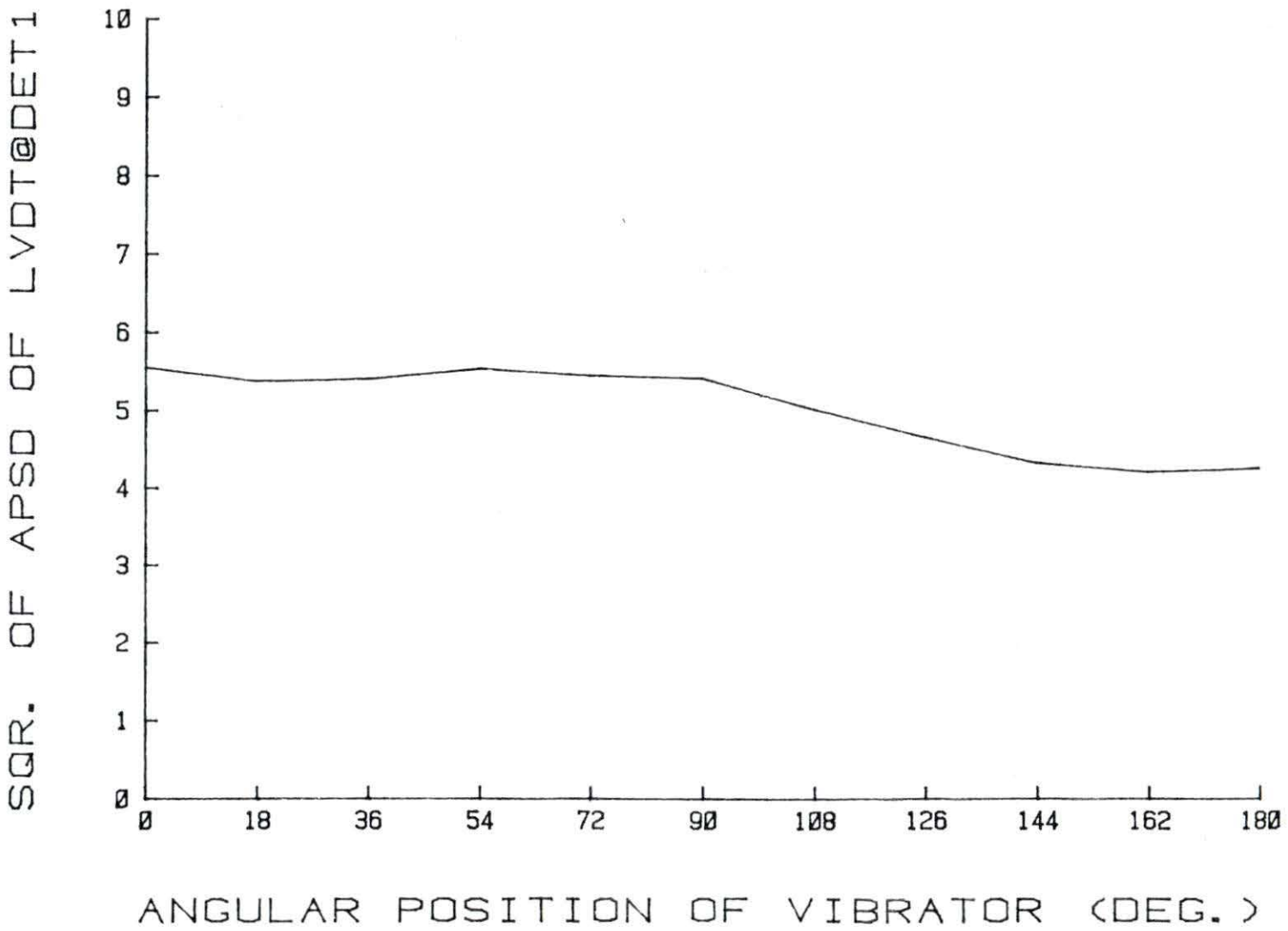

FIGURE 18. Magnitude of LVDT (@DET1) at 1.52 Hz vs angular position of the vibrator

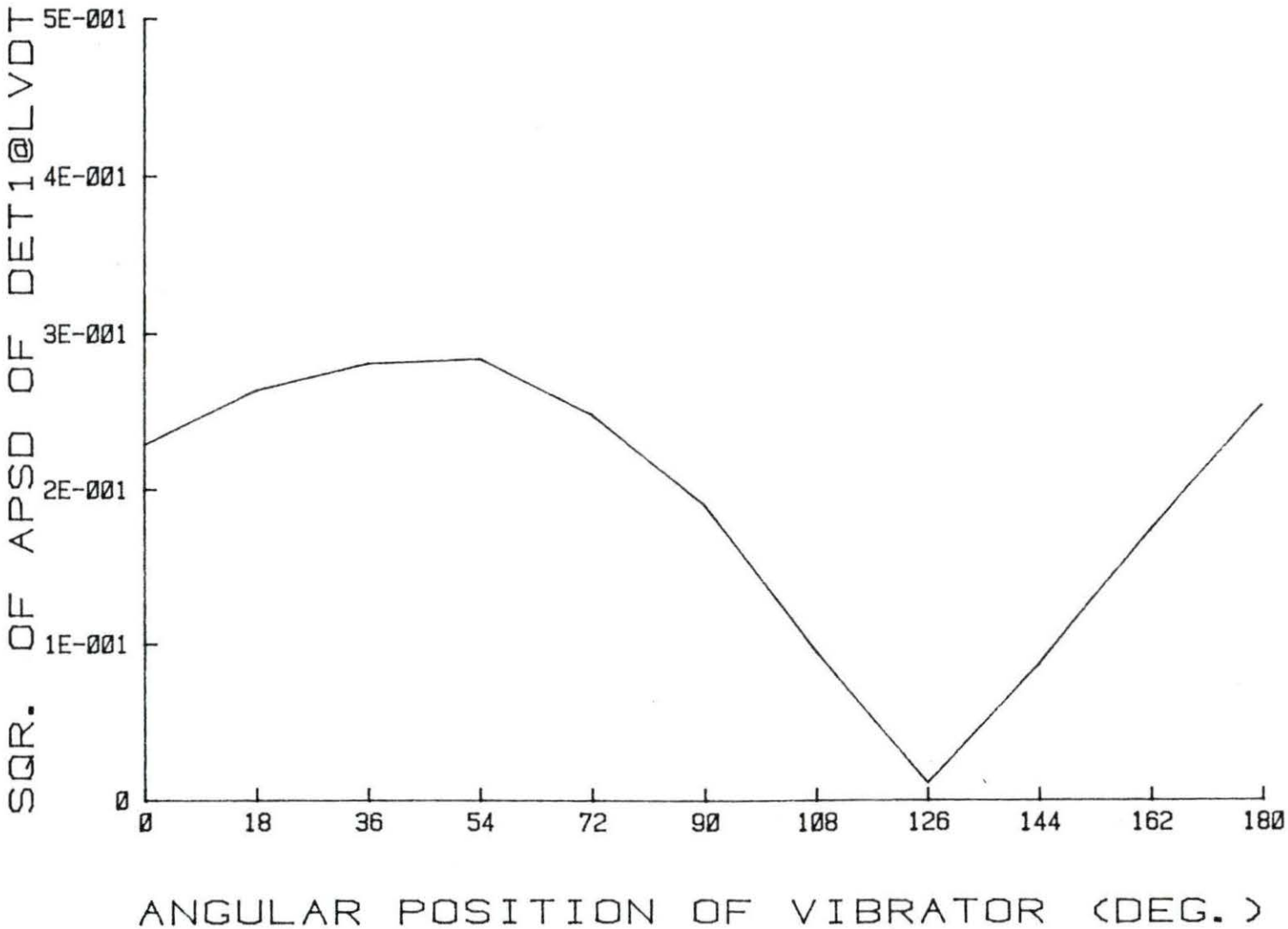

FIGURE 19. Magnitude of DET1 (@LVDT) at 1.52 Hz vs angular position of the vibrator

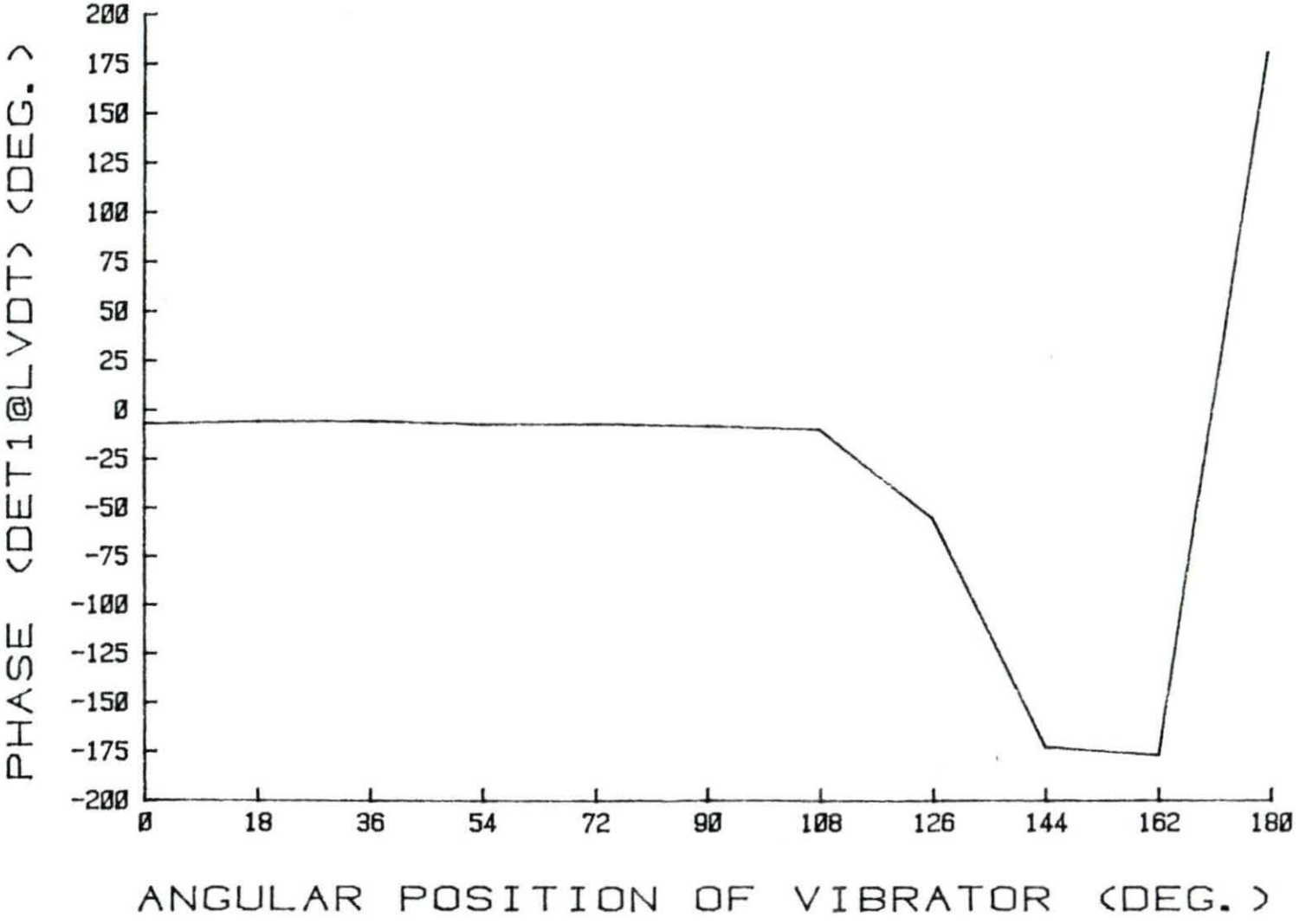

FIGURE 20. DET1-LVDT phase at 1.52 Hz vs angular position of the vibrator

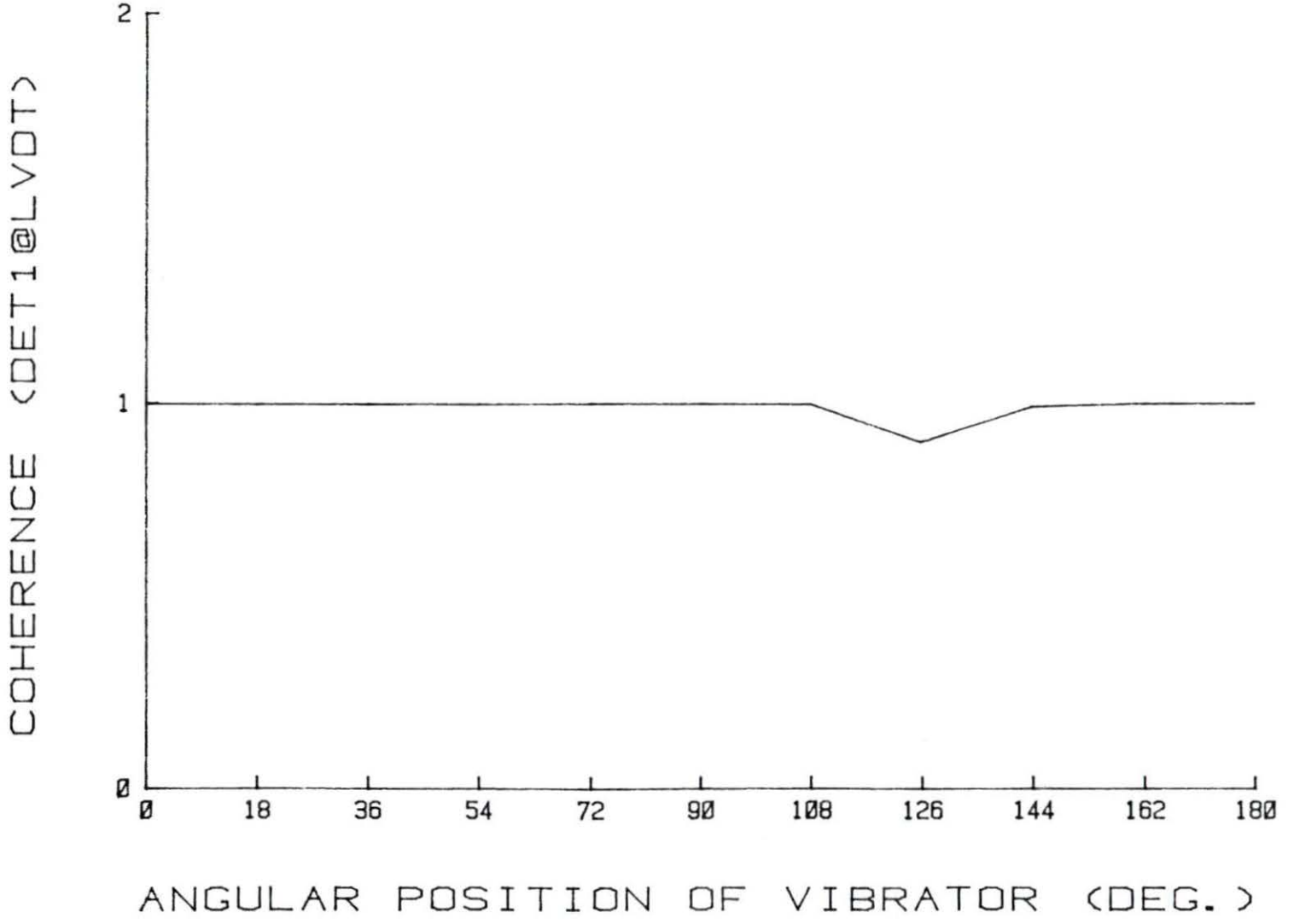

FIGURE 21. DET1-LVDT coherence at 1.52 Hz vs angular position of the vibrator

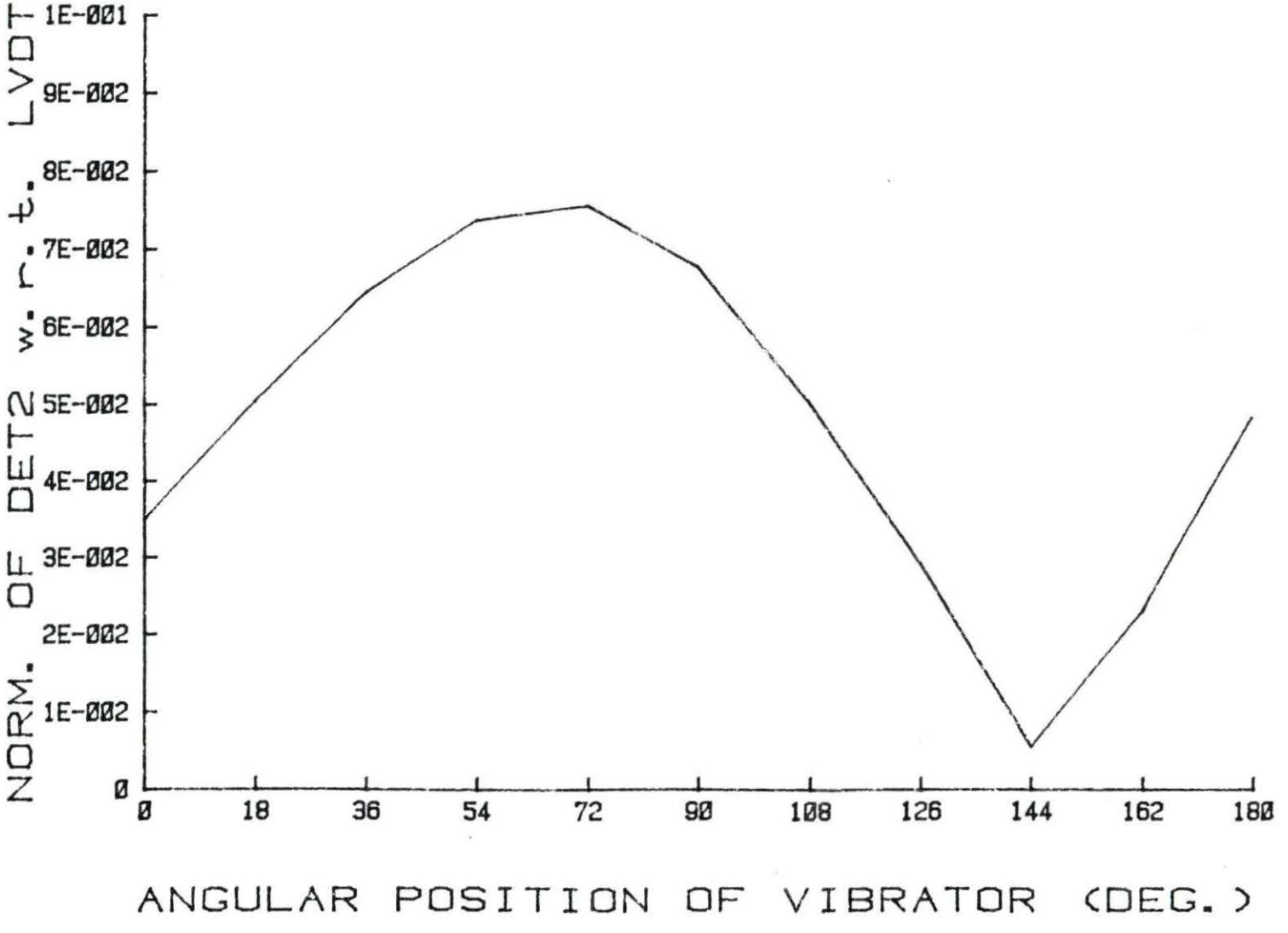

FIGURE 22. Normalization of DET2 to LVDT at 1.52 Hz vs angular position of the vibrator

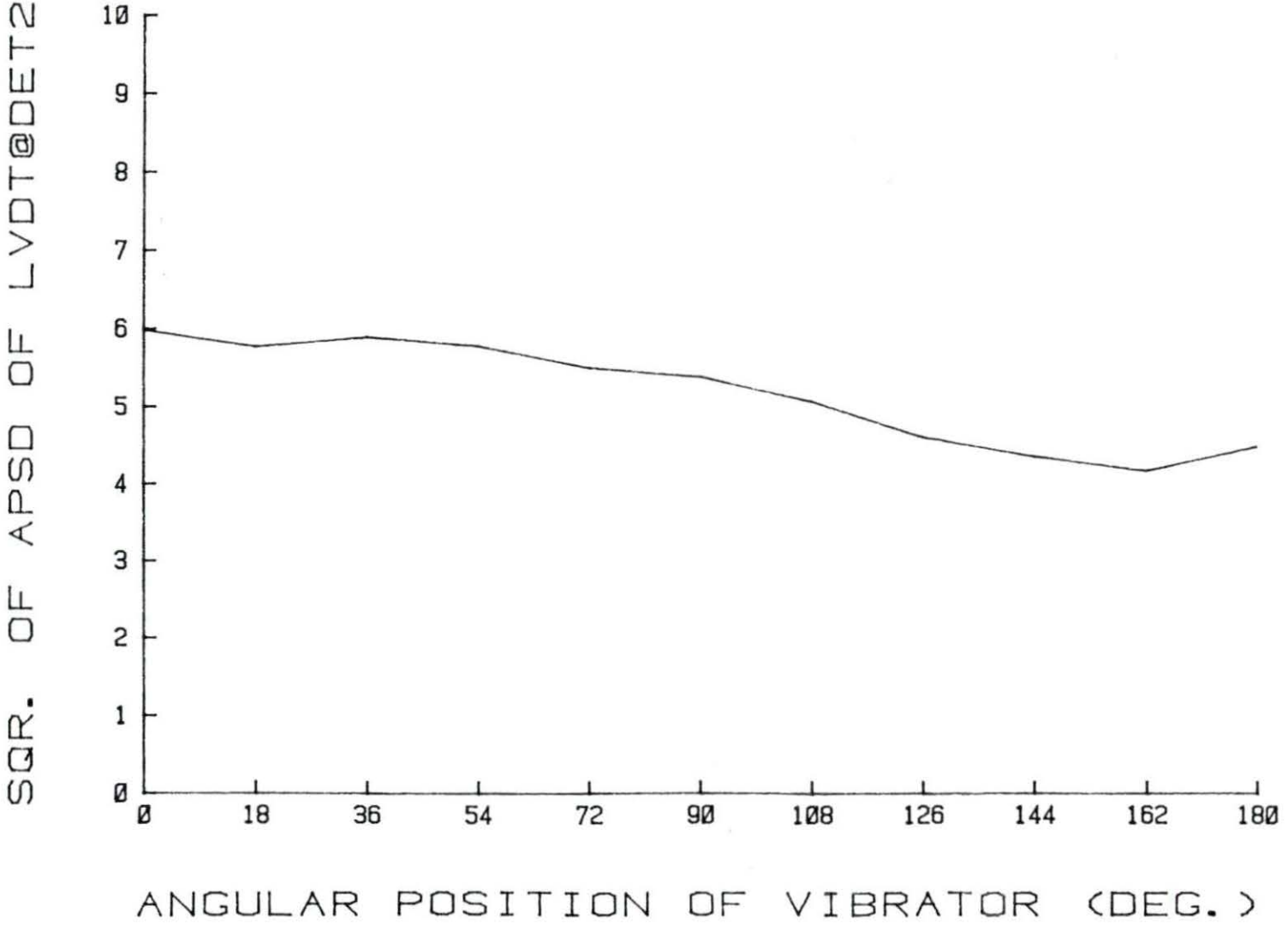

FIGURE 23. Magnitude of LVDT (@DET2) at 1.52 Hz vs angular position of the vibrator

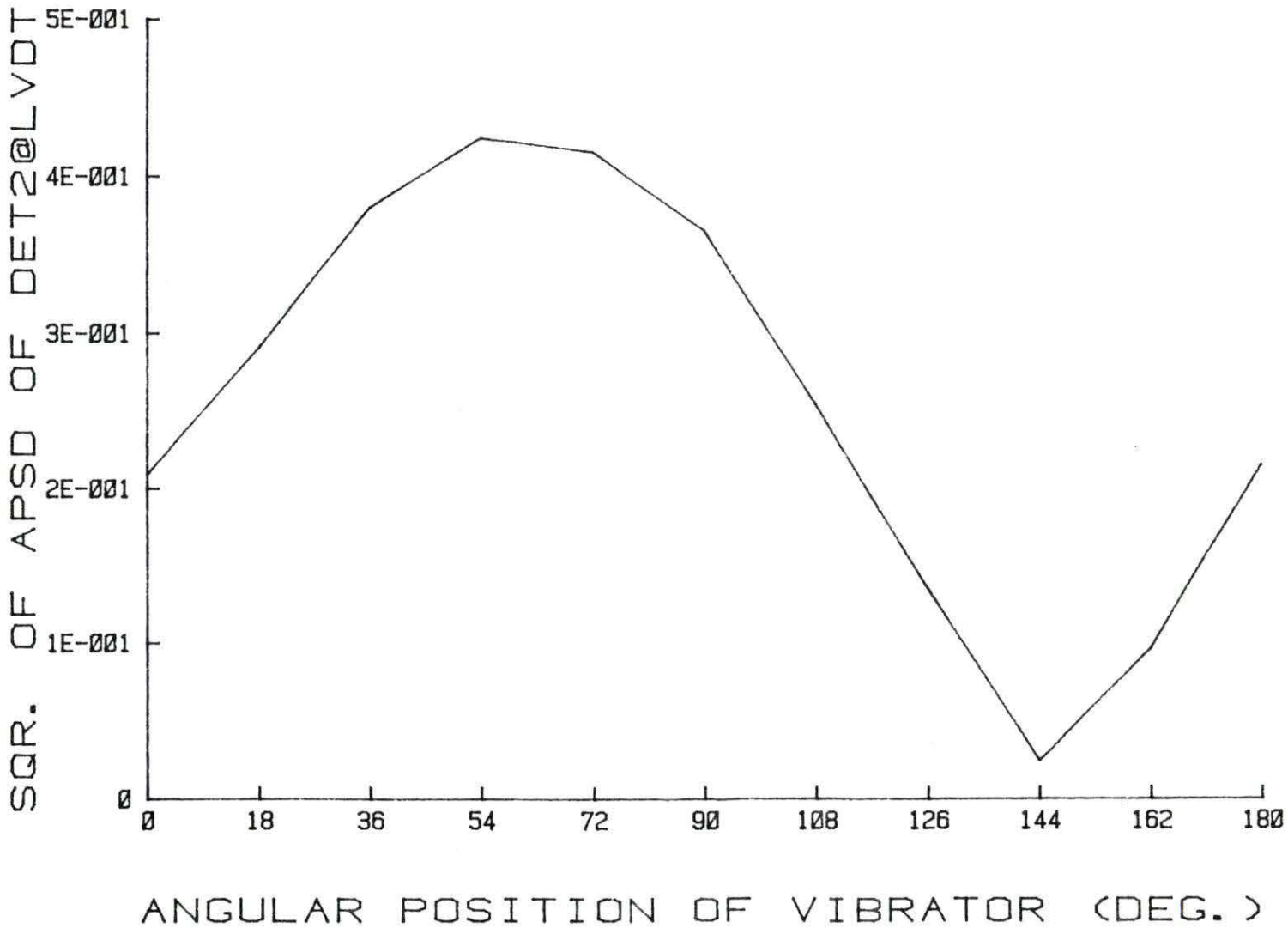

FIGURE 24. Magnitude of DET2 (@LVDT) at 1.52 Hz vs angular position of the vibrator

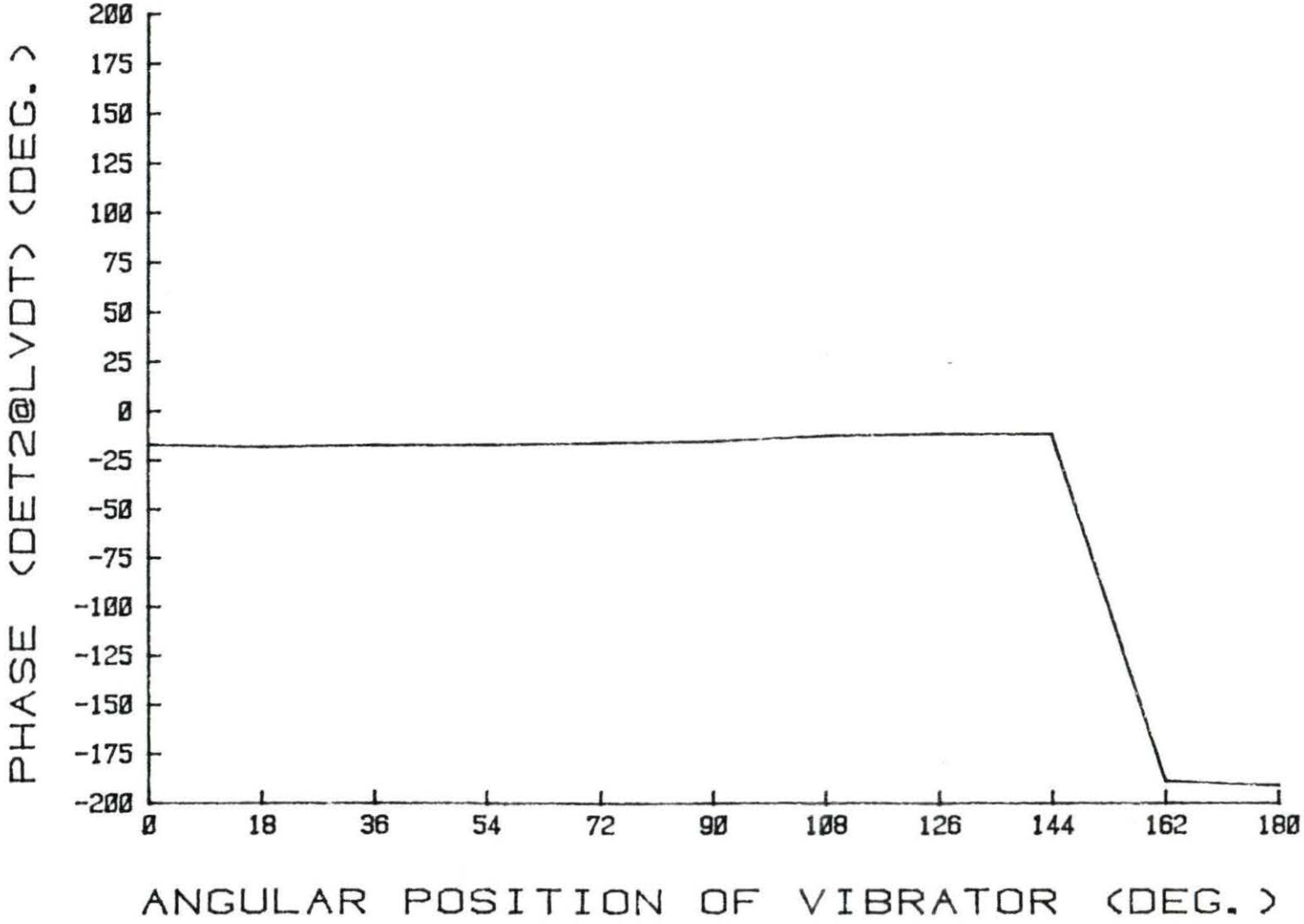

FIGURE 25. DET2-LVDT phase at 1.52 Hz vs angular position of the vibrator

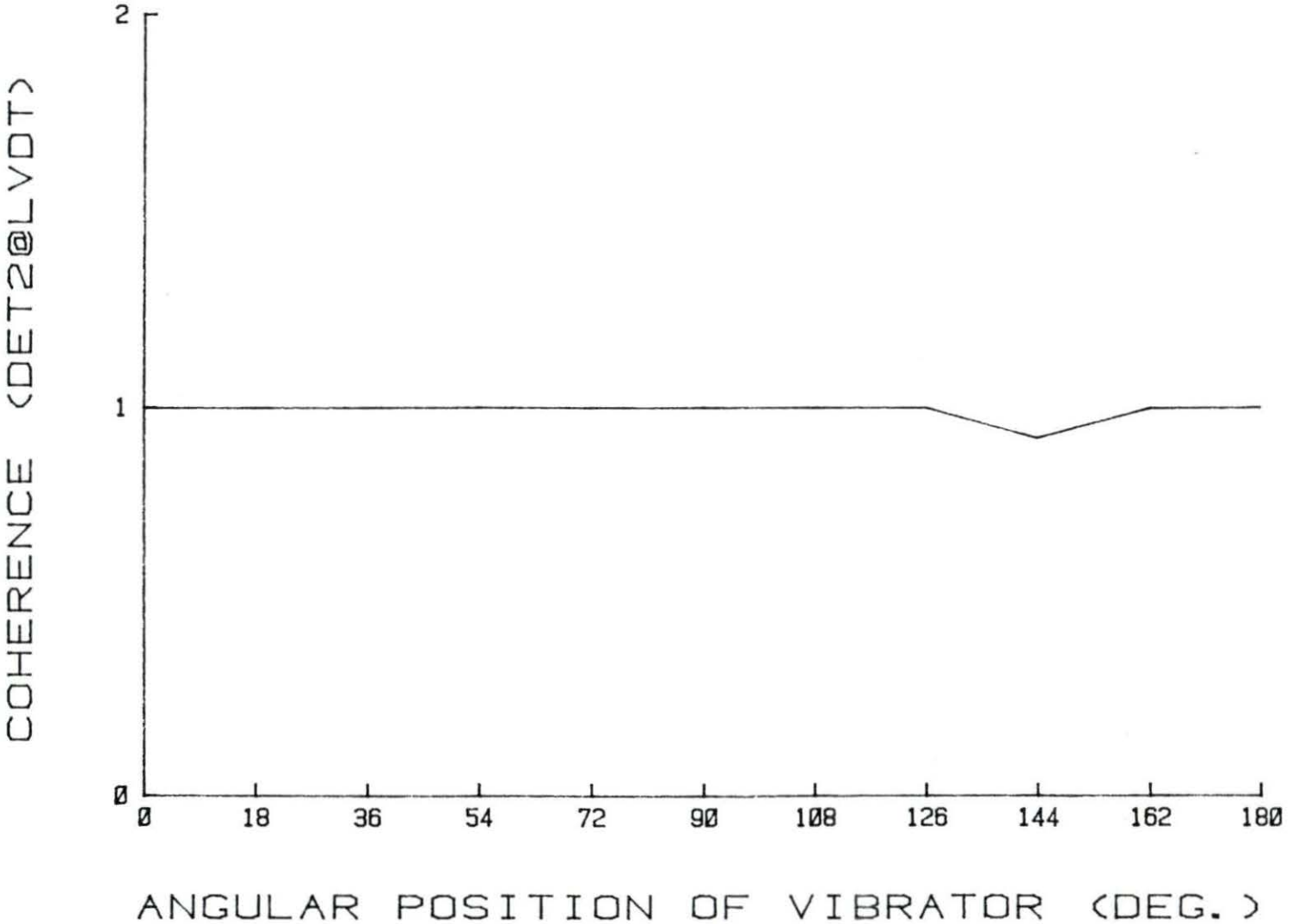

FIGURE 26. DET2-LVDT coherence at 1.52 Hz vs angular position of the vibrator

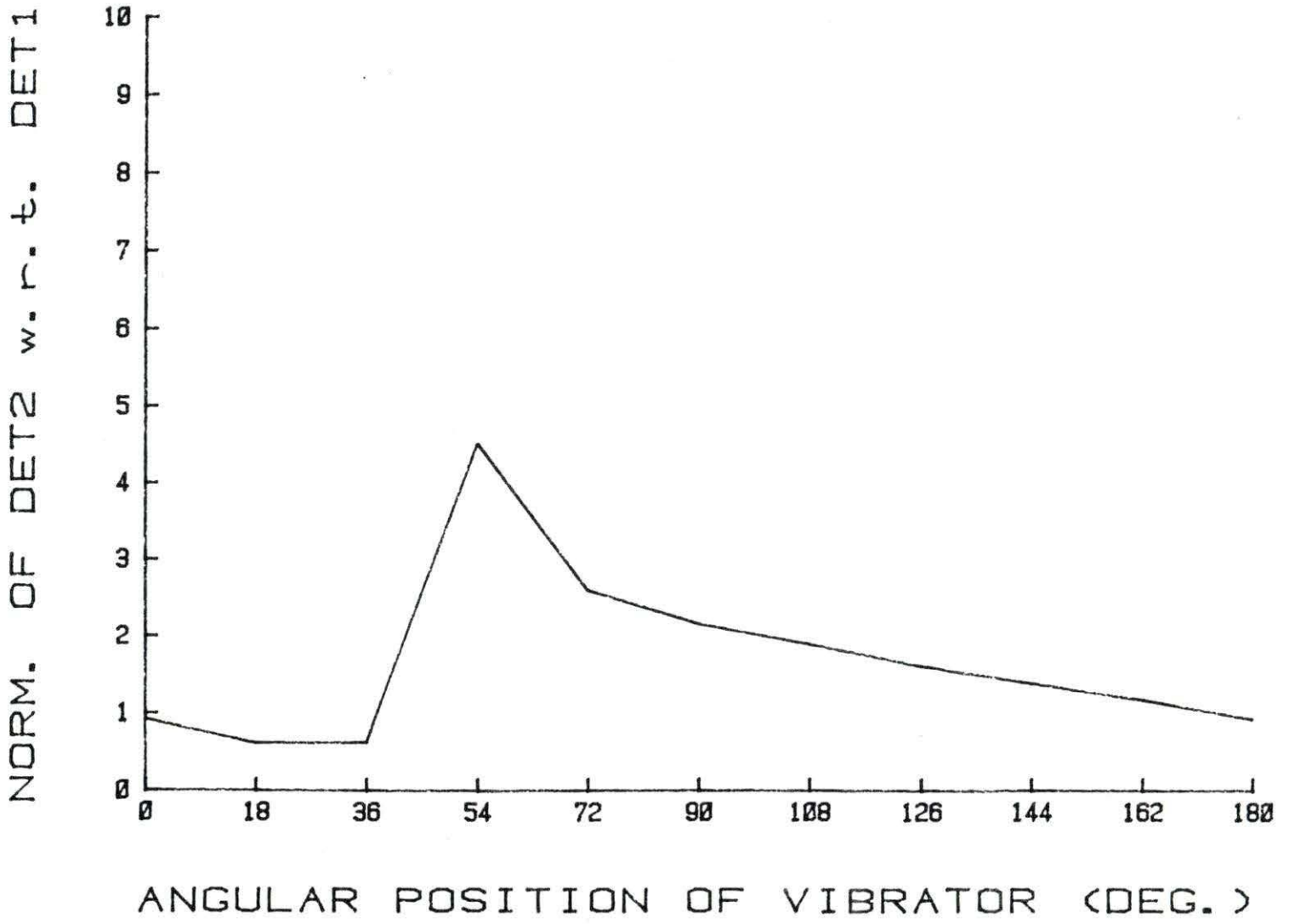

FIGURE 27. Normalization of DET2 to DET1 at 1.52 Hz vs angular position of the vibrator

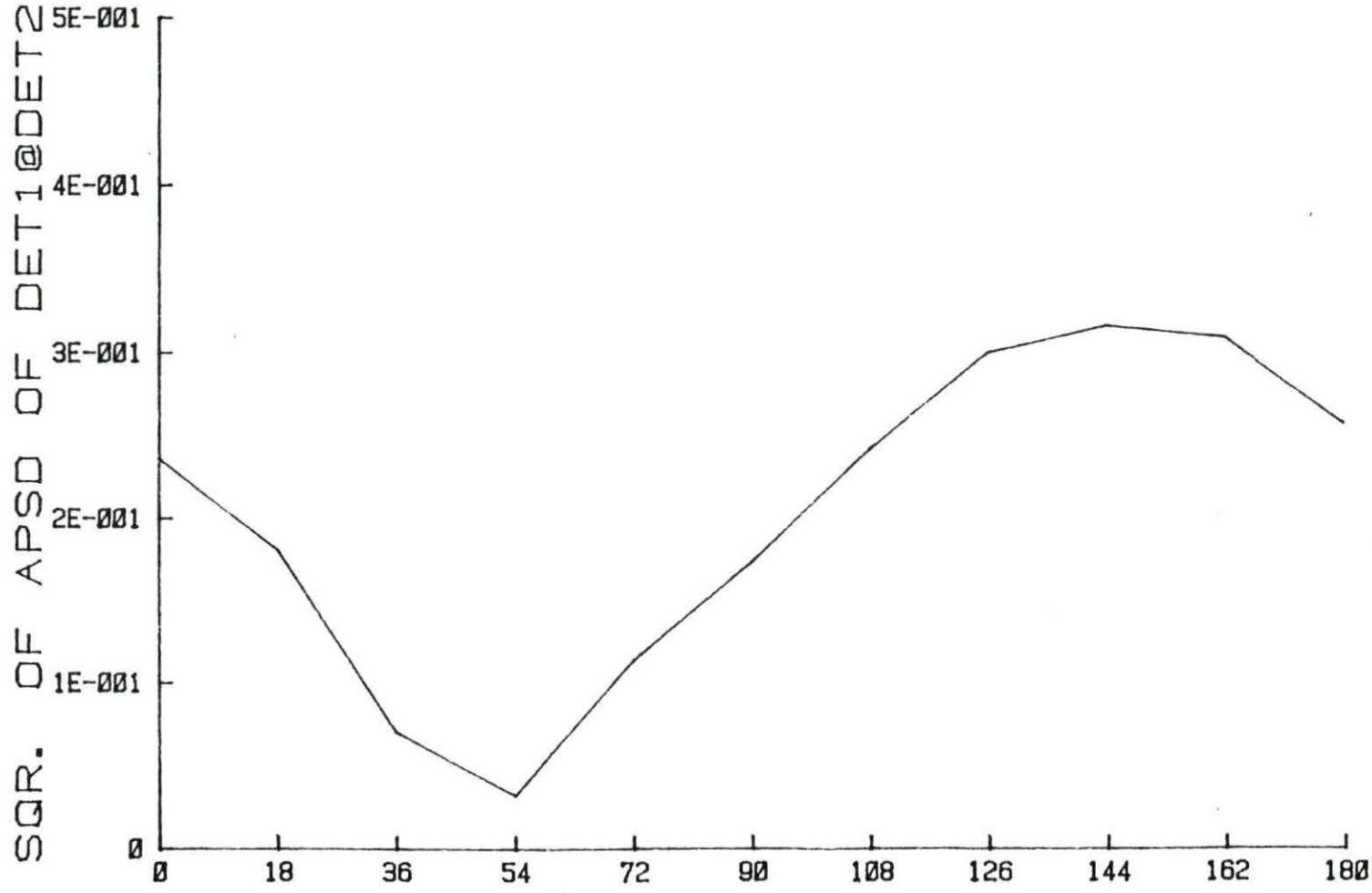

FIGURE 28. Magnitude of DET1 (@DET2) at 1.52 Hz vs angular position of the vibrator

FIGURE 29. Magnitude of DET2 (@DET1) at 1.52 Hz vs angular position of the vibrator

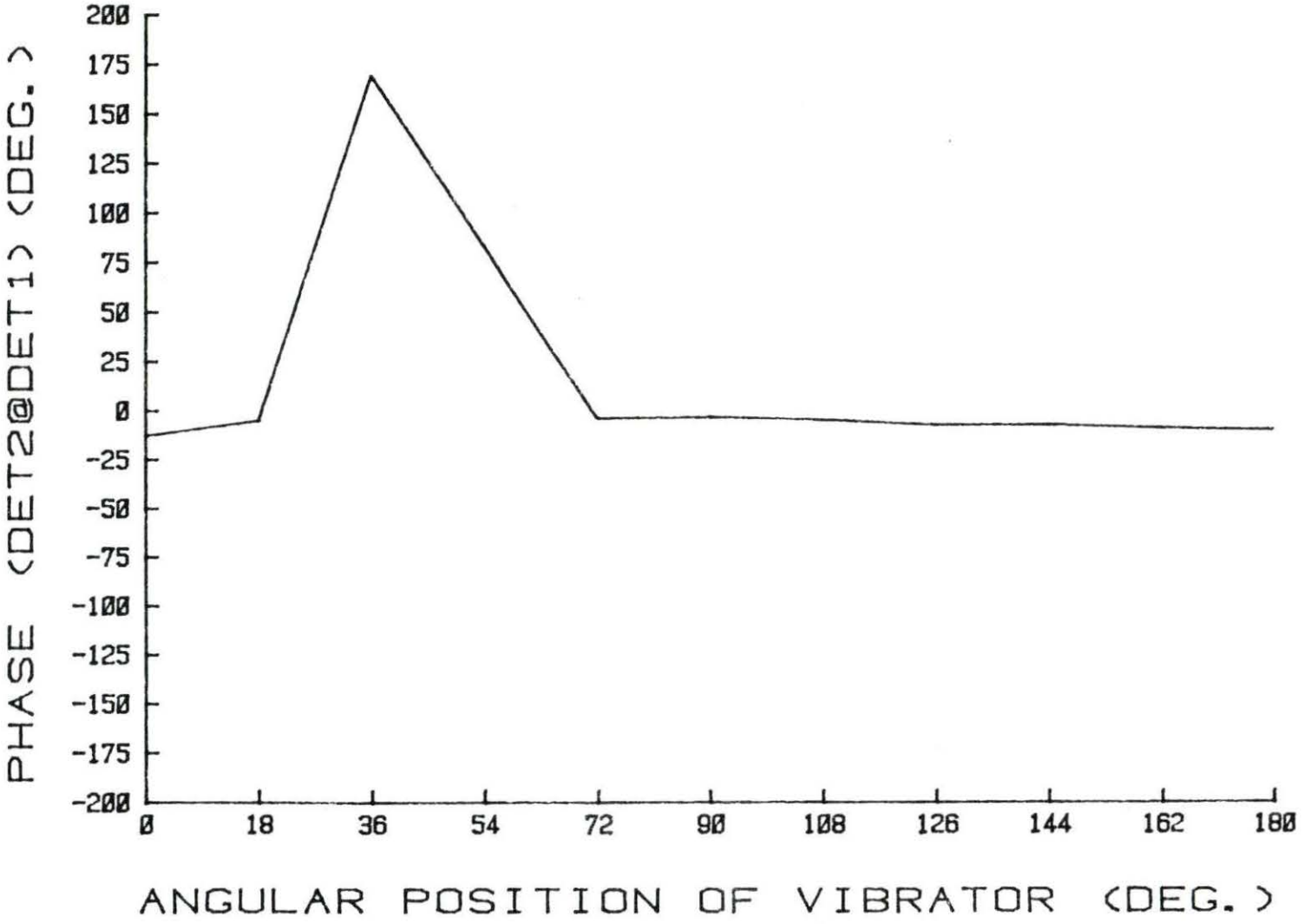

FIGURE 30. DET1-DET2 phase at 1.52 Hz vs angular position of the vibrator

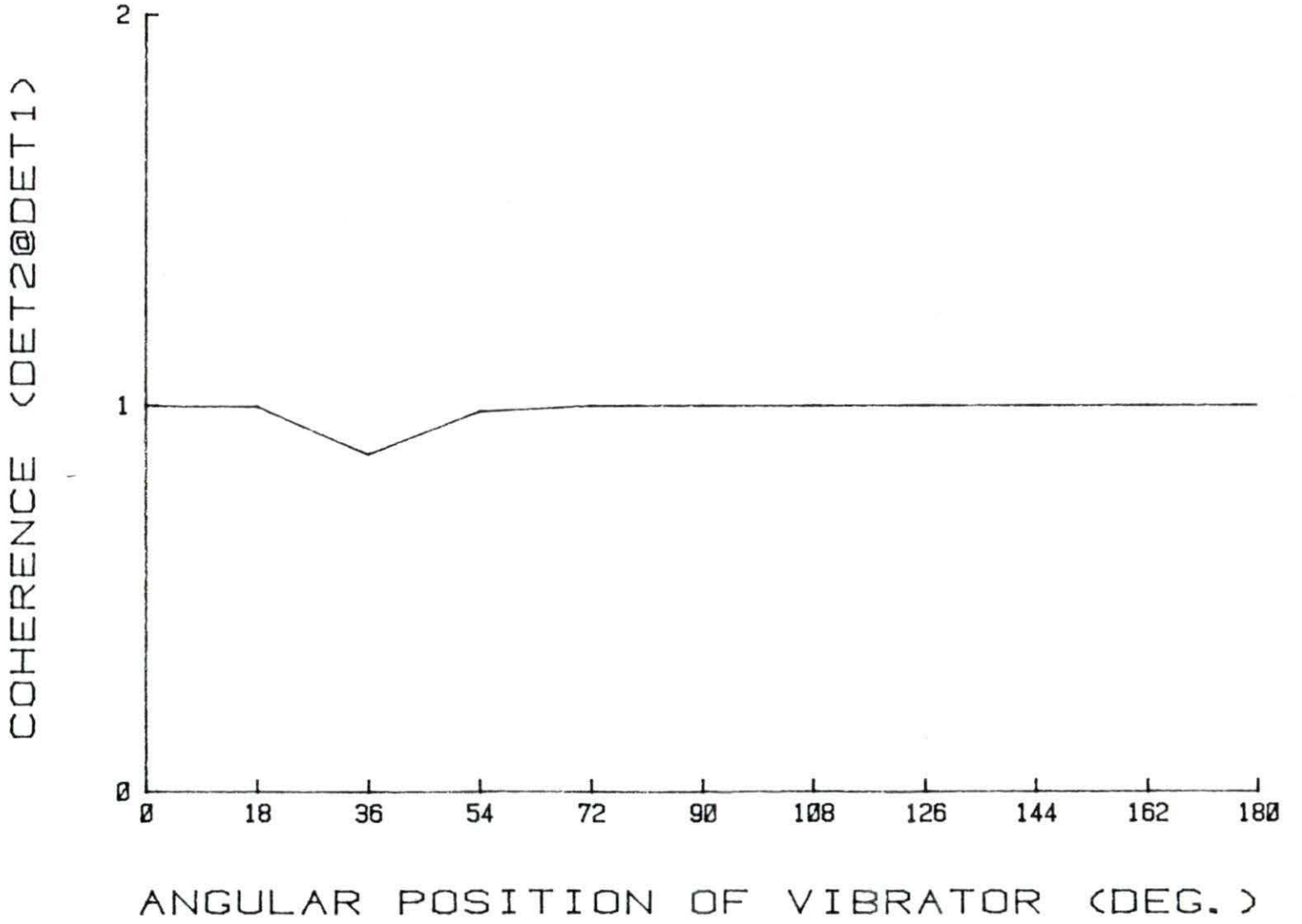

FIGURE 31. DET1-DET2 coherence at 1.52 Hz vs angular position of the vibrator

the LVDT is positioned radially. Figure 16 shows the relationship among the LVDT, DET1, and DET2 signals, and the pattern of the motion of the vibrator. Since the LVDT device was also being rotated by the motor, the phase (Figures 20, 25, 30, 35, 40, 45) show that the LVDT motion orientation changed to reverse motion around the physical 90 degrees of the vibrator relative to DET1.

When the vibrator oscillates at an angular position of 90 degrees relative to DET1, the local response of the DET1 is at double the fundamental frequency [16], and therefore zero at the fundamental frequency. Based on this, the dips shown in the data obtained from DET1 show the physical 90 degrees angular direction (Figures 19, 28, 34, 43). The response at 1.52 Hz for this case must therefore be that due to the global response only. As pointed out previously, the actual 0 degree direction of motion did not necessarily coincide with the physical 0 degree position. These dips were used to establish the physical 0 degree position and the global portion of the response. Figures 24, 29, 39, and 44 which form the response of DET2 also display these kind of dips, but at a different angular position from that of DET1. These could be due to the lack of the neutron flux gradient around those angular positions inside the UTR-10 reactor. Looking at the magnitude Figures 19, 24, 28, 29, 34, 43, and 44, one can see that as the vibrator oscillates in different angular positions relative to the DET1, the responses of DET1 and DET2 change according to the direction of the motion of the vibrator. One important point in these figures is that

they illustrate that when the vibrator is oscillating at a physical 90 degree angle relative to DET1, the response of DET1 is due only to the global effect. These figures also illustrate that the vibrator reference point was offset from the original intended one by approximately 36 degrees (physical zero degree reference = vibrations in EW direction, Figure 15)

The phase Figures 20, 25, 30, 35, 40, and 45 show that the orientation of the LVDT, with respect to the detectors, changed as the vibrating rod passed the physical 90 degree point. That is why one can see the DET1 and DET2 signals increase to 180 degree phase shift relative to the LVDT signal when the vibrator rotates towards the 180 degree angular position. The phase figures between the detectors show that there is an 18 degrees phase shift between the responses of DET1 and DET2 which is equal to the phase angle of the reactor transfer function. Also at actual 36 degrees, the DET2 response goes toward zero (explained latter) and the phase shift between the detectors goes to about 180 degrees.

It is also known that the spectrum analyzer flips the angles by ±360 degrees if the phase angles pass the ±180 degree limit of the system. This is why some of the phase angles show rapid changes in value.

The coherence functions (Figures 21, 26, 31, 36, 41, and 46) show that the analyzer's two input signals are always coherent except at the angular position of 90 degree. This could mean that the DET2 response

dropped at that particular angle due to the flux orientation inside the reactor (reactivity effect). It may also be due in part to the loss of the local component of the response. Both the unflooded and the flooded cases show the same general behavior.

Figures 47-48 show the calculated local and global responses of the unflooded case based on the method, which is explained in the following section.

The global part of the response was obtained by using the fact that when the vibrator is in motion at physical 90 degree relative to DET1, the response of DET1 at 1.52 Hz is only due to the global effect [16]. This is the only time that DET1 sees the global effect without the local effect combined with it. Therefore, this point was used to scale the global effects monitored by both detectors. The assumption was made that DET2 responds to the global effect only. The response of DET1 was divided by the response of DET2, at the physical 90 degree point only, and then this ratio was multiplied by the response of DET2 at all points. This provided the scaled global effect seen by DET1 due to the vibration. To estimate the local effect the scaled global effect was subtracted from the response of DET1. This calculation was based on the assumption that the phase angle of the reactor transfer function is negligible at 1.52 Hz frequency.

Several different assumed 90 degree points were tried (36, 54, 72, and 90 degrees), but the most consistent results were obtained using 54 degrees as corresponding to the physical 90 degree point. The resulting L/G ratios (Appendix E) are given in Table 4.

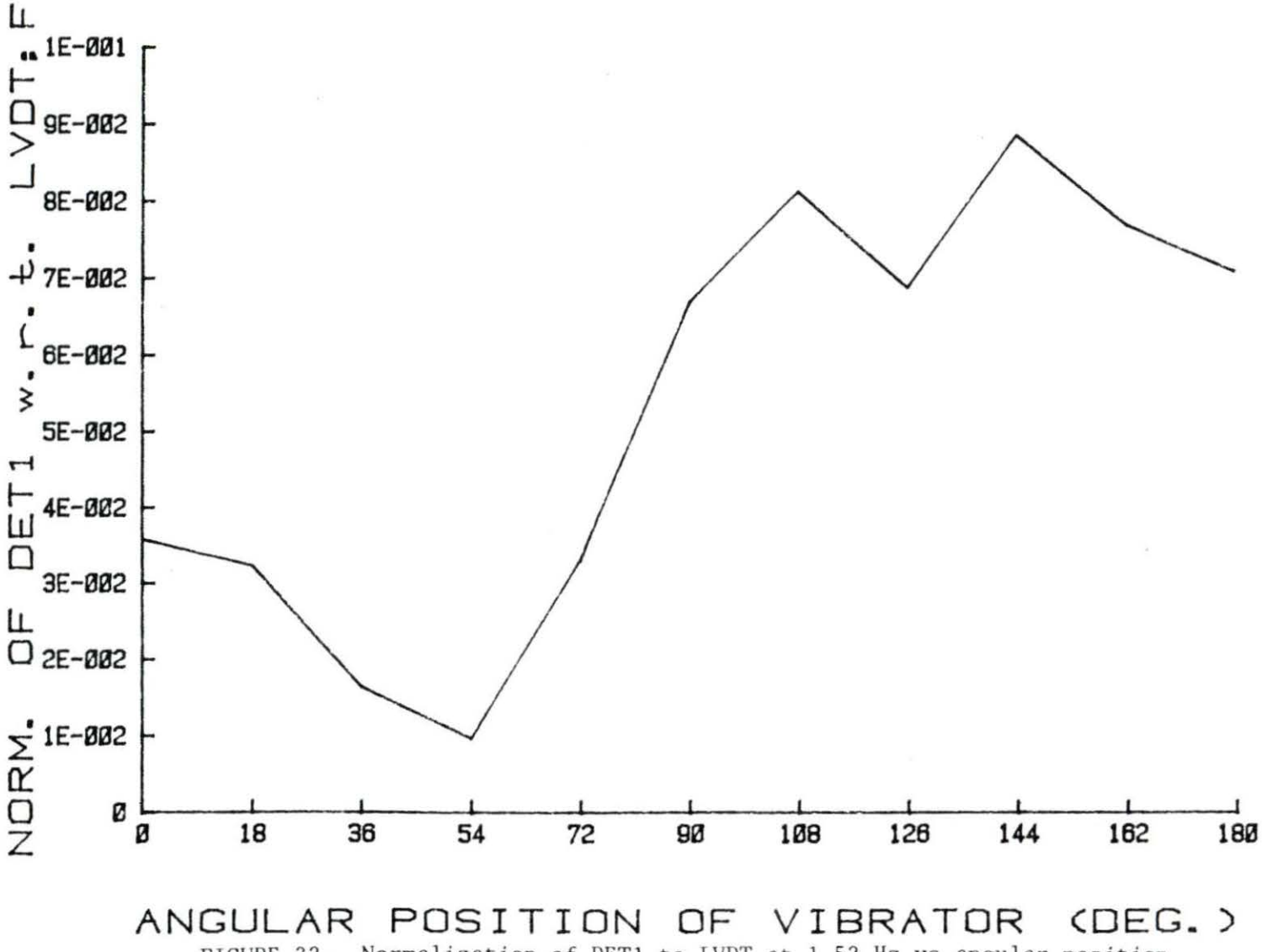

FIGURE 32. Normalization of DET1 to LVDT at 1.52 Hz vs angular position of the vibrator (flooded case)

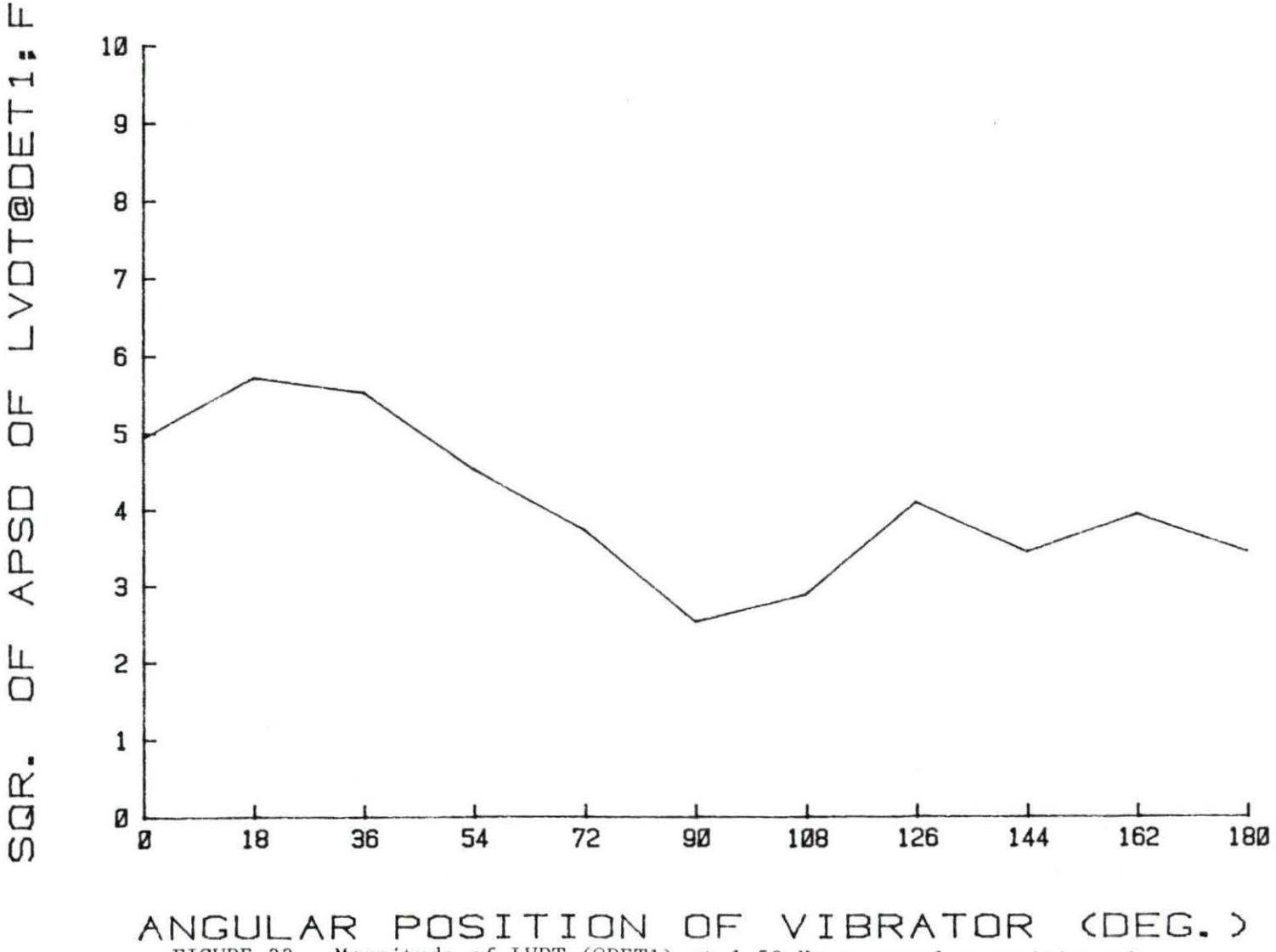

FIGURE 33. Magnitude of LVDT (@DET1) at 1.52 Hz vs angular position of the vibrator (flooded case)

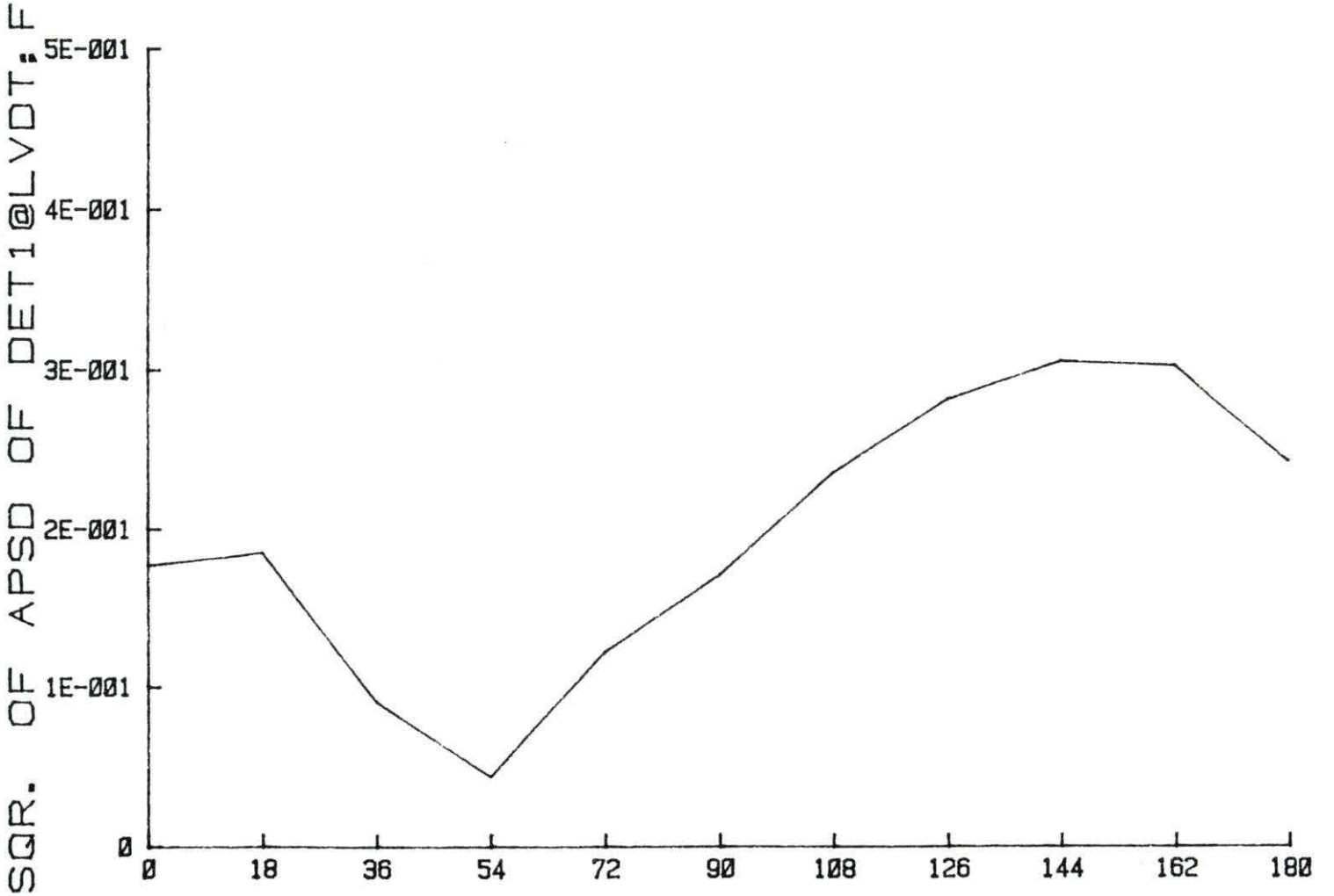

FIGURE 34. Magnitude of DET1 (@LVDT) at 1.52 Hz vs angular position of the vibrator (flooded case)

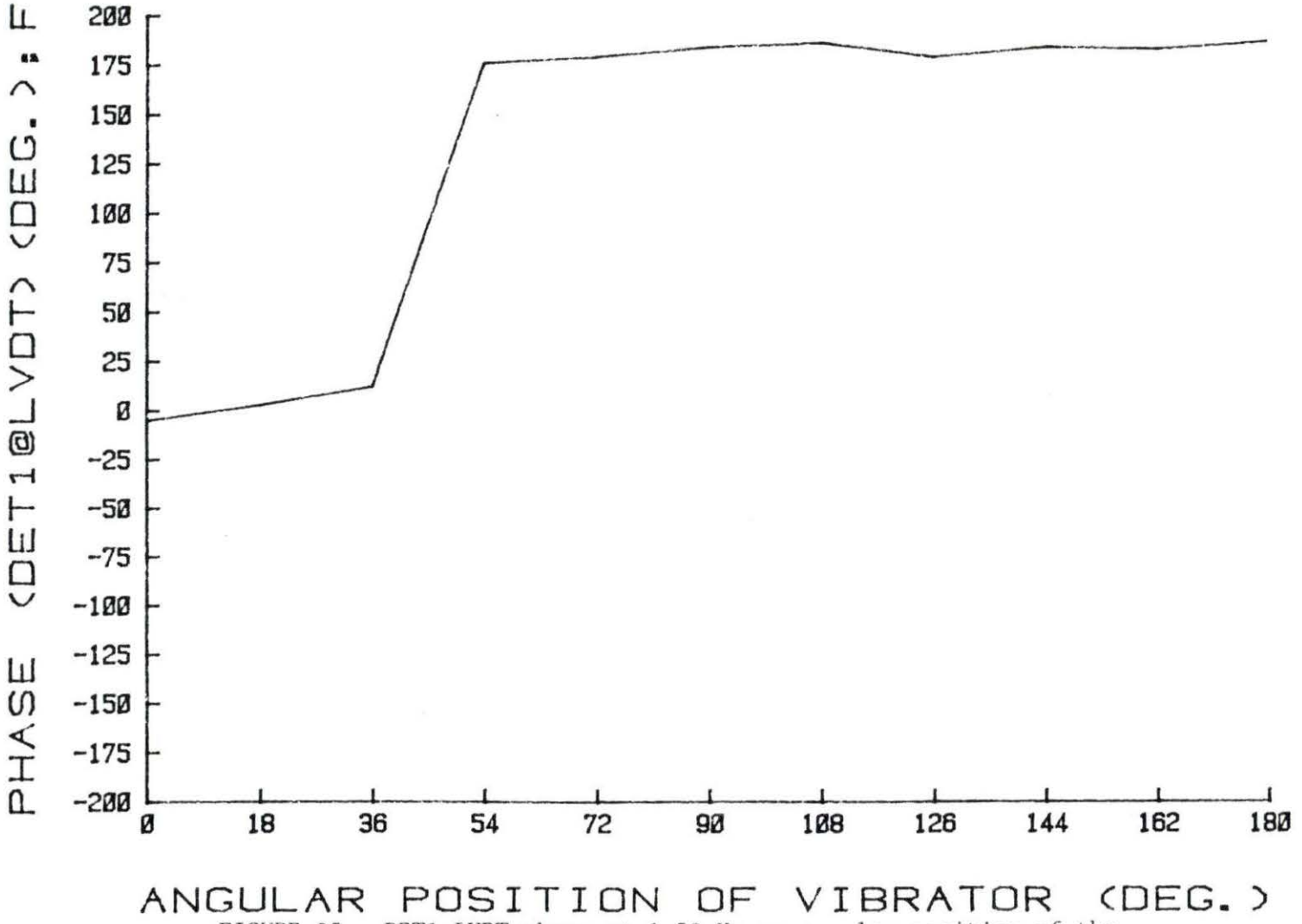

FIGURE 35. DET1-LVDT phase at 1.52 Hz vs angular position of the vibrator (flooded case)

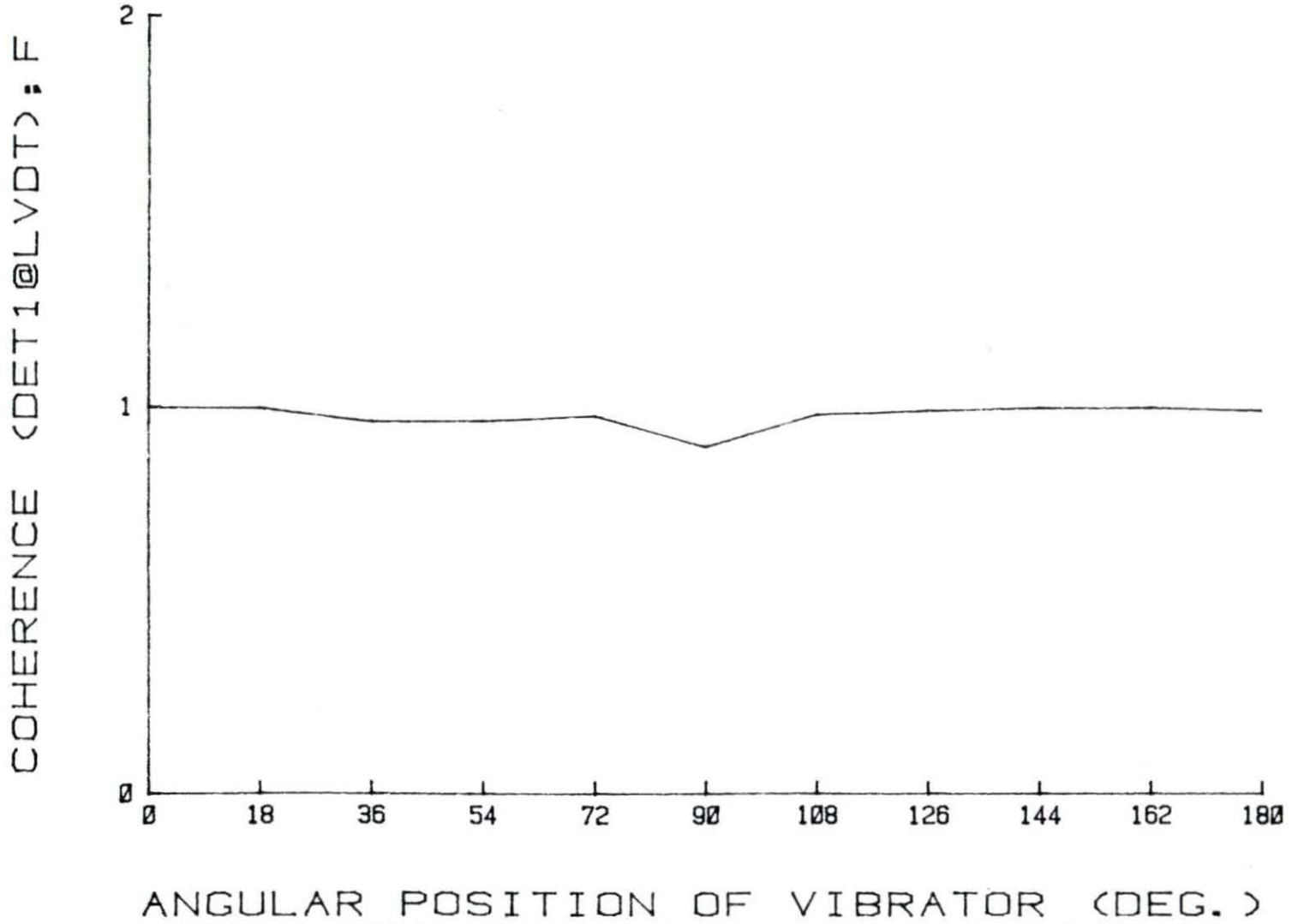

FIGURE 36. DET1-LVDT coherence at 1.52 Hz vs angular position of the vibrator (flooded case)

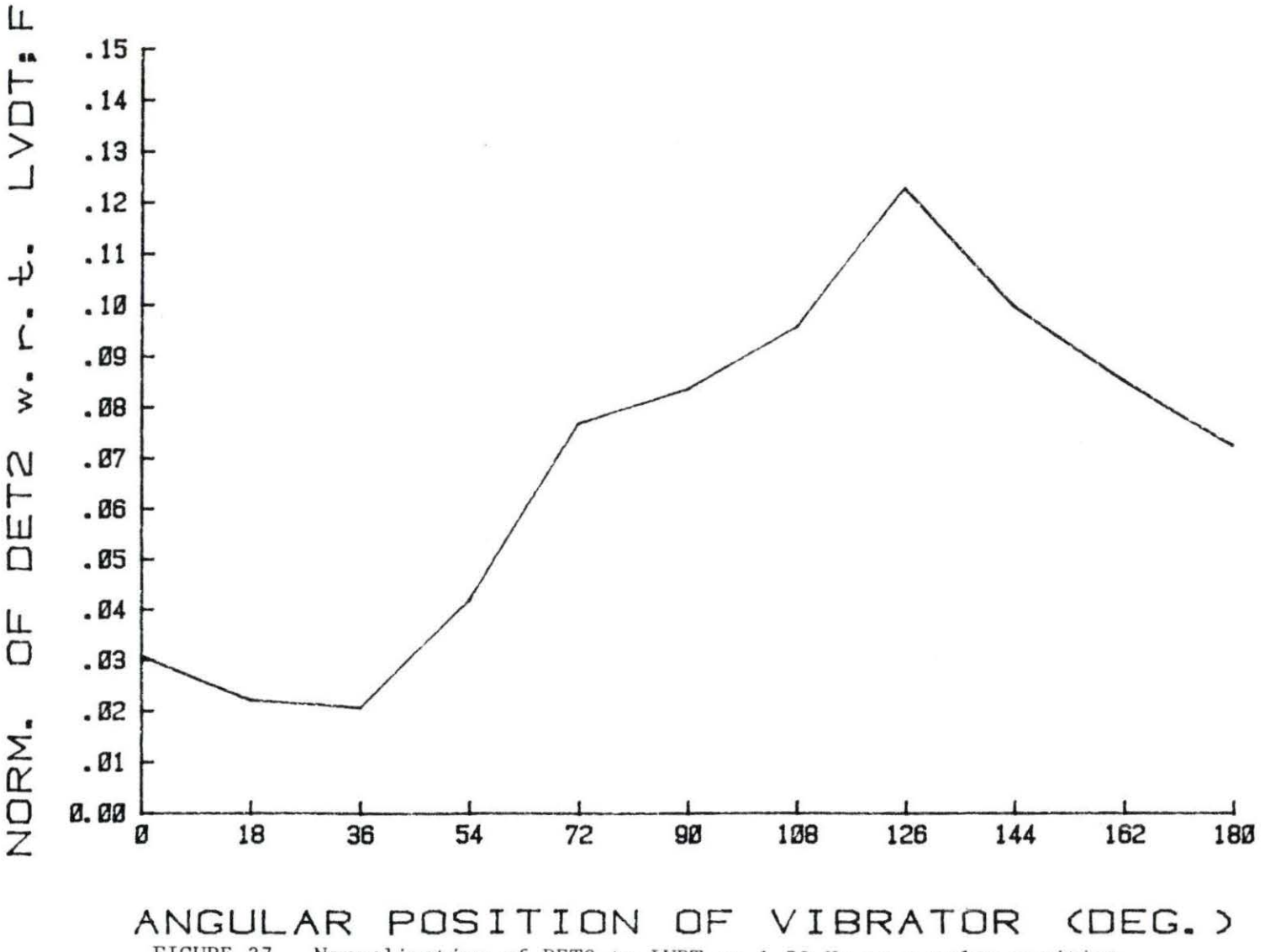

FIGURE 37. Normalization of DET2 to LVDT at 1.52 Hz vs angular position of the vibrator (flooded case)

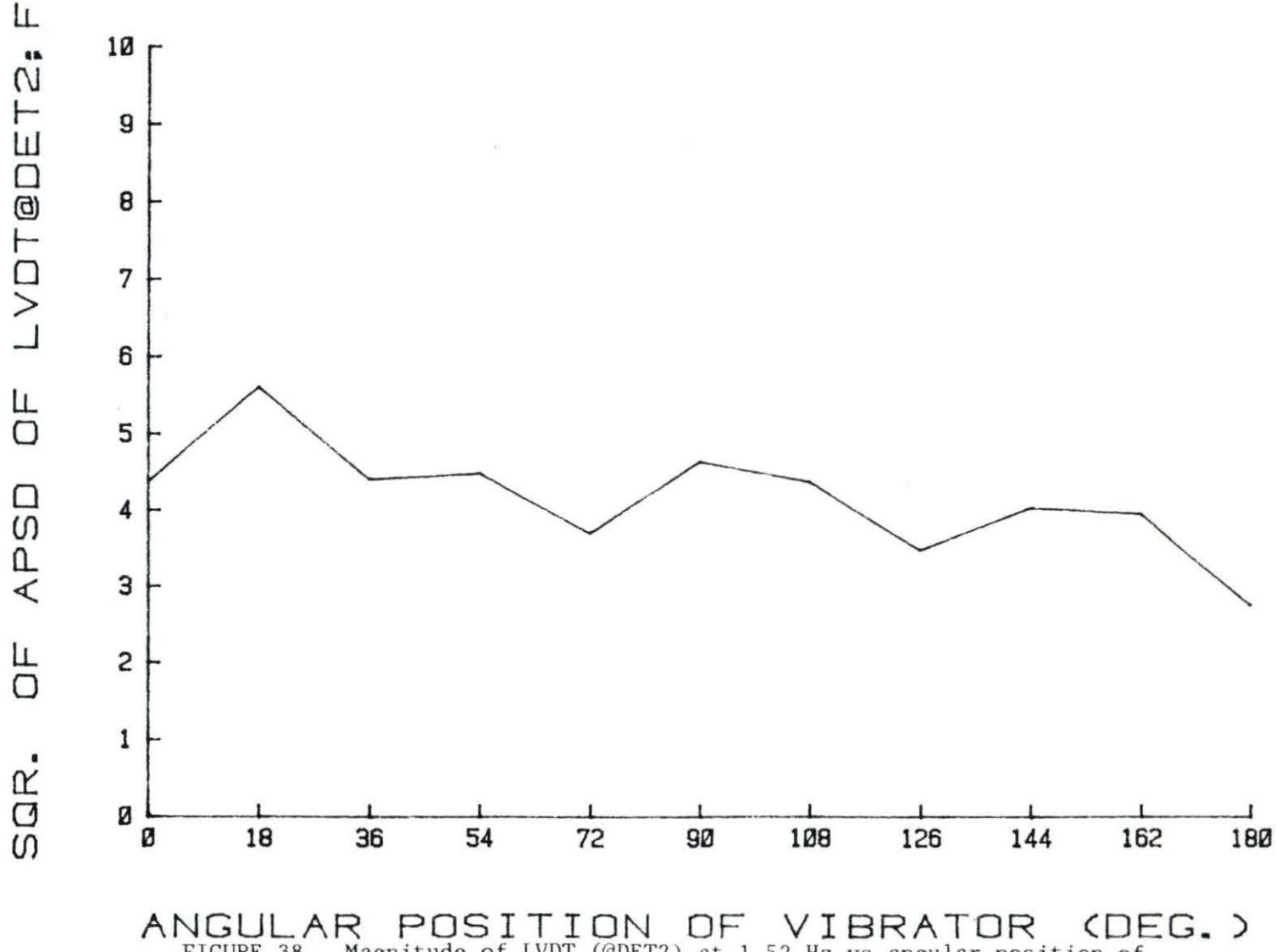

FIGURE 38. Magnitude of LVDT (@DET2) at 1.52 Hz vs angular position of the vibrator (flooded case)

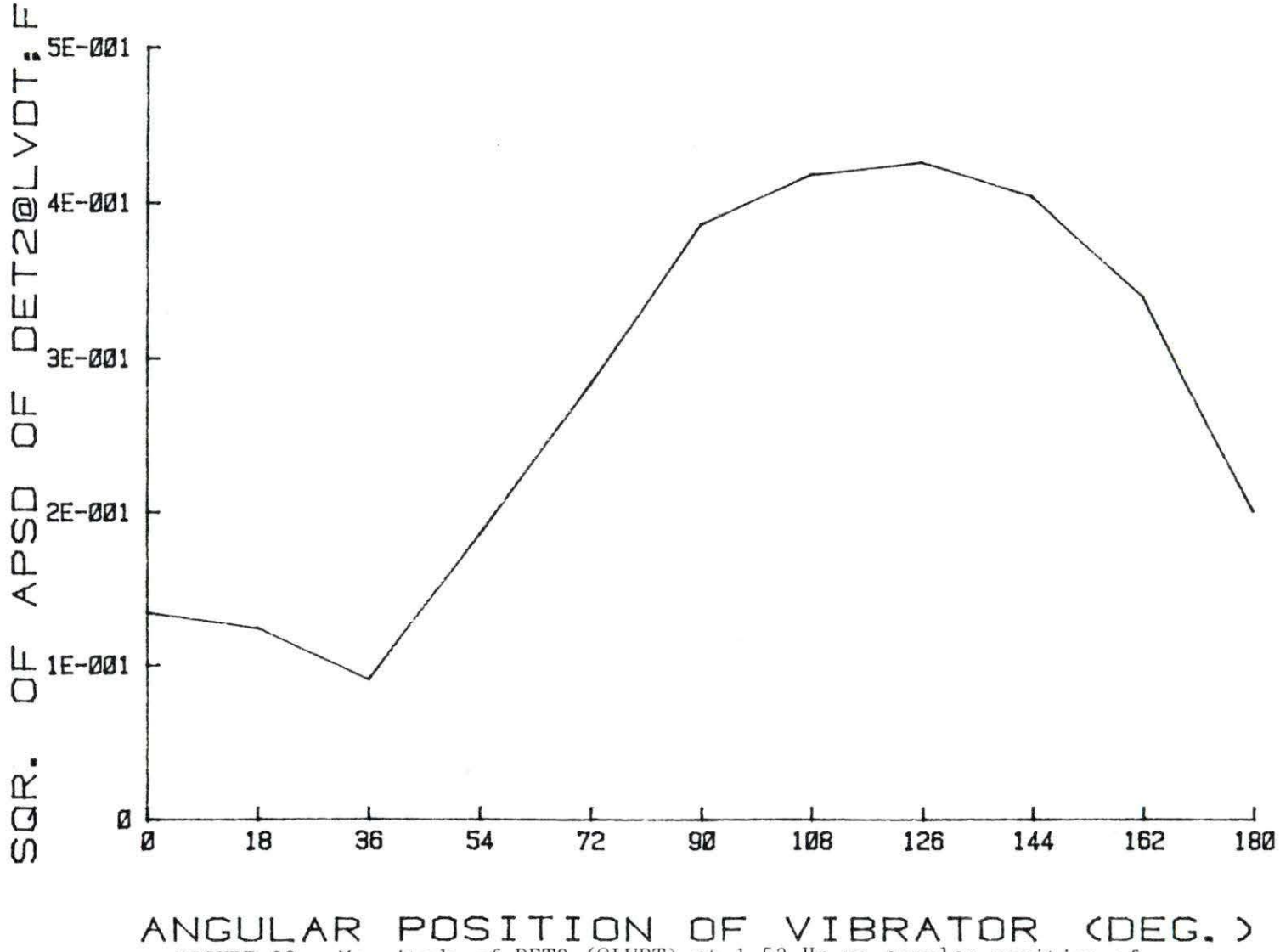

FIGURE 39. Magnitude of DET2 (@LVDT) at 1.52 Hz vs angular position of the vibrator (flooded case)

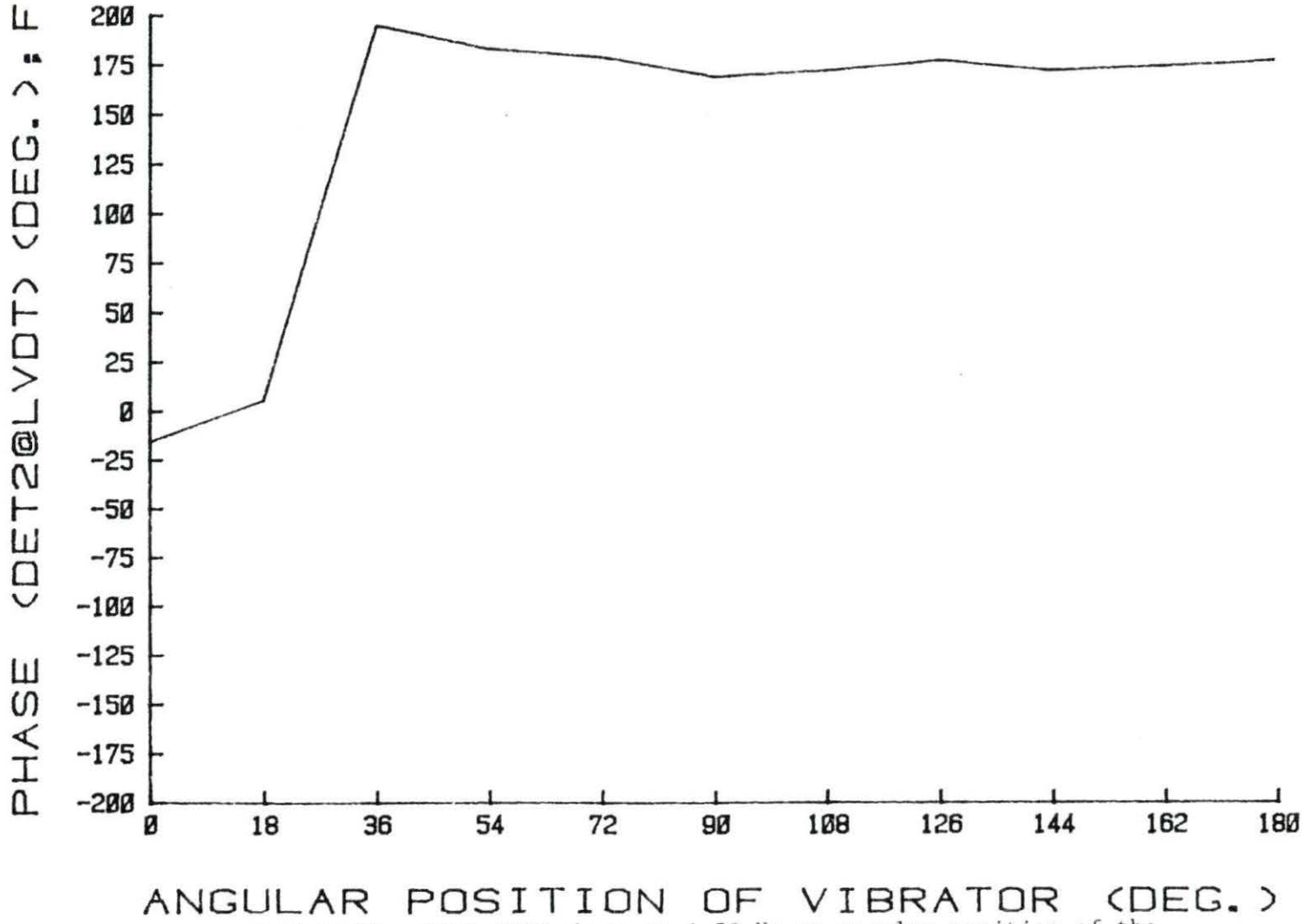

FIGURE 40. DET2-LVDT phase at 1.52 Hz vs angular position of the vibrator (flooded case)

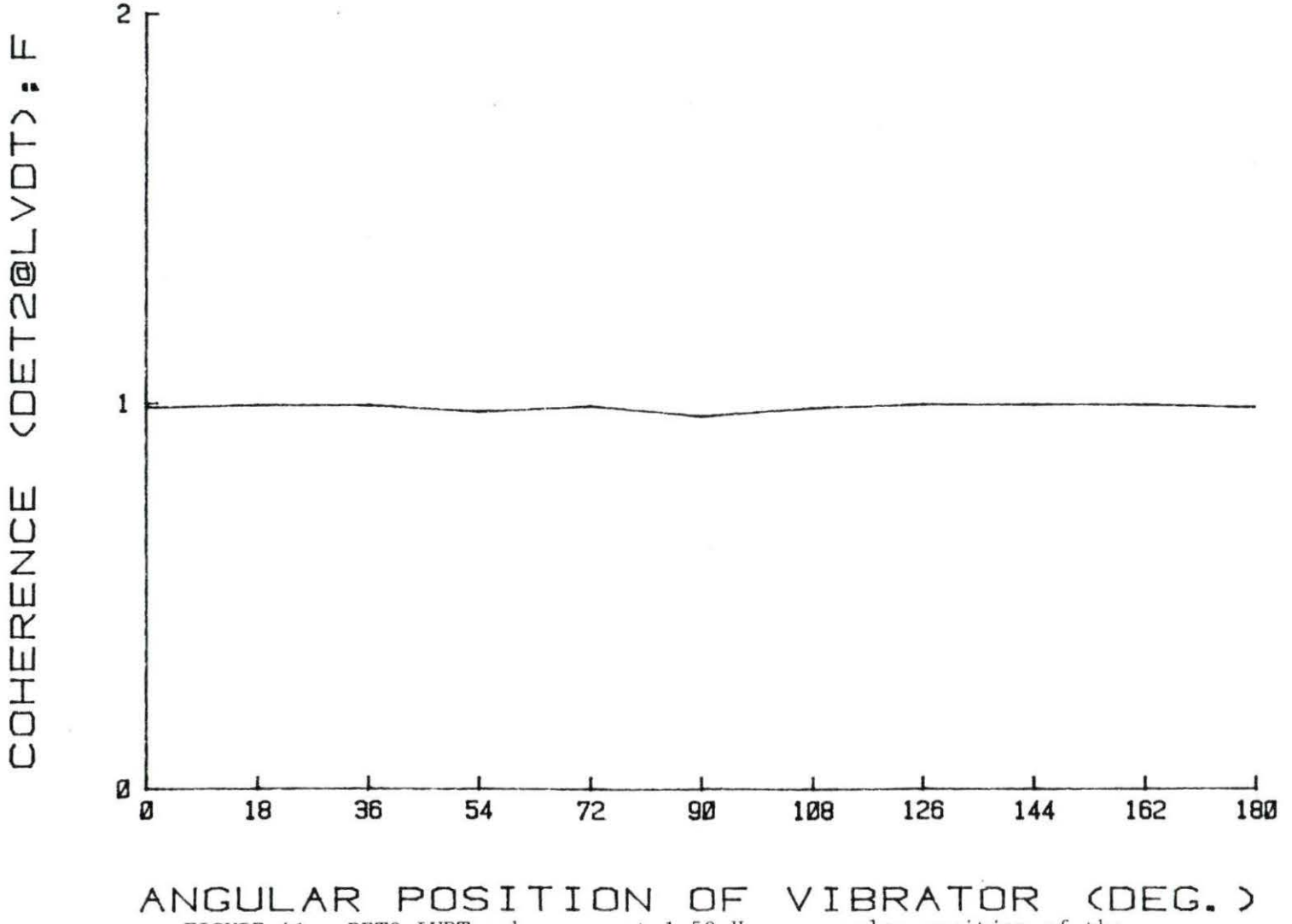

FIGURE 41. DET2-LVDT coherence at 1.52 Hz vs angular position of the vibrator (flooded case)

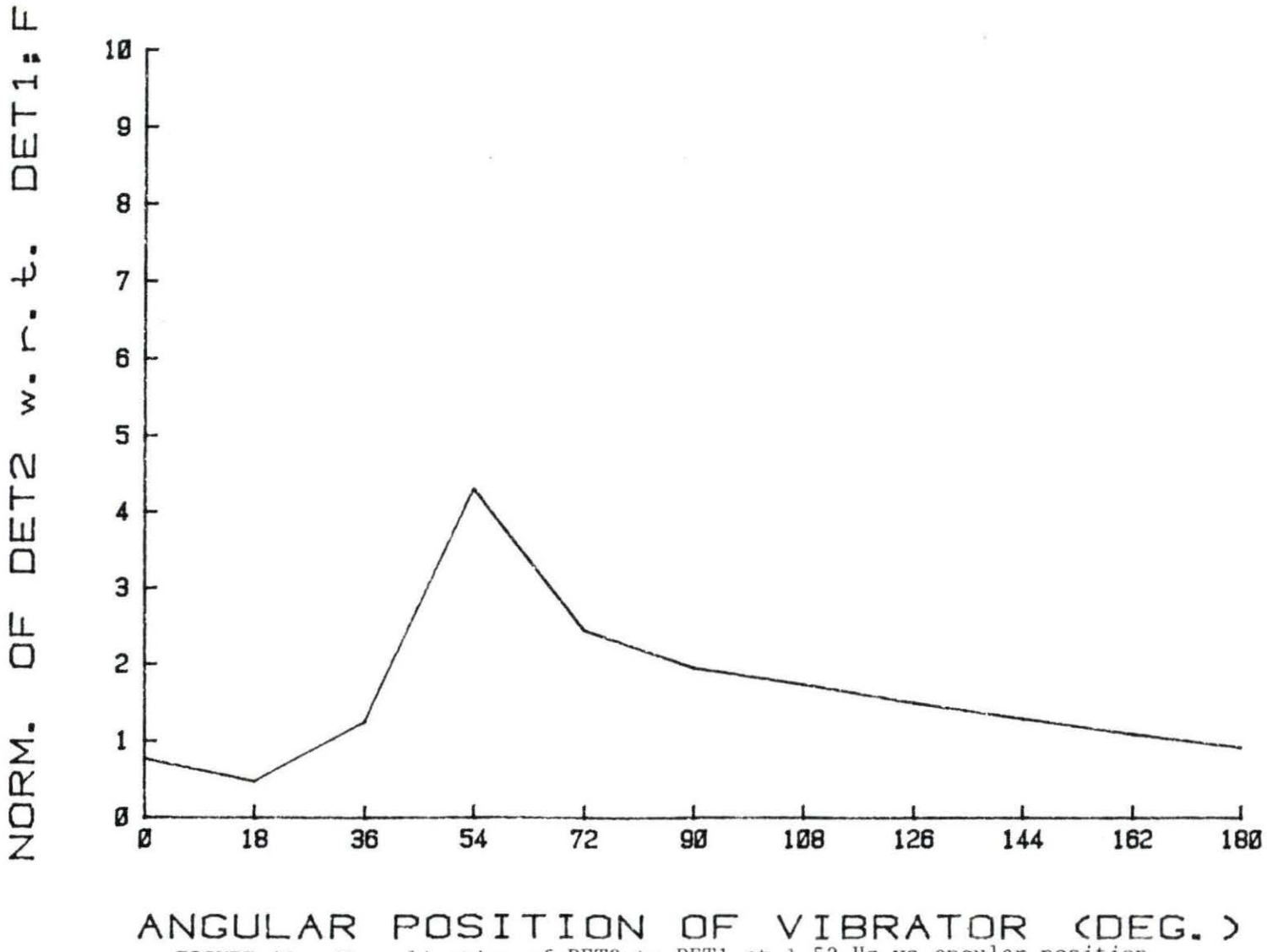

FIGURE 42. Normalization of DET2 to DET1 at 1.52 Hz vs angular position of the vibrator (flooded case)

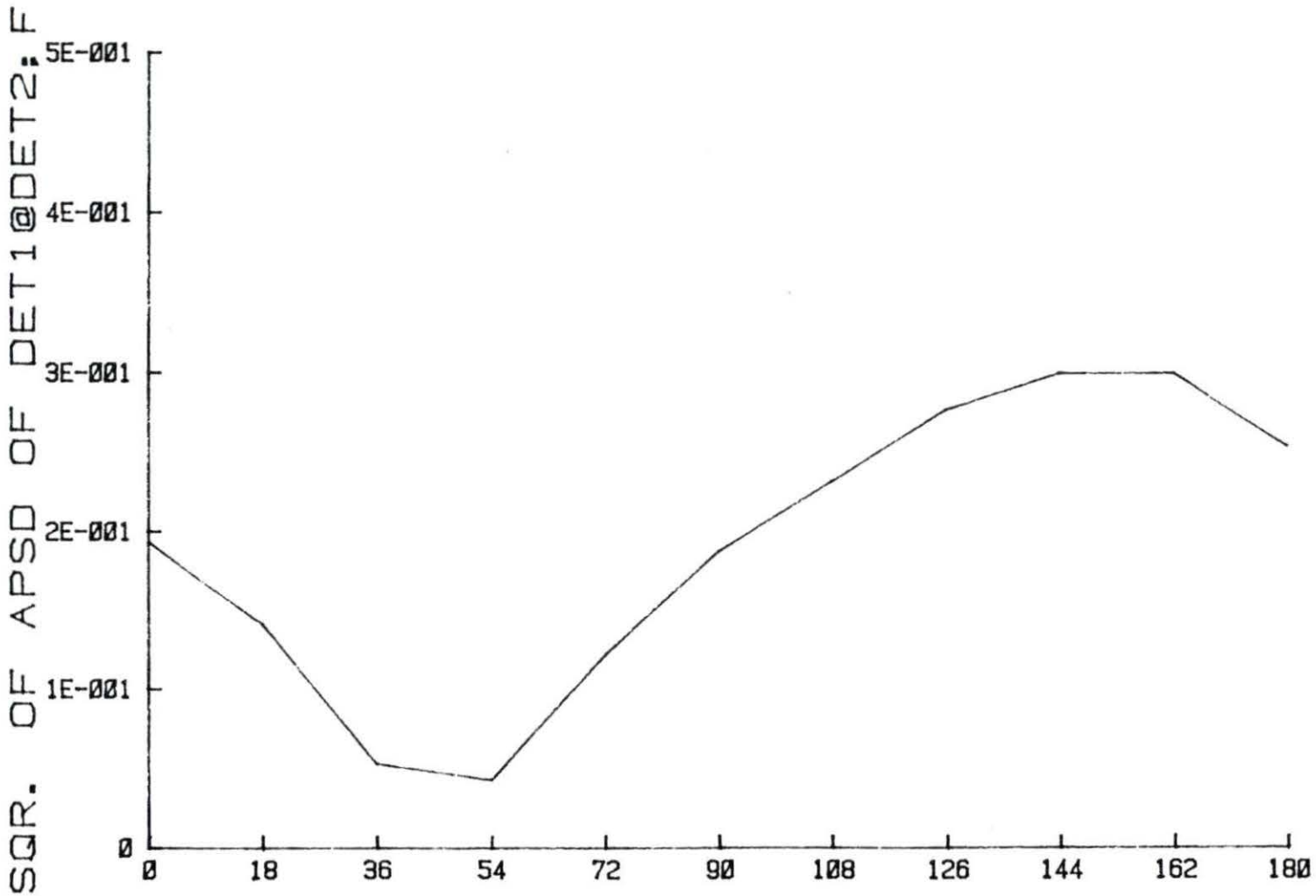

FIGURE 43. Magnitude of DET1 (@DET2) at 1.52 Hz vs angular position of the vibrator (flooded case)

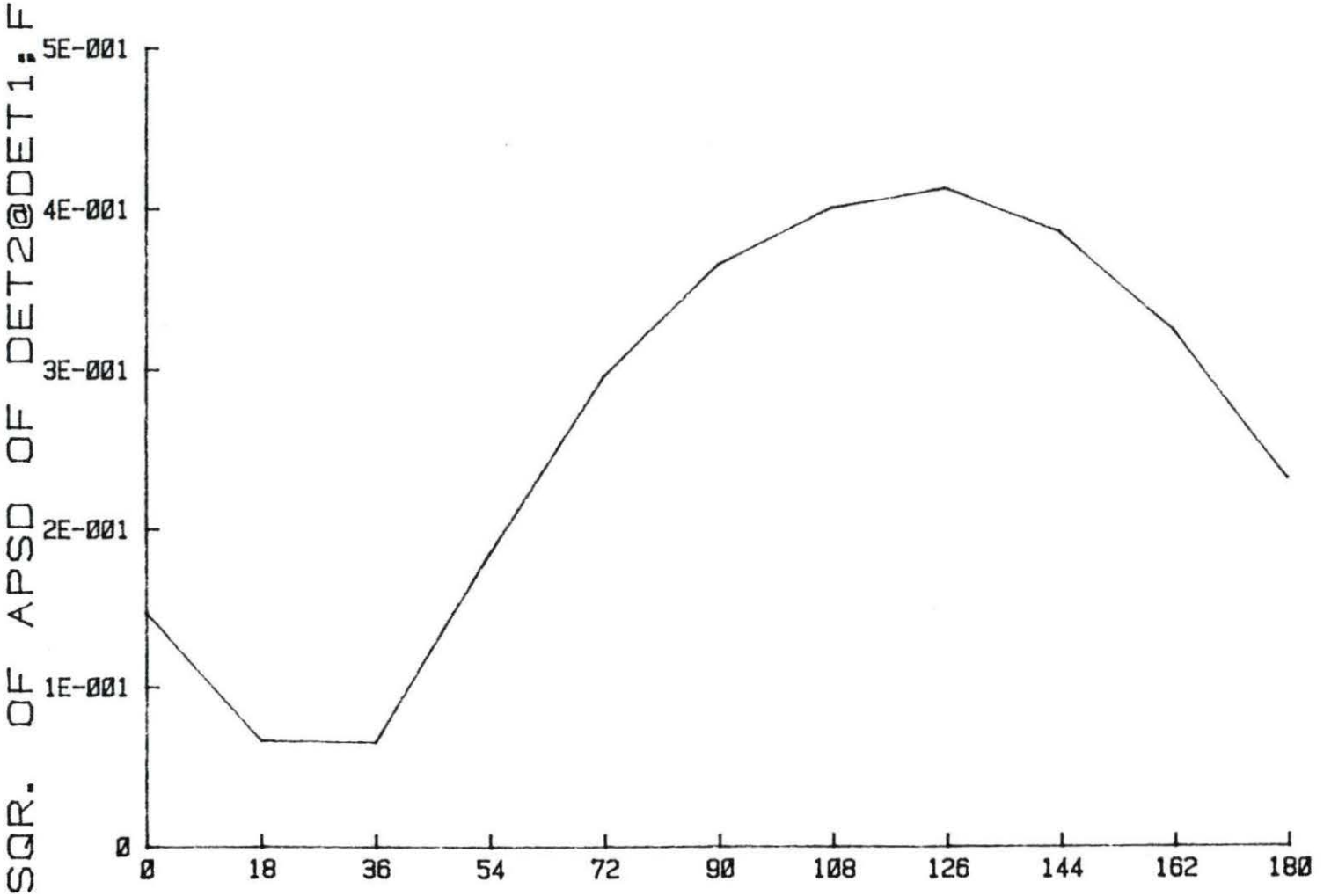

FIGURE 44. Magnitude of DET2 (@DET1) at 1.52 Hz vs angular position of the vibrator (flooded case)

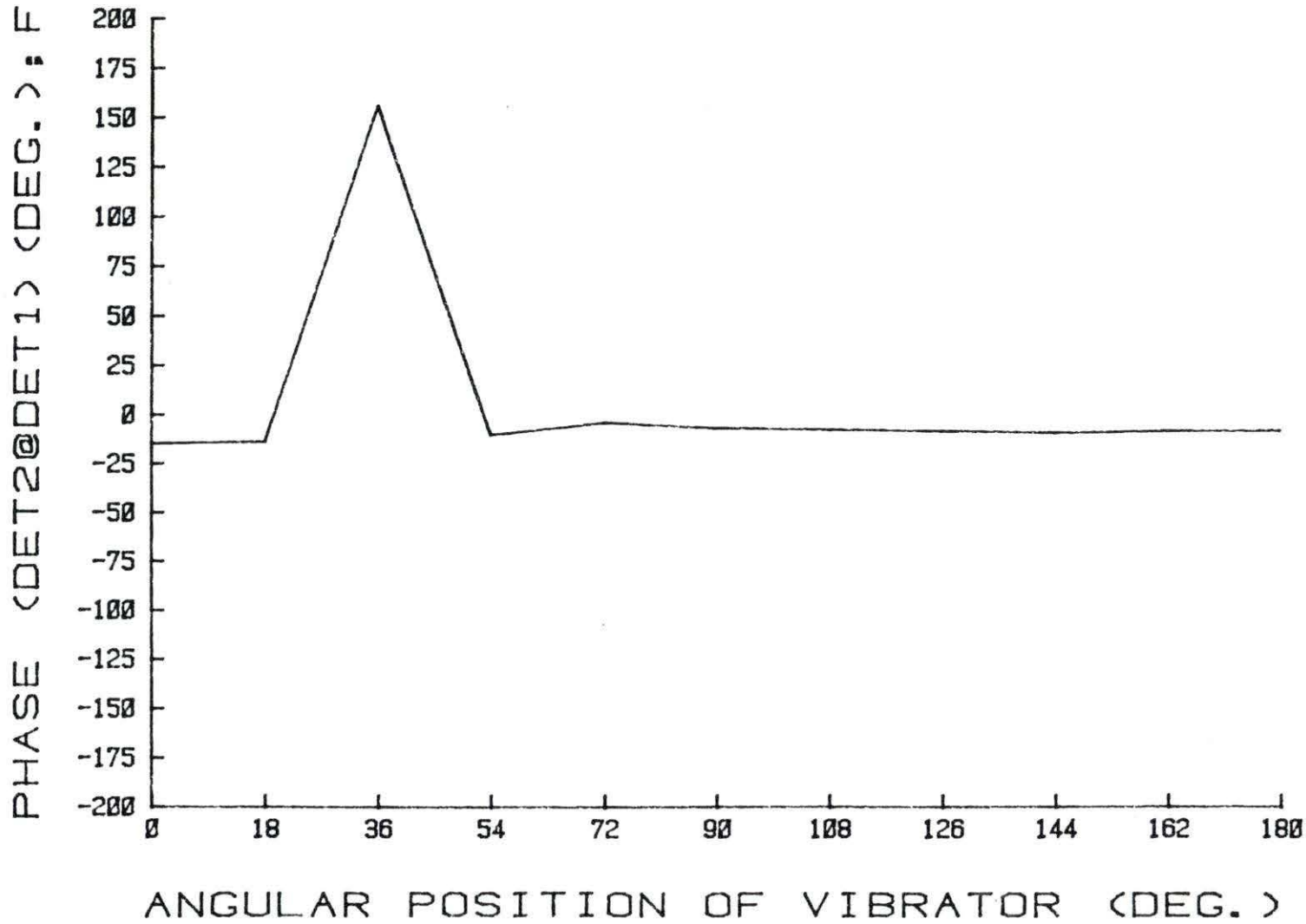

FIGURE 45. DET1-DET2 phase at 1.52 Hz vs angular position of the vibrator (flooded case)

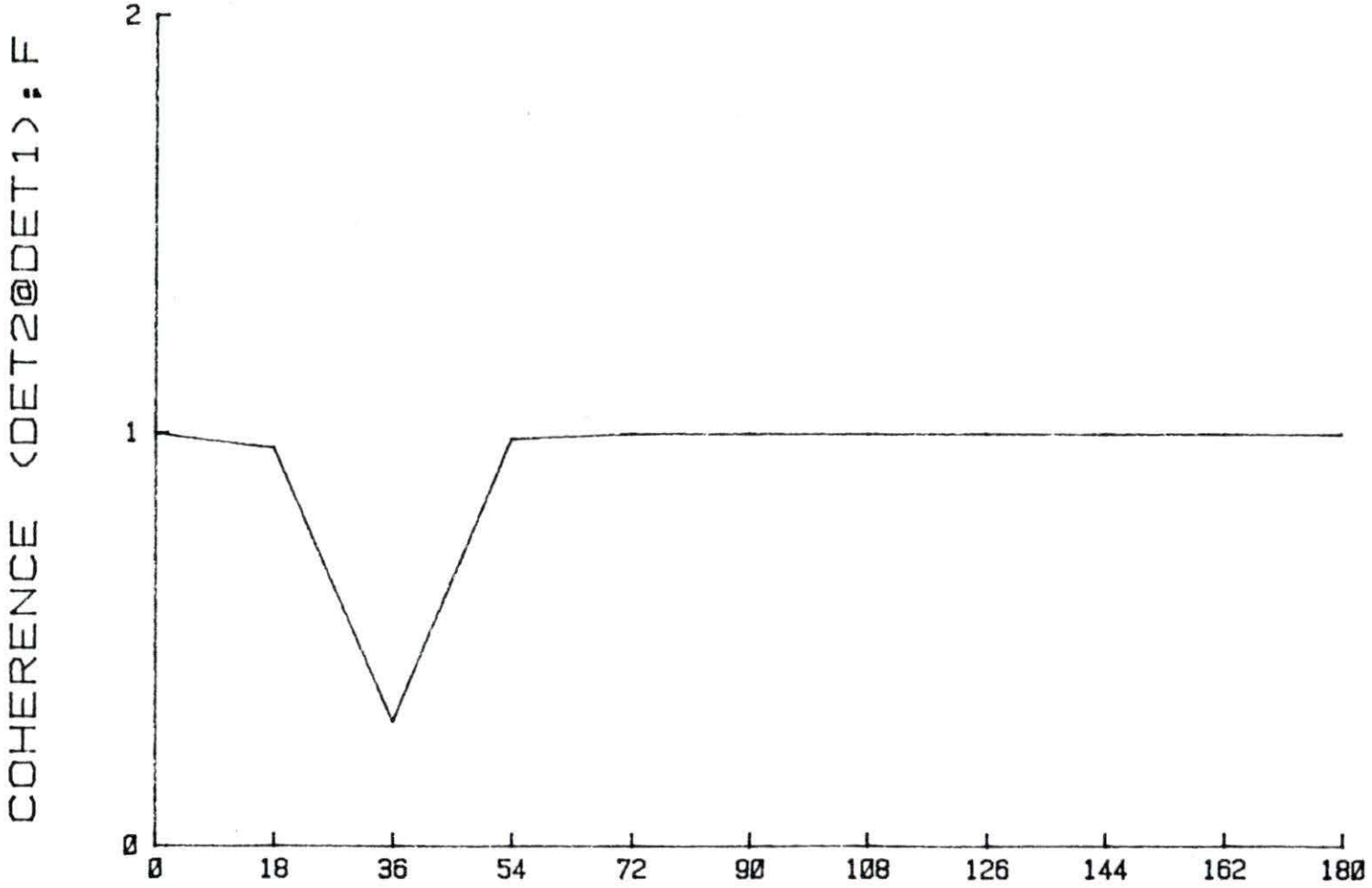

FIGURE 46. DET1-DET2 coherence at 1.52 Hz vs angular position of the vibrator (flooded case)

TABLE 4. L/G ratio at different angular positions (A.P.) (54@90)

A.P.	L/G
0	3.9
18	6.3
36	6.4
54 (physical 90)	0
72	0.7
90	1.1
108	1.4
126	1.8
144 (physical 180)	2.2
162	2.8
180	3.9

To provide a check on these data, the results obtained by Sankoorikal [10] can be noted. For east-west vibrator motion he found an L/G ratio of 1.6. East-west motion would correspond approximately to an angular position of 144 degrees (based on 90 degree corresponding exactly to 54 degrees) for the current work. A value of 2.2 was obtained for this direction. It should be pointed out that the 54 degree direction may not correspond to the exact physical 90 degrees since the data from which it was estimated were obtained in 18 degree steps. It can be concluded, therefore, that the L/G ratios for these measurements do not differ significantly from Sankoorikal's results for this direction of motion.

Since one expects the global part of the response to be a constant value, the global effect (Figure 48) basically shows the gradient of the

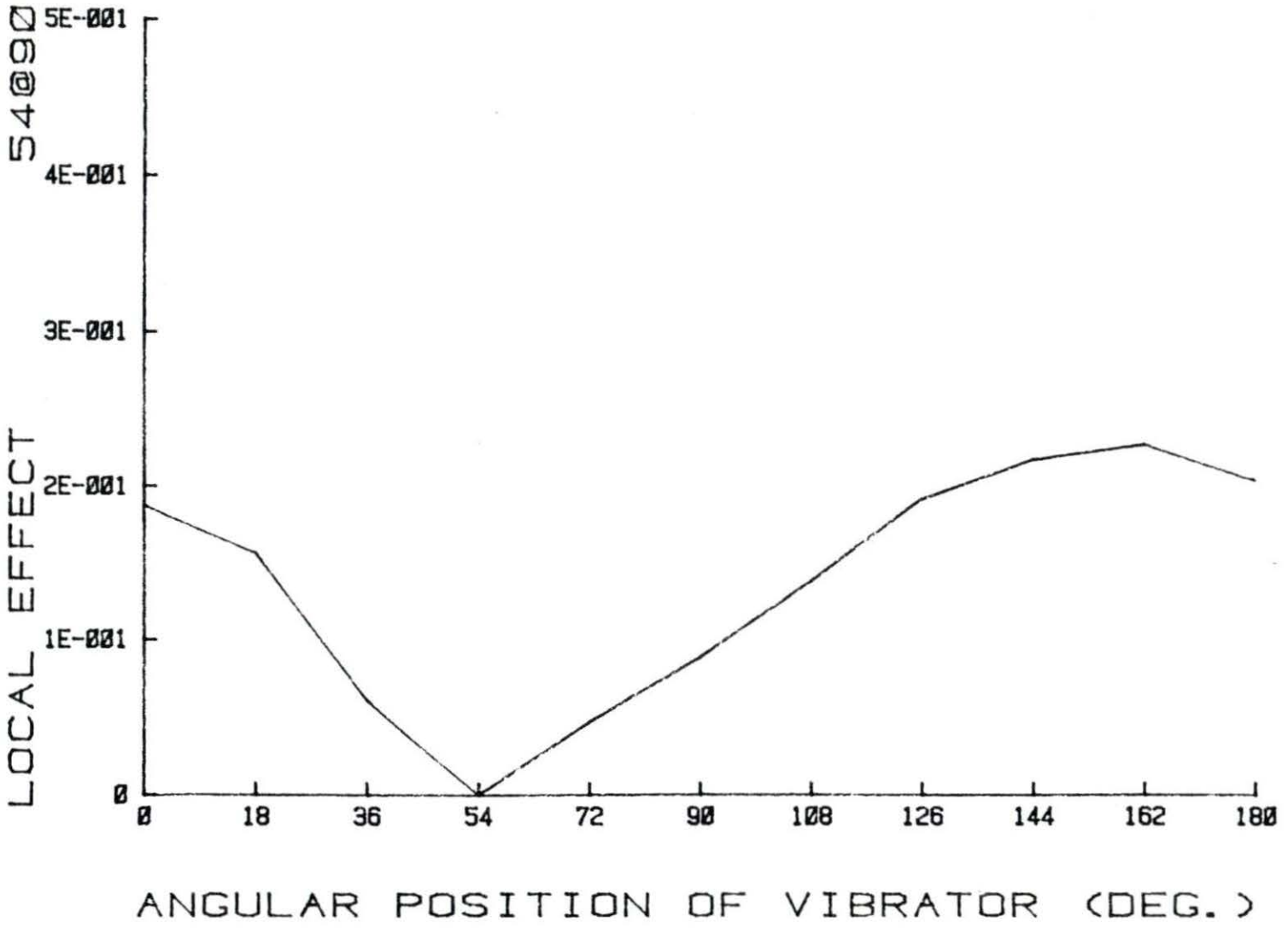

FIGURE 47. Local effect at 1.52 Hz vs angular position of the vibrator

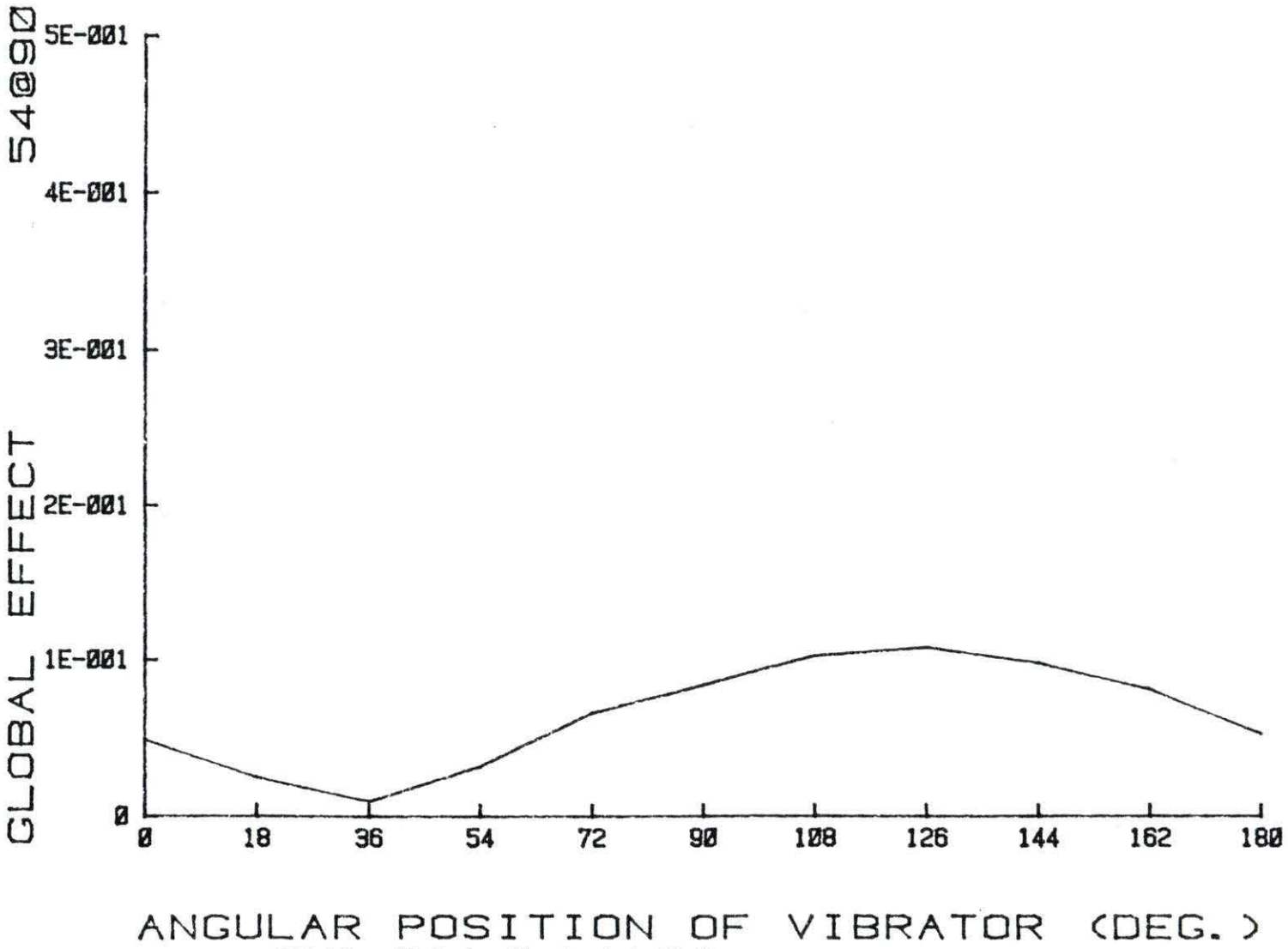

FIGURE 48. Global effect at 1.52 Hz vs angular position of the vibrator

neutron flux in different angular positions inside the UTR-10 reactor. The local effect (Figure 47) basically shows the orientation of the vibrating absorber with respect to the DET1.

VI. CONCLUSIONS

Within the scope of this study, the following conclusions are justified:

1) The direction of motion of the vibrator affects the detector response.

2) The local and global components of the response can be isolated by using the physical 90 degree motion data.

3) The suitability of a stepping motor for remote control of an experiment in a reactor has been demonstrated and procedures for the automated control and data acquisition of the experiment via software programs developed.

4) The responses for the flooded and unflooded cases, although showing somewhat the same behavior, require further study to clarify the trends observed.

5) Additional studies are required to develop an explanation for the structure or detail found in the responses.

VII. SUGGESTIONS FOR FUTURE INVESTIGATIONS

The following ideas are suggested as areas for future research.

1) Exchange the places of the vibrator and DET1 and repeat these measurements.

2) Repeat the flooded case for both orientations of the vibrator.

3) Readjust the zero reference of the vibrator system with respect to DET1, so that physical 90 degrees of the vibrator matches 90 degrees of the system's software program.

4) Insert more neutron detectors around the nuclear reactor core to obtain information required for locating the vibrating element.

5) Excite the vibrator with the pseudo random binary sequence (PRBS) signal and repeat the experiment.

6) Perform measurements at smaller angular steps to obtain finer detail of the response as a function of the vibration direction.

VIII. BIBLIOGRAPHY

1. F. J. Sweeney and J. A. Renier, Sensitivity of detecting in-core vibrations and boiling in pressurized water reactors using ex-core neutron detectors, Martin Marietta, Oak Ridge National Laboratory, NUREG/CR-2996, ORNL/TM-8549 (1984).

2. R. C. Kryter, Loose-part monitoring programs and recent operational experience in selected U.S. and Western European commercial nuclear power stations, Martin Marietta, Oak Ridge National Laboratory, NUREG/CR-3687, ORNL/TM-9107 (1984).

3. W. J. Hennessy, R. A. Danofsky and R. A. Hendrickson, Some observations of the two-dimensional neutron noise field generated by a moving neutron absorber located in the reflector region of low power reactor, Nuclear Science and Engineering 88, 513 (1984).

4. I. Pazsit and O. Glockler, On the neutron noise diagnostics of pressurized water reactor control rod vibrations, Nuclear Science and Engineering 85, 167 (1983).

5. A. M. Weinberg and H. C. Schweinler,Theory of oscillating absorber in a chain reactor, Phys. Rev. 74, 851 (1948).

6. G. Hessel, H. Koppen, P. Liewers, P. Schumann, and F. Weih, Development of nuclear power plant noise diagnostics into a processmeasuring method, Nuclear Technology 68, 102 (1984).

7. M. P. Paidoussis, A review of flow-induced vibrations in reactors and reactor components, Nuclear Engineering and Design 74, 31 (1982).

8. S. J. Lee and R. W. Albrecht, The use of neutron fluctuation to locate a vibrating control rod in a pressurized water reactor model, Nuclear Science and Engineering 83, 427 (1983).

9. R. A. Danofsky and R. A. Hendrickson, Response of the in-core neutron detector of a nuclear reactor to moving core components, National Science Foundation yearly report, ISU-ERI-Ames-84216 (1984).

10. J. T. Sankoorikal, Neutron detector response to a vibrating absorber located in a fuel assembly, M.S. Thesis, Parks Library, Iowa State University, (1983) (Unpublished).

11. H. Van Dam, Neutron noise in boiling water reactors, Atomkernenergie 27, No. 1, 8 (1976).

12. K. Behringer, G. Kosaly, and Lj. Kostic, Theoretical investigation of the local and global components of the neutron-noise field in a boiling water reactor, Nuclear Science and Engineering 63, 306 (1977).

13. I. Pazsit, Investigation of the space-dependent noise induced by a vibrating absorber, Atomkernenergie 30, No. 1, 29 (1977).

14. I. Pazsit and G. Th. Analytis, Theoretical investigation of the neutron noise diagnostics of two-dimensional control rod vibrations in a PWR, Annals of Nuclear Energy 7, 171 (1980).

15. M. Al-Ammar, Use of local-global ratio in detecting component vibration in reactors, Ph.D. dissertation, Parks Library, Iowa State University, (1981) (Unpublished).

16. R. J. Borland, Effects of neutron flux gradient and detector-vibrator geometry on the local-global responses of the UTR-10 reactor, M.S. Thesis, Parks Library, Iowa State University, (1982) (Unpublished).

17. W. J. Hennessy, An investigation of the two-dimensional neutron noise field generated by a moving neutron absorber using the UTR-10 reactor, M.S. Thesis, Parks Library, Iowa State University, (1983) (Unpublished).

18. I. Pazsit, Two-group theory of noise in reflected reactors with application to vibrating absorbers, Annals of Nuclear Energy 5, 185 (1978).

19. F. W. Byron and R. W. Fuller, Mathematics of classical and quantum physics (Addison-Wesley, Cambridge, Massachusetts, 1969).

20. J. J. Duderstadt and L. S. Hamilton, Nuclear reactor analysis (John Wiley & Sons, New York, 1976).

21. M. K. Kalbasi-Isfahani, Experimental plan including safety analysis report for an experiment using the UTR-10 reactor FR-84-01, Department of Nuclear Engineering, Iowa State University, (1984) (Unpublished).

IX. ACKNOWLEDGEMENTS

The author wishes to express his special appreciation to his major professor, Dr. R. A. Danofsky, for his encouraging guidance and many valuable suggestions and discussions throughout the course of this research. The author is very thankful to Dr. A. V. Pohm, Dr. R. A. Hendrickson, Mr. Harold Skank from Ames Laboratory, Masoud Feiz, J. T. Sankoorikal, Mr. Eric from ERI mechnical shop, and Mr. Jess from ERI electronic shop for their help and guidance. The author is also happy to thank the National Science Foundation for their support which was in the form of an assistantship with funds from NSF Grant CPE-8210254. The author is also thanking all his special friends and his parents Ahmad, and Fakhri Kalbasi for their generous and gracious love and support.

X. APPENDIXES

A. Automation

```
5 ! AUTOMATION
10 REMOTE 709
20 CLEAR 709
30 T=0
40 X=0
50 Y=0
60 A1=0
70 A9=0
80 A3=0
90 GOTO 560
100 IF A3>180 OR A3<0 THEN 110 E
LSE 130
110 DISP "ERROR...ANGLE MUST BE
BETWEEN (0) AND (180) DEGREES."
120 GOTO 1270
130 IF A3/1.8<>INT(A3/1.8) THEN
140 ELSE 160
140 DISP "ERROR...ANGLE MUST BE
A FACTOR OF 1.8."
150 GOTO 1270
160 A2=INT(A3/1.8)*2
170 IF A2-A1=0 THEN 180 ELSE 270

180 DISP "RIGHT ON THE MONEY!"
190 A9=A9+18
200 DISP "PLEASE TURN OFF THE SW
ICHING BOARD ,BECAUSE I AM GOING
 TO TURN THE VIBRATOR!(30Sec)"
201 BEEP
202 BEEP
210 WAIT 30000
220 A3=A9
230 IF A9=198 THEN 240 ELSE 260
240 A3=0
250 T=198
260 GOTO 100
270 IF A2-A1<>0 THEN 280
280 IF A2-A1>0 THEN 290 ELSE 400

290 Y=0
300 IF X=0 THEN 310 ELSE 340
310 OUTPUT 709 ;"TO400 "
320 OUTPUT 709 ;"TOO"
330 X=1
```

```
340 OUTPUT 709 :"CS3.2CF3.2"
350 WAIT 4
360 BEEP
370 A1=A1+1
380 DISP .5*A1*1.8:"DEGREES"
390 GOTO 500
400 X=0
410 IF Y=0 THEN 420 ELSE 450
420 OUTPUT 709 ;"TO400 "
430 OUTPUT 709 ;"T00"
440 Y=1
450 OUTPUT 709 :"CS3.2CF3.2"
460 WAIT 4
470 BEEP
480 A1=A1-1
490 DISP .5*A1*1.8:"DEGREES"
500 IF A1=A2 THEN 510 ELSE 550
510 DISP "RIGHT ON THE MONEY!"
520 IF A3=0 THEN 530 ELSE 540
530 GOTO 190
540 GOTO 560
550 GOTO 270
560 REMOTE 711
570 IF T=198 THEN 580 ELSE 590
580 GOTO 1270
590 DISP "CALL OPERATOR TO SEE I
F HE NEEDS TIME FOR REACTOR ADJU
STMENTS FOR ABOUT 30 SECONDS!"
600 BEEP
601 DISP "TURN ON THE SWITCH"
610 WAIT 30000
620 BEEP
630 DISP "CALL OPERATOR AND TELL
 HIM HE IS OUT OF TIME SORRY!"
640 OUTPUT 711 ;"RE"
650 WAIT 90000
660 OUTPUT 711 ;"AA1"
670 N$="A"&VAL$(A3/18+1)
680 Z=2
690 OUTPUT 711 ;"TA1"
700 WAIT 1000
710 OUTPUT 711 :"TA0"
720 OUTPUT 711 :"TB1"
730 WAIT 1000
740 OUTPUT 711 :"TB0"
750 GOTO 920
760 OUTPUT 711 :"AB1"
770 N$="B"&VAL$(A3/18+1)
780 Z=3
```

```
790 GOTO 920
800 OUTPUT 711 ;"AX1"
810 N$="M"&VAL$(A3/18+1)
820 Z=4
830 GOTO 920
840 OUTPUT 711 ;"PX1"
850 N$="P"&VAL$(A3/18+1)
860 Z=5
870 GOTO 920
880 OUTPUT 711 ;"CH1"
890 N$="C"&VAL$(A3/18+1)
900 Z=6
910 GOTO 920
920 OPTION BASE 1
930 DIM A$[2560],B(130)
940 J=1
950 REMOTE 711
960 OUTPUT 711 ;"LDS"
970 ENTER 711 ; A$
980 OUTPUT 711 ;"LSP"
990 ENTER 711 ; F
1000 CLEAR
1010 CREATE N$,1,1280
1020 ASSIGN# 1 TO N$
1030 FOR I=1 TO 1280 STEP 10
1040 B(J)=VAL(A$[I])
1050 PRINT# 1 ; B(J)
1060 J=J+1
1070 NEXT I
1080 F=F/125*127
1090 PRINT# 1 ; F
1100 ASSIGN# 1 TO *
1110 IF Z=2 THEN 1120 ELSE 1140
1120 OUTPUT 711 ;"AA0"
1130 GOTO 760
1140 IF Z=3 THEN 1150 ELSE 1170
1150 OUTPUT 711 ;"AB0"
1160 GOTO 800
1170 IF Z=4 THEN 1180 ELSE 1200
1180 OUTPUT 711 ;"AX0"
1190 GOTO 840
1200 IF Z=5 THEN 1210 ELSE 1230
1210 OUTPUT 711 ;"PX0"
1220 GOTO 880
1230 IF Z=6 THEN 1240
1240 OUTPUT 711 ;"CH0"
1250 REMOTE 709
1260 GOTO 190
1270 END
```

B. Data Reader

```
5 ! DATA READER
10 OPTION BASE 1
20 DIM A(128),B(128),C(128),G(16
),H$[90]
30 CLEAR
40 DISP "INPUT NUMBER OF DATA EN
TERIES"
50 INPUT M
60 DISP "INPUT NAME OF INPUT FIL
E"
70 INPUT D$
80 ON ERROR GOTO 40
90 FOR I=1 TO M
100 S$=D$&VAL$(I)
110 ON ERROR GOTO 130
120 GOTO 160
130 DISP I
140 INPUT Z
150 GOTO 100
160 ASSIGN# 1 TO S$
170 FOR L=1 TO 128
180 READ# 1 ; A(L)
190 NEXT L
200 G(I)=A(20)
210 NEXT I
220 DISP "ENTER STORAGE FILE"
230 INPUT R$
240 ON ERROR GOTO 220
250 CREATE R$,4
260 ASSIGN# 3 TO R$
270 FOR K=1 TO M
280 PRINT# 3 ; G(K)
290 NEXT K
300 ASSIGN# 3 TO *
310 DISP "THE END"
320 PLOTTER IS 705
330 FRAME
340 LOCATE 20,120,20,90
350 FRAME
360 DISP "ENTER XMIN,XMAX,YMIN,Y
MAX"
365 INPUT A,B,C,D
380 SCALE A,B,C,D
390 CSIZE 3 @ FXD 0
395 DISP "ENTER YOUR TIC-LABEL F
OR X&Y"
```

```
386 INPUT E,F
400 LAXES -E,F,A,C
420 FOR X=A TO B STEP E
430 PLOT X,G(X/E+1)
440 NEXT X
460 MOVE 90,-D/4
470 LORG 4 @ CSIZE 5,.5,10
480 LABEL "ANGULAR POSITIONS OF
THE VIBRATOR(DEGREES)"
490 MOVE -18,D/2
500 DEG @ LDIR 90
510 DISP "WHAT IS YOUR YAXIS LAB
EL?"
520 INPUT H$
530 LABEL H$
540 DISP "DO YOU WANT TO REDRAW?
(Y=1,N=0)"
550 INPUT G
560 IF G=1 THEN 570 ELSE 10
570 GOTO 320
580 END
```

C. Normalizer

```
5 ! NORMALIZER
10 OPTION BASE 1
20 DIM A(128),B(128),C(128),G(16
),H(11),D$[90]
30 CLEAR
40 BEEP
50 DISP "INPUT NUMBER OF DATA EN
TERIES"
60 INPUT M
70 ON ERROR GOTO 50
80 FOR J=1 TO M
90 BEEP
100 S$="B"&VAL$(J)
110 ON ERROR GOTO 100
120 ASSIGN# 1 TO S$
130 FOR L=1 TO 128
140 READ# 1 ; A(L)
150 NEXT L
160 BEEP
170 T$="A"&VAL$(J)
190 ASSIGN# 2 TO T$
200 FOR P=1 TO 128
210 READ# 2 ; B(P)
220 NEXT P
230 N=128
240 FOR I=1 TO N
250 IF I<19 OR I>21 THEN 270
260 C(I)=A(I)/B(I)
270 NEXT I
280 G(J)=(C(19)+C(20)+C(21))/3
285 H(J)=G(J)
290 NEXT J
300 BEEP
310 DISP "ENTER STORAGE FILE NAM
E"
320 INPUT R$
340 CREATE R$,4
350 ASSIGN# 3 TO R$
360 FOR K=1 TO M
370 PRINT# 3 ; G(K)
380 NEXT K
390 BEEP
400 DISP "THE END"
410 PLOTTER IS 705
420 FRAME
430 LOCATE 20,120,20,90
440 FRAME
```

```
450 DISP "ENTER YMIN,YMAX,YDIV"
460 INPUT Z,V,L
470 SCALE 0,180,Z,V
480 LAXES -18,L,0,0
490 MOVE 0,0
500 FOR U=1 TO M
510 PLOT U*18-18,G(U)
520 NEXT U
530 MOVE 0,0
540 MOVE 90,-V/4
550 LORG 4 @ CSIZE 5,.5,10
560 LABEL "APOV"
570 MOVE -18,V/2
580 DEG @ LDIR 90
590 DISP "WHAT IS YOUR YAXIS LAB
EL?"
600 INPUT D$
610 LABEL D$
620 DISP "DO YOU WANT TO REDRAW?
(Y=1,N=0)"
630 INPUT S
640 IF S=1 THEN 650 ELSE 10
650 GOTO 410
660 END
```

D. Plotter

```
10 ! PLOTTER
15 DIM G$[60]
16 DISP "ENTER YOUR DATA INPUT"
17 INPUT S$
18 ASSIGN# 1 TO S$
20 PLOTTER IS 705
50 LOCATE 30,130,25,95
60 DISP "ENTER XMIN,XMAX,YMIN,YM
AX"
70 INPUT A,B,C,D
80 SCALE A,B,C,D
90 CSIZE 3 @ FXD 0
100 DISP "ENTER YOUR TIC-LABEL F
OR X&Y"
110 INPUT E,F
120 LAXES -E,F,A,C
130 FOR X=A TO B STEP E
140 READ# 1 ; Y
150 PLOT X,Y
160 NEXT X
170 MOVE 33,370
180 CSIZE 4,1 @ LORG 5
200 MOVE A,C
210 MOVE B/2,-D/7
220 DISP "ENTER X-LABEL"
230 INPUT G$
240 LABEL G$
250 MOVE -B/9,D/2
260 DEG @ LDIR 90
270 DISP "ENTER Y-LABEL"
280 INPUT G$
290 LABEL G$
300 END
```

E. L/G Ratio

```
5 ! L/G RATIO
10 OPTION BASE 1
20 DIM B(11),L(11),G(11)
30 DISP "LOCAL"
40 INPUT L$
50 ASSIGN# 1 TO L$
60 FOR I=1 TO 11
70 READ# 1 ; L(I)
80 NEXT I
90 DISP "GLOBAL"
100 INPUT G$
110 ASSIGN# 2 TO G$
120 FOR I=1 TO 11
130 READ# 2 ; G(I)
140 NEXT I
150 FOR I=1 TO 11
160 B(I)=L(I)/G(I)
170 DISP B(I)
180 NEXT I
190 END
```